Doctoral Thesis

ASSESSMENT OF RECOVERY AND UTILIZATION OPTIONS OF RECYCLABLE COMPONENTS FROM WASTE INCINERATION BOTTOM ASH

carried out for the purpose of obtaining the degree of

Doctor technicae (Dr. techn.)

submitted at TU Wien,
Faculty of Mechanical and Industrial Engineering,
by

Dipl.-Ing. Julia MÜHL
Mat.nr. 01035093

under the supervision of

Privatdozent Dipl.-Ing. Dr. techn. Andreas Bartl
Institute of Chemical, Environmental and Bioscience Engineering

Reviewed by

Prof. Dr. Roland Pomberger
Department of Environmental and Energy Process Engineering,
Montanuniversität Leoben

Prof. Dr. David Laner
Institute of Water, Waste and Environmental Engineering,
University of Kassel

Vienna, April 2025

Affidavit

I declare in lieu of oath that I wrote this thesis and performed the associated research myself, using only the literature cited in this work. If text passages from sources are used literally, they are marked as such.

I confirm that this work is original and has not been submitted elsewhere for examination, nor is it currently under consideration for a thesis elsewhere.

I acknowledge that the submitted work will be checked electronically-technically using suitable and state-of-the-art means (plagiarism detection software). On the one hand, this ensures that the submitted work was prepared according to the high-quality standards within the applicable rules to ensure good scientific practice "Code of Conduct" at the TU Wien. On the other hand, a comparison with other student theses avoids violations of my personal copyright.

Vienna, April 2025

____

Julia Mühl

Acknowledgements

The financial support from the Austrian Federal Ministry of Economy, Energy and Tourism, the National Foundation for Research, Technology and Development and the Christian Doppler Research Association is gratefully acknowledged. Furthermore, I greatly acknowledge the financial and non-financial support of our company partners, which are, in alphabetical order: Abfallbehandlung Ahrental GmbH, Altstoff Recycling Austria AG, Brantner Österreich GmbH, Holding Graz - Kommunale Dienstleistungen GmbH, Lenzing Aktiengesellschaft, Linz Service GmbH, MM Board & Paper, Wien Energie GmbH, and Wopfinger Transportbeton Ges.m.b.H. In addition, I thank Magistratsabteilung MA 48, the public waste management provider of Vienna, for its non-financial support and Binder+Co AG as well as IFE Aufbereitungstechnik GmbH for their experimental support.

Special thanks go to the project partners Gerhard Stockinger and Christoph Schipfer, who provided valuable insights into their company and made it possible to conduct industry-related research. The support and patience of Christian Boswald and his team at the Brantner treatment plant during our experiments are also highly valued.

I would like to thank Stefan Skutan for his support and guidance into the depths of sampling, especially at the beginning of this journey. All student assistants who contributed to this work, especially Felix Feher, is thanked for their hard work, persistent shoveling and persevering hand sorting. Without their help this thesis could not have been performed to the present extent.

Thanks to my supervisor Andreas Bartl for his kind support. I am also grateful to Jakob Lederer for the chance to be part of his research group. I appreciated the freedom I had throughout my work, as well as the support he provided when needed. Moreover, he is mostly responsible for the open and supportive collaboration in the CD Laboratory. This positive atmosphere was also shaped by all of my colleagues, with whom I had the pleasure of working. Besides professional exchange I am grateful for the friendships that formed, the inspiring discussions and the enriching perspectives. Special thanks go to Anna-Maria, Lea and Simon for their support and close collaboration.

Finally, I want to thank all those who supported me along the way, in whatever form. To my mother, my sisters, and Andreas: thank you for your encouragement and belief in me. To my friends, and especially to Filipe, thank you for your listening ear, perspective, inspiration and enrichment in the past years.

My deepest thanks go to Rainer, who stood by my side even during the difficult phases and has been an unwavering source of support and encouragement. You were my greatest strength throughout this entire journey.

Abstract

Municipal solid waste (MSW) incineration, which is a significant MSW treatment path worldwide, leaves behind incineration bottom ash (IBA) as a solid residue. These ashes are often landfilled after the removal of coarse metals. However, further processing can improve metal recovery and enable the remaining mineral fraction to be used in the construction sector. The aim of this dissertation is to enhance the recovery and utilization of recyclable IBA components such as metals, minerals and glass through mechanical treatment. This was investigated in three Case Studies and explored for Austrian IBA from grate firing and fluidized bed combustion of MSW.

In a first experimental setup, a pilot-scale study assessed the optimization potential of an existing IBA treatment plant in Austria. Additional crushing and metal separation steps as well as glass removal were applied to six different IBAs. This study showed that enhanced IBA treatment can improve the suitability of the mineral fraction for recycling. Glass was recovered from both IBA types, but in higher amounts and better quality from fluidized bed IBAs. The plant extension examined in the first Case Study was subsequently implemented in the industrial treatment plant and analyzed in a second Case Study. One IBA from grate incineration and one from fluidized bed combustion were processed comparatively to create a mass balance of the treatment process and the IBA components aluminum, magnetic ferrous metals and glass. This experiment revealed the feasibility of industrial enhanced treatment and remarkable potential recycling rates above 95% for aluminum and magnetic ferrous metals >4 mm. Although glass recovery was not industrially feasible from the grate IBA, 72% of the glass contained in the fluidized bed IBA could be recovered. The promising results regarding glass separation from fluidized bed IBA led to a third Case Study. This study investigated whether the separated glass could be upgraded to meet the quality standards required by the packaging glass industry. Contaminants were removed from two glass fractions from fluidized bed IBA by additional sensor-based separation, thereby achieving very pure glass fractions. Yet, the strict standards for packaging glass recycling were not met.

In summary, the Case Studies in this dissertation demonstrated that enhanced IBA treatment can improve the circularity of IBAs from MSW incineration. Additional treatment steps enable better metal separation, which is economically relevant and improves the quality of the mineral fraction. Moreover, glass can be recovered from fluidized bed IBA and might be recycled in the future if improved upgrading is applied or if alternative recycling routes can be found. Certain disadvantages of grate IBA regarding its recyclability were ascertained in this thesis, including higher heavy metal contents in the mineral fraction and limited glass recovery. These downsides can be traced back to the incineration conditions in the grate furnace. The differences

determined between fluidized bed and grate IBA can be basis for a holistic assessment of whether fluidized bed or grate incineration is more beneficial for a circular economy. The enhanced IBA treatment steps developed in this work can be crucial for transitioning MSW incineration from a waste management strategy to an integrated part of a circular economy by closing material loops.

Kurzfassung

Bei der Abfallverbrennung, einem der relevantesten Behandlungspfade für Siedlungsabfall weltweit, entstehen Aschen als feste Verbrennungsrückstände. Die groben Aschen, Rostaschen aus der Rostfeuerung und Bettaschen aus der Wirbelschichtfeuerung von Abfällen, werden oftmals nach einer Abtrennung grober Metalle deponiert. Durch weitergehende Aufbereitung können Metalle jedoch verbessert rückgewonnen und dadurch auch die verbleibende Mineralikfraktion einer Verwertung im Bauwesen zugeführt werden. Ziel dieser Dissertation ist es, die Rückgewinnung und Verwertbarkeit recycelbarer Aschebestandteile wie Metalle, Mineralik und Glas durch mechanische Aufbereitungsverfahren zu steigern. Dies wurde in drei Fallstudien anhand verschiedener Rost- und Bettaschen aus Österreich untersucht.

In einem ersten Versuchsaufbau wurde im Technikumsmaßstab erhoben, wie eine bestehende Ascheaufbereitungsanlage in Österreich in Bezug auf die genannte Zielsetzung optimiert werden kann. Dazu wurden zusätzliche Zerkleinerungs- und Metallabtrennungsschritte sowie eine Glasabscheidung an drei Rost- und drei Bettaschen durchgeführt. Diese Fallstudie zeigte, dass eine erweiterte Ascheaufbereitung die Recyclingfähigkeit der Mineralikfraktion der Aschen steigern kann. Zudem wurde Glas aus beiden Aschearten rückgewonnen, jedoch in größeren Mengen und besserer Qualität aus den Bettaschen. Die untersuchte Anlagenerweiterung wurde anschließend an der industriellen Aufbereitungsanlage implementiert und in einer zweiten Fallstudie näher untersucht. Eine Rost- und eine Bettasche wurden dazu vergleichend aufbereitet, um eine Anlagenbilanz zu erstellen und das Verhalten der Aschebestandteile Aluminium, magnetische Eisenmetalle und Glas zu evaluieren. Mit diesem Versuch wurde nachgewiesen, dass die erweiterte Ascheaufbereitung im Industriemaßstab anwendbar ist und beachtliche potentielle Recyclingraten von über 95% für Aluminium und magnetische Eisenmetalle >4 mm festgestellt. Wenngleich Glas nicht industriell aus Rostaschen abgetrennt werden konnte, wurden jedoch 72% des in Bettaschen enthaltenen Glases durch die erweiterte Anlagenkonstellation rückgewonnen. Diese vielversprechenden Ergebnisse bezüglich Glasabscheidung aus Bettaschen wurden in einer dritten Fallstudie näher untersucht. In dieser wurde erhoben, ob Glas aus Bettaschen auf die von der Verpackungsglasindustrie geforderte Qualität aufgereinigt werden kann. Hierzu wurden Störstoffe aus zwei Glasfraktionen mittels zusätzlicher sensorbasierter Abscheidung abgeschieden, wodurch sehr reine Glasfraktionen erzeugt werden konnten. Die strengen Vorgaben der Verpackungsglasindustrie wurden durch die Aufreinigung jedoch nicht erreicht.

Zusammenfassend konnte in den Fallstudien dieser Dissertation festgestellt werden, dass eine erweiterte mechanische Aufbereitung die Kreislauffähigkeit von Rost- und Bettaschen aus der Abfallverbrennung erhöht. Durch zusätzliche Aufbereitungsschritte können Metalle besser abgeschieden werden, was ökonomisch relevant ist und zudem die Qualität der Mineralikfraktion verbessert. Aus Wirbelschicht-Bettaschen kann außerdem Glas rückgewonnen und zukünftig potentiell im Glasrecycling eingesetzt werden. Für Rostaschen wurden bestimmte Nachteile im Vergleich zur Bettasche ermittelt, wie beispielsweise höhere Schwermetallgehalte in der Mineralikfraktion und eingeschränkte Glasrückgewinnung. Diese Nachteile sind vor allem auf höhere Temperaturen und Verweilzeiten des Abfalls in der Feuerung zurückzuführen. Diese Erkenntnis kann genutzt werden, um ganzheitlich festzustellen, ob die Wirbelschicht- oder die Rostfeuerung im Sinne einer Kreislaufwirtschaft vorteilhafter ist. Die in dieser Dissertation entwickelte Aufbereitungserweiterung für Rost- und Bettaschen kann zudem entscheidend dazu beitragen, die Abfallverbrennung als relevanten Teil der Abfallwirtschaft hin zu einer Kreislaufwirtschaft zu entwickeln.

Table of contents

Publications in scientific journals

This work is based on three peer-reviewed publications which were published in scientific journals. The papers are listed below and can be found in full version in the Appendix.

Paper I:

Glass recovery and production of manufactured aggregate from MSWI bottom ashes from fluidized bed and grate incineration by means of enhanced treatment

Mühl, J.; Skutan, S.; Stockinger, G.; Blasenbauer, D.; Lederer, J.

Waste Management 168 (2023), 321–333.
Available online: June, 17th 2023
DOI: https://doi.org/10.1016/j.wasman.2023.05.048
Author contribution: Formal analysis, Investigation, Data Curation, Writing – Original Draft, Writing – Review & Editing, Visualization

Paper II:

Recovery of aluminum, magnetic ferrous metals and glass through enhanced industrial-scale treatment of different MSWI bottom ashes

Mühl, J.; Hofer, S.; Blasenbauer, D.; Lederer, J.

Waste Management 190 (2024), 557–568.
Available online: October, 28th 2024
DOI: https://doi.org/10.1016/j.wasman.2024.10.025
Author contribution: Conceptualization, Methodology, Validation, Formal analysis, Investigation, Data Curation, Writing – Original Draft, Writing – Review & Editing, Visualization, Project administration

Paper III:

Upgrading and Characterization of Glass recovered from MSWI Bottom Ashes from Fluidized Bed Combustion

Mühl, J.; Mika, S.; Tischberger-Aldrian, A.; Lederer, J.

Recycling 10,63 (2025).
Available online: April, 07th 2025
DOI: https://doi.org/10.3390/recycling10020063
Author contribution: Conceptualization, Methodology, Validation, Formal analysis, Investigation, Writing – Original Draft, Writing – Review & Editing, Visualization, Supervision

Abbreviations

CSP	Ceramics, stones, porcelain
DM	Dry matter
ECS	Eddy current separation
FB-IBA	Fluidized bed incineration bottom ash
Fe	ferrous
G-IBA	Grate incineration bottom ash
IBA	Incineration bottom ash
MSW	Municipal solid waste
MSWI	Municipal solid waste incineration
NFe	Non-ferrous
XRF	X-ray fluorescence

1 Introduction

The landfill ban on untreated waste as of 2004, set by the landfill directive, has substantially modified Austrian waste management and has generated a considerable increase in municipal solid waste incineration (MSWI) (Pomberger et al., 2017). Around twenty years later, MSWI still plays a crucial role not only in Austria but globally (Brunner and Morf, 2024; Makarichi et al., 2018; Neuwahl et al., 2019). In 2020, 36% of the total municipal solid waste (MSW) were incinerated, while only 2% were landfilled in Austria (BMK, 2023). Whereas separately collected MSW was mainly recycled in 2020, MSW from mixed residual waste collection was incinerated almost completely (94%) (BMK, 2023). In Austria, twelve MSWI plants, thereof five fluidized bed combustors and seven grate incinerators, are currently in operation (Bernhardt et al., 2024). Their annual capacity amounts to 2.8 million tons for non-hazardous waste. Another grate incineration plant is in the planning phase (Energie Graz, 2024). The high share of fluidized bed combustion for MSWI in Austria is exceptional by international standards (Leckner and Lind, 2020; Lu et al., 2017; Makarichi et al., 2018). The more established technology for waste incineration is grate firing, although fluidized bed combustion can offer advantages for MSWI (van Caneghem et al., 2012).

MSWI primarily aims to reduce waste volume and mass and destroy pollutants (Neuwahl et al., 2019). Moreover, MSWI can be utilized for the production of heat and energy. Nevertheless, solid residues remain after waste incineration, which must be processed for further recycling or disposal. The most significant residue in terms of quantity is incineration bottom ash (IBA), which is categorized into grate IBA (G-IBA) and fluidized bed IBA (FB-IBA), depending on the incineration technology from which it derives. Also, fly ash remains after incineration as a finer solid residue. In total, IBAs and fly ashes together account for 15-30% of the MSW incinerated, with the ratio of IBA to fly ash being highly dependent on the incineration technology used (Fan et al., 2022; Feil et al., 2019; Kellner et al., 2022; Qi et al., 2024; Vermeulen et al., 2012).

For many years, it was common practice in Austria only to recover coarse metals from IBAs while disposing of the remaining mineral components in landfills (BMNT, 2017). This also applies in an international context (Fletcher and Dunk, 2023). However, depending on the composition of the waste incinerated, IBAs only contain 5-20% of metals (Šyc et al., 2020). The abundant amount of IBAs was therefore landfilled, producing vast amounts of landfill volume. Additionally, valuable materials contained in the IBAs, such as glass or metals, which are difficult to separate, were removed from the recycling loop.

By new research findings and ongoing transformation of the linear waste management into a circular economy, increasing efforts are aiming at improving the circularity of

IBAs (Brunner and Morf, 2024; Silva et al., 2019; van Caneghem et al., 2019b). These developments are also considered in legal guidelines within the European Union. New recycling paths, for example in the construction sector, are examined and legally approved in several states (Blasenbauer et al., 2020). This also applies to Austria, where as of 2023 the legal framework allows IBA utilization in concrete production if complying with specific requirements, in addition to the utilization in road construction, which has been permitted before (BMK, 2023). Beyond that, the high share of FB-IBA in Austria offers the opportunity to recover glass from this ash type, which has not been reported in the scientific literature hitherto. Glass contained in IBAs is typically treated with the mineral fraction and landfilled or recycled, respectively.

To establish new recycling paths in practice, it is necessary to improve existing treatment plants, which were initially designed for metal recovery. Legal and technical requirements have to be met by the mineral fractions of IBAs to allow for their recycling. For example, heavy metal contents and residual metal pieces are limited in the construction sector. Additionally, soluble salts can impede the recyclability of the mineral material. From a technical perspective, constant quality and a specific particle size distribution are also required. Enhanced IBA treatment is indispensable to meet the legal and technical demands and to make the mineral fraction from IBA usable as a secondary raw material. Therefore, further research and comprehensive studies are necessary to develop improved IBA treatment, also on an industrial scale. Broad knowledge about the properties of IBAs and their processing and recovery options is essential for establishing industrial, long-term recycling solutions.

1.1 Scope of the Thesis and Research Questions

The objective of this thesis is to assess how the circularity of IBAs from MSWI can be improved. Therefore, various aspects of enhanced IBA treatment in Austria were investigated in this work, focusing on mineral constituents and metals in the IBAs. Thus, the utilization of IBA as a secondary raw material should be increased, thereby reducing landfill volume. Due to the high share of fluidized bed combustion in Austrian MSWI, differences between FB-IBA and G-IBA could be examined in all experiments conducted. This aspect has rarely been explored in scientific research hitherto.

The following research questions were addressed in this thesis:

- Does enhanced IBA treatment increase the utilization potential and the circularity of the IBAs?
- Which differences occur in the treatment of G-IBAs and FB-IBAs?
- Is enhanced IBA treatment on an industrial scale feasible?
- Which shares of the packaging materials aluminum, magnetic ferrous metals and glass can be industrially recovered by means of enhanced IBA treatment?

- Which properties do the glass fractions recovered from IBAs exhibit?
- Is the recycling of glass from IBAs possible in the packaging glass industry? If not, what needs to be done to enable glass recycling?

1.2 Case Study Description and Thesis Structure

To answer the research questions, several treatment experiments with FB-IBA and G-IBA were conducted as part of this dissertation. The investigations were realized in three Case Studies, which are outlined in the following section. The related publications can be found in the Appendix of this thesis.

1.2.1 Case Study I

In the first Case Study, enhanced treatment steps on a pilot scale were investigated, using three FB-IBAs and three G-IBAs. The six IBAs used were first processed at the industrial IBA treatment plant operated by *Brantner Österreich GmbH*, which has been primarily designed for metal recovery. Subsequently, enhanced pilot-scale treatment was applied to the IBAs, including sieving and crushing of the mineral material and additional metal separation steps for magnetic ferrous and non-magnetic, non-ferrous metals. Moreover, glass was recovered from the coarse mineral fraction using sensor-based glass sorting.

The amounts of mineral material and glass were quantified in this experiment, in order to reveal the potential of glass recovery and differences between the IBAs. Additionally, chemical analyses of the mineral fractions were conducted to determine whether they met the legal requirements for utilization in Austria. The findings from Case Study I were summarized and published in the first paper of this thesis, entitled "*Glass recovery and production of manufactured aggregate from MSWI bottom ashes from fluidized bed and grate incineration by means of enhanced treatment*" (Mühl et al., 2023).

1.2.2 Case Study II

Following Case Study I, the enhanced treatment investigated was implemented at the industrial IBA treatment plant of Brantner Österreich GmbH in 2021. The plant extension included a crusher, additional sieves, further magnetic metal, and eddy current separators, as well as a glass sorter. This allowed for a comparative examination of enhanced IBA treatment on an industrial scale compared to the pilot-scale treatment in Case Study I. By sampling and manual sorting of all output flows during the experiment, the amounts and compositions of all outputs of the treatment plant were determined. Thereby, the distribution of the IBAs itself and of the components aluminum, magnetic ferrous metals and glass was examined after the treatment. From this data, a material flow analysis was established for the IBAs and the three packaging materials >4 mm. As a result, recovered amounts of potentially recyclable material from industrially treated IBA and the quality of the glass recovered could be determined. The findings of Case Study II were published in the second paper "*Recovery of aluminum, magnetic ferrous metals and glass through enhanced industrial-scale treatment of different MSWI bottom ashes*".

1.2.3 Case Study III

The first two Case Studies clearly showed that FB-IBAs from fluidized bed combustion contain significant amounts of glass, which can also be technically recovered. However, little information has been reported regarding the composition and properties of glass from FB-IBA. Moreover, due to their share of extraneous material, the glass fractions recovered from FB-IBA in Case Studies I and II cannot be recycled in the Austrian packaging glass industry without further upgrading. Closed-loop recycling in the packaging glass industry underlies strict requirements concerning the content of extraneous material and metals, or regarding the heavy metals Pb, Cd, Hg and Cr(VI). Therefore, glass recovered from FB-IBA was upgraded and assessed more closely in a third experiment, Case Study III. The glass usability for recycling in the packaging glass industry after additional sensor-based upgrading steps was examined in different setups. In the course of this upgrading, extraneous material, including non-glass mineral-based material (e.g., ceramics, stones, porcelain, building material), metals and lead glass, were further removed through sensor-based sorting to purify the glass fractions. To characterize the glass fractions, manual sorting and XRF analysis were applied. The glass fraction produced during the second Case Study and another glass fraction recovered from industrial enhanced IBA treatment were used for the investigations. The results of Case Study III, including upgrading and characterization of the glass fractions, were published in the paper "*Upgrading and Characterization of Glass recovered from MSWI Bottom Ashes from Fluidized Bed Combustion*", which constitutes the third publication of this thesis.

1.2.4 Thesis structure

The structure of the thesis is summarized in Figure 1.

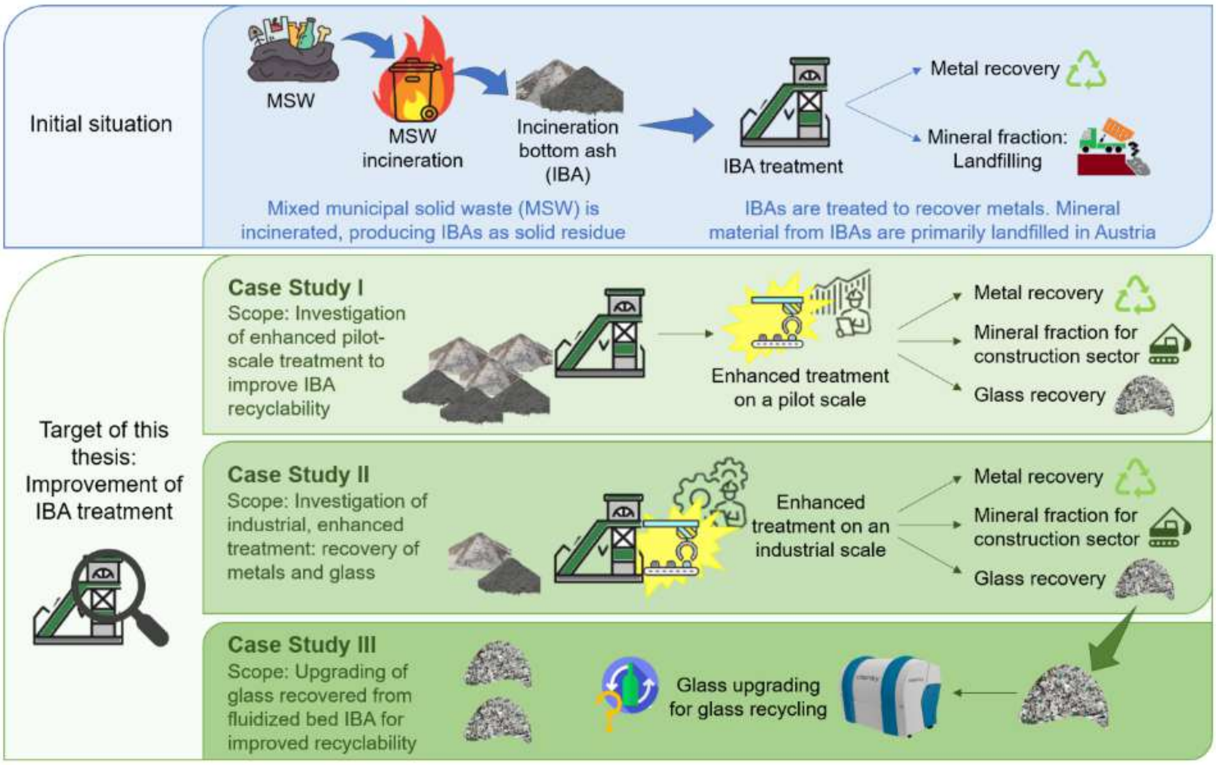

Figure 1: Thesis structure

2 Theoretical Background on Incineration Bottom Ash

IBAs remain as solid residues after fluidized bed and grate incineration, respectively. The incineration technology essentially affects the properties of these ashes, leading to notable differences between FB-IBAs and G-IBAs (Astrup et al., 2016; Blasenbauer et al., 2023; Maldonado-Alameda et al., 2023). Moreover, the composition of the MSW incinerated as well as the discharge process, which can be designed as dry or wet discharge (quenching), influences the IBA properties (Back and Sakanakura, 2022; Costa et al., 2020; Inkaew et al., 2016; Šyc et al., 2018; Yeo et al., 2024). In Austria, solely dry discharge is used for FB-IBAs after fluidized bed combustion, whereas G-IBAs are quenched in a water bath. Not only the characteristics but also the share of ash in relation to the MSW incinerated is influenced significantly by the firing technology (Leckner and Lind, 2020; Vermeulen et al., 2012). The proportions of IBAs and fly ashes from grate incineration and fluidized bed combustion relative to the amount of waste incinerated are depicted in Table 1. More G-IBA remains after grate incineration than FB-IBA after fluidized bed combustion. G-IBAs account for 17-30% of the MSW incinerated, whereas FB-IBAs account for similar shares than fly ashes from fluidized bed combustion, in the range of 8-14% of the MSW fed into combustion (Kellner et al., 2022; Qi et al., 2024).

Table 1: Overview of the shares of solid residues from municipal solid waste incineration in Austria according to Kellner et al. (2022)

	Fluidized bed combustion (FB-IBA)	**Grate incineration (G-IBA)**
Share of incineration bottom ash relative to the waste incinerated	8-14%	17-30%
Share of fly ash relative to the waste incinerated	8-17%	2-5%
Share of incineration bottom ash relative to the total mass of solid residues	38-58%	82-94%

IBA primarily consists of mineral material, such as molten agglomerates, which are formed during incineration, and of refractory, inert material (e.g. building material, glass) (Chimenos et al., 1999; Eusden et al., 1999; Neuwahl et al., 2019; Šyc et al., 2018). Furthermore, IBA contains metals in the range of 5-20% (Šyc et al., 2020). Especially in G-IBA, unburnt material can also occur.

In order to utilize not only the economically valuable metals but also other IBA components according to a circular economy, enhanced IBA treatment is indispensable. IBA treatment has been focused on metal recovery for a long time (Simon and Kalbe, 2023). During the last years, however, processing technologies for IBA have been increasingly expanded and specialized to enable the recycling of further IBA components, as depicted in the following section.

2.1 IBA Treatment

Modern IBA treatment aims not only to recover metals but also to utilize the mineral fraction of IBA (Holm and Simon, 2017; Keulen et al., 2016). For this, several processes and combinations of these are necessary, which are often carried out in multiple stages (Huber, 2020). Fundamental processes for IBA treatment are sieving and magnetic metal separation to recover magnetic ferrous metals (Chen et al., 2023; Dou et al., 2017; Holm and Simon, 2017; Huber, 2020). For the separation of non-magnetic metals (often referred to as non-ferrous, NFe, metals) eddy current separation (ECS) is applied. Crushers are commonly used for particle size reduction but also to liberate metals embedded in a mineral matrix (Chen et al., 2023; Holm and Simon, 2017). By crushing, metals enclosed by molten agglomerates can be made available for subsequent metal recovery (Huber, 2020; van de Wouw et al., 2020). For coarse IBA constituents, manual sorting is still occasionally used.

To generate a mineral fraction suitable for utilization further treatment processes are needed (Saikia et al., 2008; Vateva et al., 2025). Technologies for density separation, such as jigs or hydro cyclones, are frequently used in this context (Holm and Simon, 2017; Huber, 2020). Since soluble salts in the mineral fraction are limited for some recycling paths, water contact is also part of the IBA treatment in many cases (Alderete et al., 2021; Chen et al., 2023; Lam et al., 2010; Sorlini et al., 2017; Tian et al., 2024). This can be realized through wet treatment processes like wet sieving or washing (Abbas et al., 2003; Alam et al., 2017; Bansal et al., 2024; Kalbe and Simon, 2020). Also, outdoor storage of the IBA exposed to weather conditions, which is referred to as aging or weathering, can support washing out soluble salts (Freyssinet et al., 2002; Glauser et al., 2021). Additionally, aging is used to lower the pH value and to carbonate metal oxides in the mineral fraction, which contributes to immobilizing heavy metals (Dhir et al., 2018b; Luo et al., 2019; Xuan et al., 2018).

Novel developments in the IBA treatment include sensor-based sorting, for instance glass removal from IBA using visible light; inductive sorting of stainless steel; or metal sorting using X-ray fluorescence (XRF) (Huber, 2020; Makari, 2014; Pfandl et al., 2020).

2.2 Utilization Options for IBA

To efficiently process IBA, it is crucial to have a detailed understanding of the desired properties and quality requirements for potential applications of the treated material. Depending on the ash component, different utilization paths exist, each with specific material requirements.

2.2.1 Metals

Metals from IBA are typically classified into magnetic and non-magnetic metals. Magnetic metals, often ferrous metals such as steel, can be recovered from the ash at very high rates (>80%) and are suitable for reuse in steel production (Allegrini et al., 2014; Bunge, 2016; Neuwahl et al., 2019). Lower recovery rates are reported for non-magnetic metals (NFe metals), which are usually transferred to metal processors, where they undergo further treatment before being directed into pure metal recycling streams (Allegrini et al., 2014; Bunge, 2016). Whereas recovery of coarse metals is widely implemented and well developed, metals in the fine IBA fractions are more challenging to separate, detrimental to the recycling of the mineral fraction and are therefore subject of several research projects (Biganzoli et al., 2013; Muñiz Sierra et al., 2023; Perrin et al., 2023; Pienkoß et al., 2022; Šyc et al., 2024)

Recovering metals from IBA offers not only economic and environmental benefits but also contributes to national recycling rates for metals, thereby supporting compliance with related regulatory requirements (Lederer and Schuch, 2024; Mehr et al., 2021; van Caneghem et al., 2019a).

2.2.2 Mineral material

In recent years, the utilization of the mineral fraction of IBA has increasingly gained attention in scientific research. Applications in construction are particularly promising due to the oxidic composition of this fraction. The high contents of SiO_2, CaO, and Al_2O_3 resemble the composition of cementitious materials, as well as raw materials used in ceramics and glass production (Dhir et al., 2018b; Yeo et al., 2024). Frequently assessed recycling paths are the utilization as manufactured aggregate in concrete or cement production as well as in road construction (Bawab et al., 2021; Rübner et al., 2008). The actual utilization of the mineral fraction, however, is also strongly influenced by national regulations, since country-specific laws regulate its application (Blasenbauer et al., 2020). These stipulations aim to minimize the release of pollutants contained in the ashes into the environment. In Austria, the mineral fraction was legally regulated only for road construction before 2023. Since the publication of the Federal Waste Management Plan in 2023, its use as an aggregate in concrete production has also been permitted (BMK, 2023). The relevant limit values for utilizing the mineral fraction according to the Federal Waste Management Plan are provided in Table 2.

Table 2: Requirements for the utilization of the incineration bottom ash (IBA) mineral fraction in road construction or as manufactured aggregate in concrete production according to the Austrian Federal Waste Management Plan 2023 (BMK, 2023). DM: dry matter, Fe: ferrous metals, NFe: non-ferrous metals

Parameter	Unit	Limit value for 10-20% addition in concrete	Limit value for ≤10% addition in concrete	Limit value for road construction
Residual metal pieces, Fe > 4mm	% DM	0.5	0.5	1
Residual metal pieces, NFe > 4mm	% DM	0.4	0.4	0.8
Total contents				
Pb	mg/kg TS	500	600	900
Cd	mg/kg TS	3	4	10
Cr	mg/kg TS	400	500	800
Ni	mg/kg TS	200	200	300
TOC	%	1	1	1
Leaching contents				
pH	-	12	12	12
Electrical conductivity	mS/m	to be determined		
Sb	mg/kg TS	0.6	0.6	0.6
As	mg/kg TS	0.5	0.5	0.5
Pb	mg/kg TS	0.5	0.5	0.5
Cr	mg/kg TS	0.5	0.5	0.5
Cu	mg/kg TS	2	2	4
Mo	mg/kg TS	0.8	0.8	1
Ni	mg/kg TS	0.4	0.4	0.4
Chloride	mg/kg TS	2000	2500	3000
Sulfate	mg/kg TS	3000	5000	5000

2.2.3 Glass

Depending on the incineration process and the grade of separate collection in a country, IBA contains different glass shares (Barbato et al., 2024; Blasenbauer et al., 2023; Del Valle-Zermeño et al., 2017; Eusden et al., 1999). For G-IBA, glass contents in the range of 5-30% are usually reported (Šyc et al., 2020; Vateva and Laner, 2020). Blasenbauer et al. (2023) found that IBA from a fluidized bed contains significantly higher glass shares (nearly 50%). This is, inter alia, traced back to glass losses in the grate incineration, which are based on the formation of molten agglomerates (Eusden et al., 1999; Inkaew et al., 2016; Sepúlveda Olea et al., 2024).

Refractory glass can technically be recovered from IBA using sensor-based sorting (Makari, 2014; Šyc et al., 2020). No industrial application of glass recovery from IBA has been reported in the literature hitherto. One reason for this is that research on IBAs predominantly deals with IBAs from grate incineration. To date, there is hardly any scientific evidence or research available regarding the recovery of glass from FB-IBA. Typically, glass remains in the mineral fraction after IBA treatment and is either recycled together with it or disposed of in a landfill.

Nevertheless, waste glass is perfectly suitable for recycling. One of the frequently promoted advantages of this material lies in its endless recyclability without quality loss (Barbato et al., 2024; Larsen et al., 2009). Waste glass cullet can for instance be recycled in the packaging glass industry and thereby contribute to raw material and energy savings (Butler and Hooper, 2019; Scalet et al., 2013). Glass cullet with lower quality, meaning more contamination or higher shares of extraneous material, can potentially also be used in other applications of the construction sector (Blengini et al., 2012; Deschamps et al., 2018). For example, utilization of waste glass in the foam glass industry, the cement or concrete production and in road construction were already investigated (Dhir et al., 2018a; Kazmi et al., 2020; Mohajerani et al., 2017).

3 Material and Methods

3.1 Material: Austrian incineration bottom ashes

For the investigations in the present thesis, six different IBAs from Austrian MSWI plants were used. Three FB-IBAs from a dry discharge of a fluidized bed and three G-IBAs from wet discharge after grate incineration were assessed. The composition of the MSW incinerated in these MSWI plants is given in Table 3.

Table 3: Composition of the municipal solid waste (MSW) incinerated in the plants, where the incineration bottom ashes (IBAs) investigated derive from. Adopted from Mühl et al. (2023)

Incineration plant	**Nomenclature of the incineration bottom ash**	**Composition of the input material into the incineration plant [w.%]**
Fluidized bed combustion A	FB-IBA A	13% pretreated MSW, 50% industrial and commercial waste, 17% sewage sludge, 20% other waste
Fluidized bed combustion B	FB-IBA B	33% mixed MSW, 16% pretreated MSW, 51% industrial and commercial waste, other waste and bulky waste
Fluidized bed combustion C	FB-IBA C	98% pretreated MSW, 1% industrial and commercial waste, 1% sewage sludge
Grate incineration X	G-IBA X	27% mixed MSW, 73% industrial and commercial waste
Grate incineration Y	G-IBA Y	13% pretreated & 40% mixed MSW, 18% industrial and commercial waste, 3% sewage sludge, 24% bulky waste, 2% other waste
Grate incineration Z	G-IBA Z	14% pretreated & 65% mixed MSW, 15% industrial and commercial waste, 2% bulky waste, 3% other waste

The capacities of the MSWI plants examined make up 690,000 t/a in the case of fluidized bed and 670,000 t/a in the case of grate incinerators, according to data from 2024 (Bernhardt et al., 2024). Compared to the total capacity of 990,000 t/a and 1,380,000 t/a of fluidized bed and grate incinerators, respectively, this amounts to 70% and 37% of the Austrian MSWI plant capacity (Kellner et al., 2022). This illustrates the high relevance of the work within this thesis for Austrian waste management (Mühl et al., 2023).

The IBAs provided for the treatment experiments were delivered directly from the MSWI plants in industrial amounts of at least 100 t. The following figures depict FB-IBAs (Figure 2) and G-IBAs (Figure 3) on a pile and in detail exemplarily, which are both freshly delivered and not treated.

Figure 2: Fresh fluidized bed combustion bottom ashes before the industrial bottom ash treatment (pile left, detail right)

Figure 3: Fresh grate incineration bottom ashes before the industrial bottom ash treatment (pile left, detail right)

Industrial IBA treatment was applied to these IBAs to recover metals and to produce mineral material fractions, which were subject to further investigations. For example, glass, which was removed from these IBAs, was examined in the third Case Study.

3.2 Methods

3.2.1 IBA treatment

Industrial-scale IBA treatment

The processing of the IBAs was carried out at the industrial treatment plant of Brantner Österreich GmbH in Hohenruppersdorf, Austria. The plant is highly sophisticated and suitable for treating both G-IBA and FB-IBA. During the experiments conducted as part of this dissertation, the plant was extended and improved. In the following figures, the schemes of the treatment plant before (Figure 4) and after (Figure 5) the extension are given.

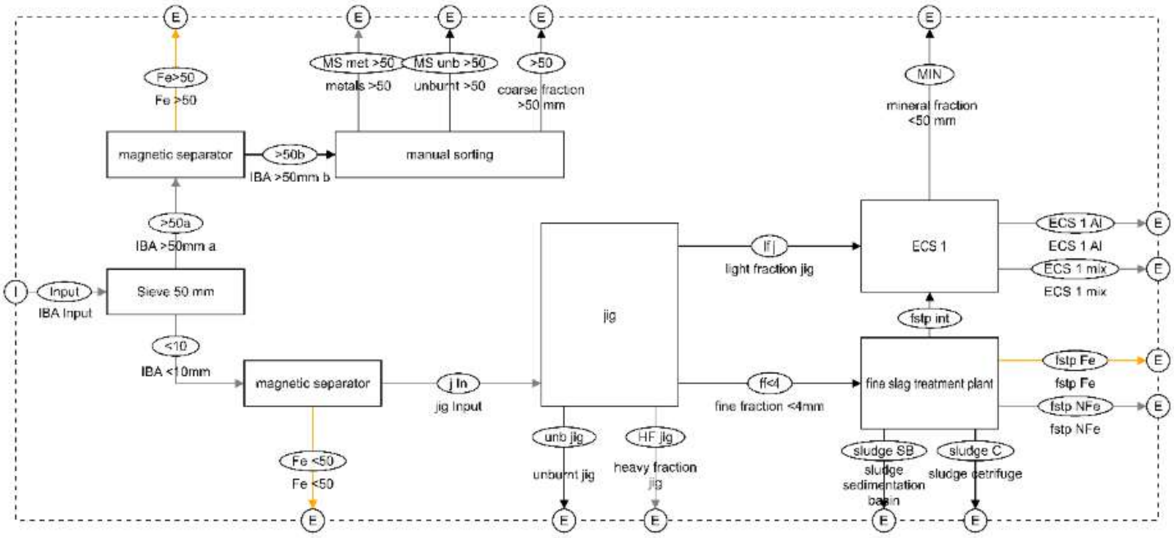

Figure 4: Scheme of the Brantner treatment plant before its extension

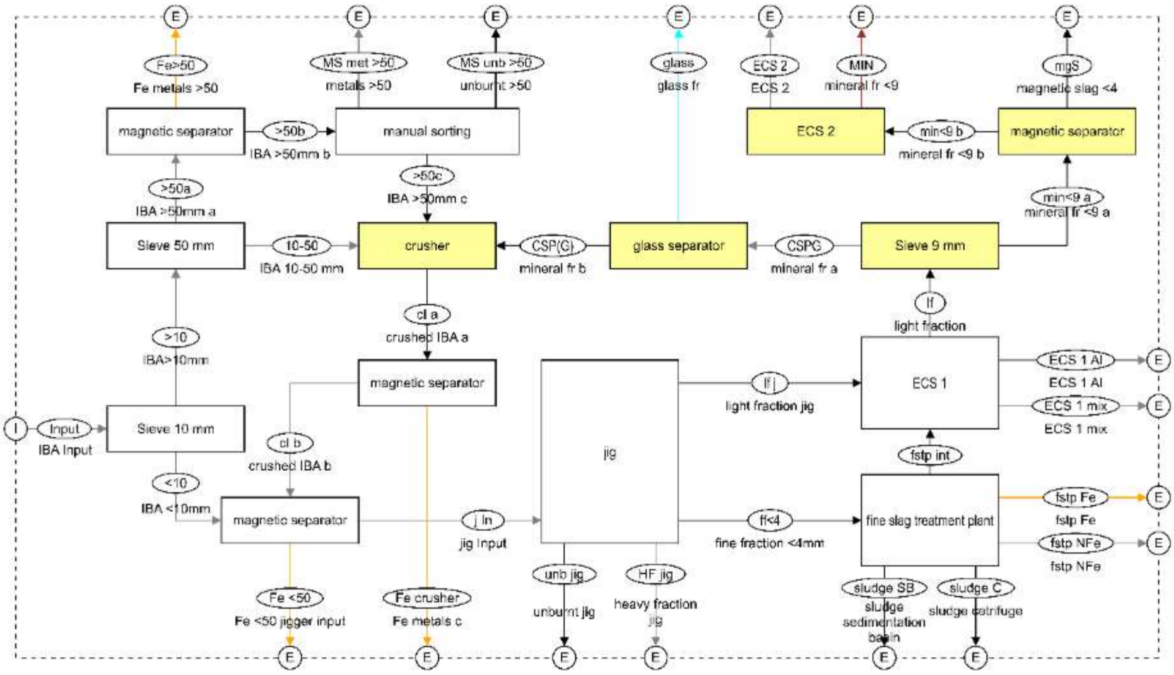

Figure 5: Scheme of the Brantner treatment plant after its extension in 2021 (own illustration, from: Mühl et al. (2024))

The Brantner treatment plant before its extension was used for Case Study I, discussed in the first publication of this thesis. The other two investigations were conducted at the extended plant.

In general, the treatment plant aims to recover as much metal as possible from the IBAs by mechanical treatment steps. Multi-step screening and several metal separation steps via magnetic separators and ECS are the basic components for meeting this target. Additionally, the jig builds the central element of the plant. This device works with a pulsating water bath and can separate the IBA into four different fractions depending on their density and sinking speed. Flowing, unburnt material is removed from the water surface. Fine material <4 mm is sieved at the bottom and led into a fine slag treatment plant, where fine metals are recovered in a separate process. The abundant amount of metals and mineral material is divided into a heavy and a lightweight fraction according to their sinking speed in the water bath. Mineral material is primarily enriched in the lighter fraction, and metals are mainly found in the heavy fraction.

With the incentive to also utilize mineral material from the IBAs, the extension of the treatment plant was implemented in 2021. This included a crusher, a glass separator and further metal separation, according to the work of the first publication. In total, the extended treatment plant produces about 15 output flows.

Pilot-scale IBA treatment

In Case Study I, the potential improvement of the Brantner treatment plant was assessed. This was done by additional pilot-scale treatment of subsets of the industrially treated IBAs. The pilot-scale treatment included sieving with a circular motion vibrating screen (manufacturer *Keestrack*) with 8 and 35 mm meshes. Coarse material >8 mm was crushed with a mobile jaw crusher (manufacturer *Rubble Master HMH GmbH*). Additionally, the sieved material was passed through metal separation using a magnetic separator and subsequently an ECS (both of manufacturer *IFE Aufbereitungstechnik GmbH*). Finally, the particle size fraction 8-35 mm was used for glass separation using a sensor-based sorter by *Binder+Co AG*. The same sensor-based glass separator was also used in the investigations regarding glass purification presented in the publication of Case Study III.

3.2.2 Aging of the mineral fractions

Aging, also referred to as weathering, is a standard method to reduce the leaching contents of the mineral fraction of IBAs, as described in section 2.1. In practice, aging is performed by storing the material outdoors, exposed to the weather conditions and precipitation for about three months (Dhir et al., 2018b; Margallo et al., 2015; Verbinnen et al., 2017).

To ensure comparable samples of aged IBA material in the course of the investigations of this thesis, the aging was conducted on a smaller scale. Therefore, subsets of the mineral fractions were stored in purpose-built aging boxes, which were built from standard Euro-pallets and pallet collars. To allow water to drain, a permeable fleece was used as the inner lining of the box. In the first Case Study, the aging process was controlled, using defined amounts of water in a specific interval of two weeks.

3.2.3 Sampling

IBA is, like many waste streams, a very heterogeneous material. This makes it hard to determine its exact composition and properties. A key factor for the reliable characterization of heterogeneous material is correct sampling (Astrup, 2007; Saqib and Bäckström, 2014; Skutan and Brunner, 2012). The goal of proper sampling is to obtain a representative sample that reflects the properties of the entire material. At the same time, the sample mass should be kept as small as possible to minimize handling and analytical effort (Gy, 2004). Especially in the case of low contents of the analyte, though, small sample masses and correct analysis contradict each other (Morf et al., 2013). Consequently, sampling frequently requires finding a compromise between effort and representativeness (Bunge and Bunge, 1999). To address these challenges, various measures were considered in the present thesis.

Sample extraction

Special attention was paid to ensuring technically correct sampling. Therefore, the principle established by Gy (1992) was applied, which states that all particles should have an equal chance of being included in the sample. Based on this, different sampling techniques were developed and discussed in the literature. For example, the widely spread grab sampling, which is also recommended in technical standards such as the Austrian standard ÖNORM S 2127 (Austrian Standards Institute, 2011), was classified as not suitable for correct sampling by Gerlach and Nocerino (2003). Equally, grid sampling was evaluated as complicated but incorrect by Gy (1992). Both publications, as well as the methods report by Skutan et al. (2018), recommend sampling from the conveyor belt or the falling stream as an alternative. Therefore, this technique was also used in the present investigations of this thesis. Yet, this technique requires considering the plant operation, since, for example, conveyor belts have to be stopped or sampling needs to be done under falling material. In the case of the Brantner treatment plant, most output flows are discharged into containers in a falling stream. In many cases, this falling stream could be used for sampling with purpose-built sampling devices. Examples of these individual sampling devices adapted to the specific output flows can be seen in Figure 6.

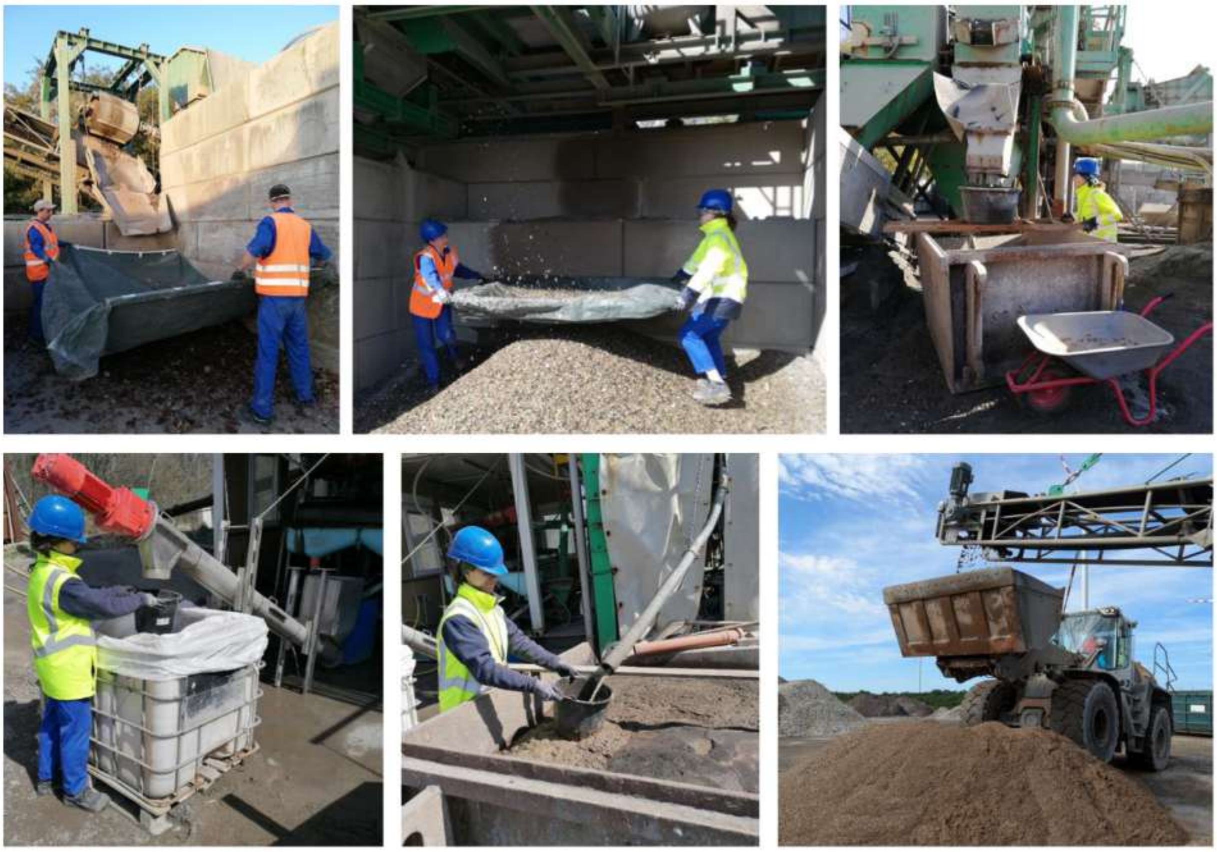

Figure 6: Sampling devices used for sampling at the Brantner treatment plant

Sample masses and number of increments

Besides the sampling technique, also the required sample mass for a representative sample had to be determined in advance. Therefore, the equation developed by Skutan and Brunner (2005), which is based on Bunge and Bunge (1999) and was also applied to IBAs by Huber et al. (2020), can be applied. This calculation of the minimum sample mass is based on the appearance of rare carrier particles, containing a certain mass fraction of analyte. Also, Skutan et al. (2018) recommend minimum sample masses for different IBA fractions depending on their particle size. Both these approaches were used to estimate the required minimum sample masses of the output fractions in the Case Studies. Nevertheless, especially when considering the equation by Skutan and Brunner (2005) based on Bunge and Bunge (1999), enormous sample masses of several tons would have been required as primary sample mass in some cases. As analyses of these amounts would not have been possible due to limited personnel and financial resources, compromises had to be found for several output fractions of the Brantner treatment plant. In some cases, especially regarding manual sorting of the mineral and glass fractions, a more practical approach, using technical standards, was chosen to determine the masses used for analysis. Since the mineral fraction should be analyzed for its use as an aggregate in concrete production, the standard EN 933-11 was chosen for its manual sorting (European Committee for

Standardization, 2009). This standard was also applied to the manual sorting of the glass fractions and to some coarse output fractions.

As heterogeneous material usually exhibits grouping or segregation effects, sampling from a treatment plant should also be spread over time to represent a larger amount of processed material (Gy, 1992). This can be ensured by taking multiple increments and blending them into one sample (Gerlach and Nocerino, 2003). As recommended in the literature, a minimum of 30 increments was defined for the sampling in the present Case Studies. This number was derived from Gerlach and Nocerino (2003) in order to reduce the grouping and segregation error in relation to the fundamental error. While increasing the number of increments could further enhance the representativeness of the sample, the limit of 30 was set to balance improved accuracy with practical considerations of workload (Skutan et al., 2018).

Reduction of sample masses

In many cases the sample mass has to be reduced for the analysis, for example subsequently to particle size reduction of the sample. Various techniques are available for this purpose as well, differing in terms of effort and accuracy. Fractional shoveling was preferably chosen for the work within this thesis, since this was recommended by the authors already cited (Gerlach and Nocerino, 2003; Gy, 1992; Skutan et al., 2018). Even though sample reduction using riffle splitters or sectorial splitters would also be suggested, they could only be used in a few cases, since these splitters have to suit the particle size and sample masses. Coning and quartering were avoided entirely, as this technique does not ensure correct sampling and is insufficiently precise (Gerlach and Nocerino, 2003; Skutan et al., 2018).

3.2.4 Characterization and material analysis

For the IBAs considered in this thesis, different characterization methods were used depending on the target of analysis.

Manual sorting

Since FB-IBAs and G-IBAs obviously differ in composition, the macroscopic constituents >4 mm of many output fractions were determined by manual sorting. Thereby, also the share of recyclable material, such as aluminum, magnetic ferrous metals or glass, could be assessed. Manual sorting was only applied to material >4 mm. Finer particles <4 mm were removed by screening before sorting since the manual separation and visual classification of material <4 mm is very intense and time-consuming. Moreover, the abundant amount of aluminum, magnetic ferrous metals and glass in IBA can be found in coarser particle size fractions >4 mm (Huber et al., 2020; Šyc et al., 2018; Vateva and Laner, 2020). This counts especially for magnetic ferrous metals and glass.

The IBA components were separated by manual sorting into the main categories metals, mineral material (excl. glass), glass and unburnt material with different sub-categories, which are shown in Table 4.

Table 4: Categories of manual sorting in the Case Studies of this thesis

Main category	Case Study I	Case Study II	Case Study III
Metals	Metals	Magnetic metals	Metals
		Aluminum	
		Other metals (e.g. stainless steel, brass, copper, coins)	
Mineral material (excl. glass)	Mineral agglomerates	Mineral material (excl. glass)	Non-glass mineral-based material (CSP, building material (e.g. concrete, brick), molten agglomerates
	Other inert material, i.e. ceramics, stones, porcelain, building material		
Glass	Glass	Glass	Clear (flint) glass
			Green glass
			Amber glass
			Other glass (other colors, molten glass agglomerates, highly tarnished glass)
Unburnt material	Unburnt material	Unburnt material	Unburnt material

Most components could be separated by visual inspection. For classification of the metals in Case Studies I and II, magnetic metals were removed by a magnet. Aluminum was identified among other metals either based on specific products like aluminum cans, trays, or foil, or, especially finer particles, were distinguished by its matte silver-grey color and characteristic softness when filed.

During manual sorting of some, especially coarser, output fractions produced in the experiment assessed in the second Case Study, molten agglomerates, e.g. mineral adhesions on metals, were separated by crushing before the manual sorting. Thereby, metals and mineral material could be distinguished. This was not necessary in the case of the other experiments as smaller particles (mineral fraction <8 mm) or particles with barely any mineral adhesions (glass fractions), respectively, were sorted.

In the third Case Study also lead glass was manually sorted from white glass. This cannot be done only by visual inspection. Therefore, a UV-C lamp with a wavelength of 254 nm (manufacturer *analytikjena*) was used, which causes blue fluorescence in lead glass as shown in Figure 7.

Figure 7: Fluorescence of lead glass on the right side when exposed to UV-C light

Determination of residual metal pieces in the mineral fraction

To utilize the mineral fraction of the IBAs in the construction industry in Austria, residual metal pieces in this fraction are limited to 0.5 % for ferrous metals and 0.4% for non-ferrous metals (BMK, 2023). The determination method of the share of residual metal pieces is specified in BMK (2023) and was used for the investigations of Case Study I. The method is based on crushing all mineral material in the dried mineral fraction. It is assumed that metal pieces are not comminuted by the crusher, but are flattened (Chen et al., 2023). Thereby, flat metal pieces can be sieved off from the crushed mineral material. The process is depicted in Figure 8.

Figure 8: Determination of residual metal pieces, from left to right: mineral fraction <8 mm, crushing of the mineral fraction, sieving of the crushed material, metals after crushing (top) and crushed mineral material (bottom)

Chemical analysis of the mineral fraction

Besides the residual metal pieces, some chemical parameters are also limited in the mineral fraction of IBA if used in the construction sector. These are the total and leaching contents of specific heavy metals, the total content of TOC, the pH value, and leaching contents of chloride and sulfate (BMK, 2023). The analyses have to be conducted following the standard ÖNORM S2127 according to the Austrian landfill ordinance (Austrian Standards Institute, 2011; BMLFUW, 2008). These guidelines require, amongst others, an aqua regia digestion and inductively coupled plasma optical emission spectroscopy (ICP-OES) for the total contents and a liquid-to-solid ratio of 10/1 l/kg for the leaching contents (European Committee for Standardization, 2002a; German Institute for Standardization, 2012, 2003). The chemical analysis of the treated mineral fraction regarding its suitability in concrete production was conducted in Case Study I for the six IBAs considered.

Chemical analysis of the glass fraction

In the third Case Study, which focused on glass in IBAs, the glass fractions were also chemically analyzed. These measurements were especially performed to assess heavy metal contents of Pb, Cd and Hg, which are limited for glass cullet in the packaging glass industry (Bundesverband Glasindustrie e.V. et al., 2014; EC, 2025). Since aqua regia digestion cannot be used to dissolve glass, XRF analysis was used to determine the heavy metal contents in the glass (Schaeffer and Langfeld, 2020; Turner, 2019). The glass samples were crushed and milled to a particle size <500 µm. Subsequently the powder was pressed into pellets, which were used for the measurements with a hand-held XRF analyzer (manufacturer *ThermoScientific*).

Based on packaging regulations of the EU, the packaging glass industry also specifies a threshold for the Cr(VI) content in glass (EC, 2025). Therefore, this parameter was also analyzed in accordance with technical standards (Deutsches Institut für Normung e.V., 2020; European Committee for Standardization, 2002b).

3.2.5 Material flow analysis

Material flow analysis (MFA) as developed by Brunner and Rechberger (2017) was used as a tool to determine and quantify the material flows within the treatment experiments. This was applied to the enhanced treatment steps (Case Study I), the extended Brantner treatment plant (Case Study II) and to the glass upgrading (Case Study III). The materials investigated, referred to as goods, were the IBAs (Case Studies I and II) and the glass fraction from FB-IBA (Case Study III), respectively. Sub-goods denote the constituents of the goods (e.g. aluminum, ferrous metals or glass in IBA; white glass and metals in the glass fraction).

MFA is based on the principle of mass conversation within the system considered. This means that the sum of all masses of input flows equals the sum of all output flow masses and stocks, if applicable (Brunner and Rechberger, 2017). To examine the distribution of a good or sub-good within the system, transfer coefficients *TC* for a good or sub-good *i* into an output flow *j* are calculated as shown in equation 1.

$$TC_{i,j} = \frac{m_{i,j}}{\sum_{j=1}^{n} m_{i,input}} \qquad (1)$$

in which $m_{i,j}$ is the mass of a good or sub-good *i* in an output flow *j* and $\sum_{j=1}^{n} m_{i,input}$ equals the sum of this good or sub-good in the input into the process. The sum of all transfer coefficients equals 1.

The input data for the material flow analyses were determined from the Case Studies. Material flows were weighed, if possible; their water content was assessed and manual sorting was performed to obtain the composition of various output flows. MFA was used to understand the treatment processes, to examine the distribution of single constituents (sub-goods) within these processes and to calculate the composition of the input material. Calculations of the material flows were conducted using the software *STAN*, version 2.6. The system boundaries and targets of the MFAs conducted in each Case Study are summarized in Table 5.

Table 5: Overview of material flow analyses in the Case Studies of this thesis

Case Study	System boundary	Input data obtained from the experiments	Calculated material flows by MFA
Case Study I	Enhanced IBA treatment on a pilot-scale	Masses of output flows of the enhanced treatment	Input masses, unknown output masses and mass flows between processes
Case Study II	Industrial IBA treatment plant (Brantner extended)	Masses of input and output flows (excl. mineral fraction), results from manual sorting of all output flows, water contents of all flows	Mass of mineral fraction produced; composition of IBA input into the treatment plant, distribution of aluminum, magnetic ferrous metals and glass into output flows, MFA on a dry matter basis
Case Study III	Upgrading steps for glass fraction	Masses of output flows of glass purification, results from manual sorting	Input composition of glass fractions before purification; composition of glass fractions after second and third purification

4 Results

In the following section the major findings of the Case Studies performed are summarized. The detailed results can be found in the corresponding publications, which are given in the Appendix.

4.1 Results of Case Study I

In Case Study I enhanced IBA treatment was investigated using six different IBAs with the aim to improve metal recovery, to produce manufactured aggregate suitable for recycling and to examine glass recovery from IBA (Mühl et al., 2023).

The improvement of the treatment was assessed by the total contents of heavy metals in the mineral fraction and the content of residual metal pieces. Compared to the literature, contents of Cd, Cr, Pb and Ni were lower than in previous works by Allegrini et al. (2014), Glauser et al. (2021), Huber (2020) or Kalbe and Simon (2020), which proves the success of the additional treatment. Residual metal pieces made up 0.00% (FB-IBAs) and up to 0.03% (G-IBAs) in the case of magnetic ferrous metals >4 mm and up to 0.1% and 0.2% for non-ferrous metals >4 mm in FB-IBAs and G-IBAs, respectively. These values are well below the limit value for concrete production stipulated by BMK (2023), accounting for 0.5% and 0.4% for magnetic ferrous and non-ferrous metals. For concrete production, also further parameters have to comply with limit values, which are set for up to 10% and up to 20% of manufactured aggregate addition in the concrete. In the case of FB-IBA, these total and leaching contents required were all met for up to 10% addition of manufactured aggregate. Only sulfate in one FB-IBA exceeded the threshold for 20% addition, the other two FB-IBAs would be suitable. Single exceedances of the 20% thresholds were found in all G-IBAs and only one G-IBA would be permitted for a 10% addition in concrete. These results indicate that the enhanced treatment was successful to a certain extent, but some potential of improvement is left. For example, the contents of soluble salts were lower in comparable studies which applied washing of the mineral fraction to reduce the content of chloride and sulfate (Keulen et al., 2016; Sorlini et al., 2017).

The findings of Case Study I also show that differences between FB-IBAs and G-IBAs occur, which has also been described by Blasenbauer et al. (2023). Manual sorting of the mineral fractions also revealed that mineral agglomerates 4-8 mm, mainly containing molten agglomerates, constitute a high share of the mineral fraction of G-IBAs but do barely occur in FB-IBAs. Contrary to that, the mineral fraction 4-8 mm of FB-IBAs primarily contains inert material (including glass). This can be traced back to the quenching process or to melting of glass and other inert material during grate incineration (Bayuseno and Schmahl, 2010; Eusden et al., 1999; Inkaew et al., 2016).

A lower amount of glass in G-IBA was also observed in the glass separation assessed in Case Study I. Therein it was found that the glass recovery potential of G-IBAs is significantly lower than in FB-IBAs. By enhanced treatment of FB-IBAs 23-49% of the mineral material 8-35 mm were recovered as glass fraction, whereas in the case of G-IBAs only 2-5% of the mineral material 8-35 mm were separated as glass fraction. Besides the melting and quenching reactions mentioned above, also coatings and adhesions on glass in the G-IBA potentially inhibit its recovery by means of sensor based sorting (Makari, 2014). Yet, this Case Study showed that glass recovery from IBAs is technically feasible, especially for FB-IBAs, which has not been investigated before. Due to the higher glass amount in a better quality, the glass fractions obtained from FB-IBA treatment were examined more closely. These three glass fractions were mainly (71-76%) of a particle size 8-16 mm. Besides glass, the glass fractions also contained extraneous material like mineral-based non-glass material or metals in the range of 2-14%. As the packaging glass industry requires extremely low contents of extraneous material in the range of up to 20 g/t for utilization in the melt furnace (Bundesverband Glasindustrie e.V. et al., 2014), additional upgrading of the glass fractions is definitely necessary.

Concluding, this comparative assessment of enhanced IBA treatment applied to different IBA types indicated that the varying properties of FB-IBAs and G-IBAs also affect their treatment and recycling potential. Glass can technically be recovered from IBAs, but seems far more feasible for FB-IBAs regarding the amount and quality of the glass. Furthermore, enhanced treated IBAs are potentially able to meet the environmental thresholds stipulated by BMK (2023) for utilization as manufactured aggregate. It remained open after Case Study I if the manufactured aggregate can be used from a technical perspective. Moreover, the upscaling to an industrial scale of the enhanced treatment and the upgrading of the glass fraction need further investigation.

4.2 Results of Case Study II

After Case Study I, the Brantner IBA treatment was extended according to the investigations made in Case Study I. Therefore, the aim of Case Study II was to assess the upscaled, industrial IBA treatment with one FB-IBA and one G-IBA (Mühl et al., 2024). The plant's function was examined in detail, considering all output flows. Special focus was given to the IBA constituents aluminum, magnetic ferrous metals and glass, all >4 mm, during the treatment. This Case Study is one of few that inspected an industrial IBA treatment plant in detail during regular plant operation. The whole experiment is described in Mühl et al. (2024), which constitutes the second publication of this thesis.

Regarding the output flows of the treatment process it could be shown that the mineral fraction makes up 68% of the G-IBA treated and 34% of the FB-IBA. Only the glass fraction produced from FB-IBA treatment makes up a higher amount, accounting for 35% of the FB-IBA input. The study also revealed that only 5% and 11% of FB-IBA and G-IBA, respectively, are disposed of directly after the treatment. Material in the other output fractions can potentially be recovered by additional upgrading steps or utilized as manufactured aggregate produced from the mineral fraction.

The packaging metals aluminum and magnetic ferrous metals were investigated more closely in Case Study II. The total amount of these metals in the FB-IBA amounts to 7.0% and 6.9% of aluminum and magnetic ferrous metals, respectively. The G-IBA contained 2.9% of aluminum and 3.8% of magnetic ferrous metals, which is clearly less than in the FB-IBA. This tendency can also be seen in earlier results by Blasenbauer et al. (2023) and Huber et al. (2020). Not only the input into the MSWI but also the incineration conditions affect the production of molten agglomerates and fly ash in fluidized bed and grate incineration, which can cause the difference in metal amounts (Blasenbauer et al., 2023; Saqib and Bäckström, 2014).

Through IBA treatment aluminum and magnetic ferrous metals were distributed into various output flows of the treatment plant. These metals can still be recovered and recycled from specific output flows, but are disposed of in others. The Brantner treatment plant is able to enrich more that 95% of aluminum and magnetic ferrous metals >4 mm from FB-IBA and G-IBA in output flows, where metals can potentially be recovered after further upgrading. Especially in the case of non-ferrous metals this is an extraordinary potential recovery rate, since comparable rates reported in the literature do only rarely surpass 90% (Allegrini et al., 2014; Bunge, 2016; Neuwahl et al., 2019).

The content and recovery of glass >4 mm was also examined in Case Study II. One of the most important aspects regarding glass was the fact that sensor-based glass sorting cannot be applied to IBA from grate incineration at the Brantner treatment plant. This can be traced back to low amounts of glass, surface coatings on the glass cullets and extraneous material in the IBA that reduce the feasibility of glass recovery from G-IBA (Mühl et al., 2023). In the G-IBA a glass content of only 7% was calculated from the material flow analysis, whereas the FB-IBA contained 42% and therefore six times more glass. In the case of FB-IBA, the Brantner treatment plant is designed to remove glass >9 mm into a glass fraction. During the experiment 72% of the total glass >4 mm could be enriched in this glass fraction, which amounts to 300 kg per one ton of FB-IBA treated. However, the glass fraction produced on an industrial scale contained 14% of extraneous material, whereas the glass fraction of the same FB-IBA only contained 2% of extraneous material when treated on a pilot scale in Case Study I (Mühl et al., 2023). Both values do not comply with the limit values of the packaging glass industry. It can be concluded from this that pilot-scale glass removal from IBAs works better than on an industrial scale. Upscaling inhibited glass recovery from G-IBA and reduced the glass quality recovered from FB-IBA. Yet, glass extraction from FB-IBA was industrially successful, enabling large amounts of the FB-IBA to be recovered as potentially recyclable glass.

In summary, this Case Study showed that industrial, enhanced treatment of IBAs is able to improve the recovery of aluminum and magnetic ferrous metals. These metals can be industrially recovered to a very high extent. Furthermore, glass recovery could be upscaled in the case of FB-IBA. With the exception of glass recovery from G-IBA, this Case Study confirmed that enhanced IBA treatment developed in Case Study I can also be applied industrially and thereby enhance the recyclability of IBAs.

4.3 Results of Case Study III

Case Study III of this thesis focused on characterization and upgrading of the glass fractions recovered from FB-IBA through industrial IBA treatment (Mühl et al., 2025).

To enable a recycling path for the glass fraction produced from IBA treatment, Case Study III investigated the upgrading of two FB-IBA glass fractions produced by industrial-scale treatment. Different upgrading setups were assessed, using four-step upgrading and single-step upgrading of the glass 8-16 mm after sieving. In both cases, the share of extraneous material in the IBAs could be reduced, improving the glass quality. Especially the four-step upgrading could produce a very pure glass fraction with extraneous material below 0.1%. The other glass fractions after single-step upgrading of sieved or unsieved glass contained 1.2-2.2% of extraneous material, which is also a clear decrease compared to 9% and 13%, respectively, of extraneous material in the glass fractions before upgrading.

Manual sorting of the fractions showed that the glass in FB-IBA is primarily clear glass, followed by green and smaller amounts of amber glass. The abundant amount of extraneous material found was non-glass mineral-based material, whereas metals occurred subordinately.

The two glass fractions used for the upgrading process contained 85-89% of glass. During upgrading some glass is incorrectly separated into the extraneous material fractions and therefore lost. In the case of four-step upgrading this accounted for 34% and 17% of glass in the two FB-IBAs investigated. Previous sieving of the glass fraction before the upgrading of the glass fraction 8-16 mm led to higher glass losses, since glass is also removed with the sieved material <8 mm and > 16 mm. In the upgrading setup including sieving, 49% (FB-IBA B) and 36% (FB-IBA C) were lost into extraneous material fractions and sieved fractions. From this result it can be concluded that sieving of the glass fraction before upgrading causes high glass losses and is therefore not recommended, if glass is not recovered from the sieved fractions <8 mm and >16 mm as well. Yet, the upgrading process in general can be seen as indispensable for further glass recycling options as it enables a clear reduction of extraneous material. Nevertheless, the compliance with the strict quality requirements of the packaging glass industry could not be ensured. Whereas humidity and organic material of glass from FB-IBA do not impede this recycling path, other limit values concerning the content of extraneous material were clearly exceeded by glass fractions recovered from FB-IBA. It was not feasible to generate valid results in the range of few grams per ton by manual sorting. Since it was also reported for separately collected and upgraded waste glass that these limit values were exceeded, the applicability of these limit values needs to be discussed with potential glass recyclers (Aldrian et al., 2018).

The XRF analysis of the heavy metals in the output fractions showed that particularly Pb is a relevant parameter for the limit value set by the packaging glass industry for Cd, Hg, Pb and Cr(VI). Cd, Hg and Cr(VI) were determined to be below the limit of detection in the glass fractions. Pb contents, on the contrary, were in the range of 110-260 mg/kg in the glass fractions intended for recycling. The threshold of 200 mg/kg could only be met by three of the six glass fractions after upgrading. Glass produced by four-step upgrading showed the lowest and therefore most promising Pb contents (110 and 140 mg/kg). The XRF analysis of the different fractions also showed that upgrading is suitable for Pb depletion in the glass fractions. All other fractions, sieved fractions and extraneous material fractions, contained significantly higher Pb contents than the glass fractions after upgrading.

Another observation made in Case Study III are the differences occurring between the glass fractions of the two FB-IBAs B and C. Lower shares of extraneous material and better upgrading results were determined for FB-IBA C. This presumably derives from the lower incineration temperature in the respective MSWI plant, resulting in fewer melt reactions and surface contamination than in FB-IBA B (Jones et al., 2013). Therefore, the combustion conditions influence the glass recovery and upgrading success.

Concluding, Case Study III showed that glass recovered from FB-IBAs can be upgraded by sensor-based sorting, producing a cleaner glass fraction potentially suitable for recycling. Especially by four-step upgrading very low shares of extraneous material and heavy metals could be ensured. However, utilization in the packaging glass industry presumably needs further improvement and the cooperation of potential recyclers. Additionally, other recycling paths and their requirements should be investigated more closely, for example utilization in the foam glass industry (Blengini et al., 2012).

5 Summary and Conclusions

In the scope of this thesis three Case Studies examined enhanced treatment of different IBAs in order to improve their recyclability. Summarizing the main findings, it can be stated that potential for improvement of IBA recyclability was successfully investigated within this research work. In this section concise answers to the research questions are given followed by concluding considerations.

5.1 Answers to the Research Questions

- Does enhanced IBA treatment increase the utilization potential and the circularity of the IBAs?

The enhanced IBA treatment steps assessed in this thesis, including additional metal separation and glass recovery, present an opportunity to recycle both mineral material and glass. Moreover, examinations of Case Study II on an industrial scale were successful in recovering the valuable packaging metals aluminum and magnetic ferrous metals from a G-IBA and a FB-IBA almost completely. It was also proven in pilot-scale and subsequent industrial-scale experiments that metal pieces can be removed from the mineral fraction to a very high extent, which is a condition for utilization of the mineral fraction in the construction sector. The pilot-scale experiment of Case Study I showed that the mineral fraction meets most of the environmental limit values of BMK (2023) after enhanced treatment, especially in the case of the FB-IBA. With further adaptions of the treatment, the enhanced treatment seems to be a promising path to allow for the recycling of the mineral fraction as manufactured aggregate. This would significantly strengthen the circularity of MSWI since the mineral fraction accounts for a predominant output flow of IBA, as shown in Case Study II. The limit values for heavy metals could most likely not be met without additional metal separation.

Glass removal in course of the enhanced treatment offers an opportunity to increase the IBAs' recyclability as well. The potential of glass recovery from FB-IBA was verified in all Case Studies conducted. Since it was demonstrated in Case Study II that glass constitutes the major material in FB-IBAs, its recovery and recycling would clearly improve the circularity of waste incineration. Without the enhanced treatment steps assessed, no glass could be recovered from FB-IBA.

The utilization potential of IBAs is significantly increased by the enhanced treatment steps investigated in this dissertation.

- Which differences occur in the treatment of G-IBAs and FB-IBAs?

An issue that could be observed in all Case Studies are differences between FB-IBAs and G-IBAs. This was also reported in previous studies but was emphasized in this thesis (Blasenbauer et al., 2023). These differences are not only visible (cf. Figure 2 and Figure 3), but can also be designated by characterization and analysis. Manual sorting of mineral fractions produced by enhanced IBA treatment in Case Study I revealed that G-IBAs contain more mineral agglomerates 4-8 mm, which are melt products that barely occur in FB-IBA. This is traced back to the wet IBA discharge and higher temperatures in grate incineration (Bayuseno and Schmahl, 2010; Blasenbauer et al., 2023; Eusden et al., 1999). All three Case Studies determined significantly more refractory glass in the case of FB-IBA and the possibility to recover glass only from this IBA type in relevant amounts and high quality. Additionally, FB-IBAs show lower heavy metal contents in the mineral fraction, which is advantageous regarding its recycling options in the construction sector (Mühl et al., 2023). In G-IBAs more metals are embedded in mineral coatings, often in mineral agglomerates, which inhibits their recovery. Furthermore, metals recovered from G-IBA exhibit more mineral adhesions, which reduce their scrap quality (Haupt et al., 2017). This downside of G-IBA compared to FB-IBA was also shown for steel scrap in previous studies (López-Delgado et al., 2003; Tayibi et al., 2007). The differences in the composition of G-IBAs and FB-IBAs also influence the treatment process. Different shares of output flows were produced in Case Study I and II, with major differences in the amounts of glass and mineral fraction. Less unburnt material occurs in FB-IBAs.

Concluding, FB-IBA show advantages compared to G-IBA in several aspects. Glass can be recovered, metals do not have to be liberated by energy-intense crushing and the mineral fraction shows lower heavy metal contents. This makes fluidized bed combustion preferable to grate incineration when it comes to recycling of the IBA. This information is a crucial aspect for a holistic comparison of these two incineration MSWI technologies.

- Is enhanced IBA treatment on an industrial scale feasible?

In 2021, the Brantner treatment plant in Austria was extended according to examinations of Case Study I. The plant is in regular operation since then and can produce potentially recyclable mineral and glass fractions, proving the feasibility of industrial-scale enhanced IBA treatment. Investigations of Case Study II also confirmed the function and success of the industrial treatment by showing large glass amounts recovered from FB-IBAs, high potential recovery rates for the metals aluminum and magnetic ferrous metals and very low contents of residual metal pieces in the mineral fractions of both IBAs (Mühl et al., 2024).

- Which shares of the packaging materials aluminum, magnetic ferrous metals and glass can be industrially recovered by means of enhanced IBA treatment?

Results of Case Study II show that the packaging metals aluminum and magnetic ferrous metals could be enriched in potentially recyclable fractions to more than 95% through enhanced industrial IBA treatment (Mühl et al., 2024). In the case of glass, no glass fraction could be industrially produced by G-IBA treatment, but 72% of the glass >4 mm contained in FB-IBA could be recovered in the glass fraction. It has to be considered that further upgrading of the recovered materials is necessary for some of the potentially recyclable fractions. For example, the high-density fraction from the jig needs further treatment to separate metals from other material like glass and mineral material and to distinguish different metals (e.g. stainless steel, copper, magnetic ferrous metals). These additional upgrading steps might lead to material losses which reduces the practical recycling rates. Nevertheless, the recovery results of the treatment plant investigated can be seen as very progressive, since the potential recovery rates achieved lie above comparable recovery rates reported in the literature.

- Which properties do the glass fractions recovered from IBAs exhibit?

Glass from IBAs was examined in all Case Studies of this thesis. However, the first Case Study exhibited that glass from G-IBA can only be recovered in small amounts and bad quality, meaning high shares of extraneous material. In addition, industrial implementation of the glass sorter at the Brantner treatment plant showed that glass recovery from G-IBA is not feasible yet. The low amounts of glass in G-IBA can be traced back to three factors. First, parts of the glass in grate MSWI melts and merges with other IBA constituents. Thereby, glass loses its transparency and cannot be detected by the sensor-based sorter anymore. The same effect arises from higher surface contamination occurring in the G-IBA. As a third aspect, grate incineration produces more IBA than fluidized bed combustion and therefore the same amount of glass incinerated leads to a lower share of glass in G-IBA compared to FB-IBA. These disadvantages of glass in G-IBA led to the decision to focus only on glass from FB-IBA in this thesis.

Regarding glass fractions recovered from FB-IBAs, certain amounts of extraneous material remain in these fractions due to imperfections that occur in each industrial mechanical sorting step, including sensor-based sorting. The glass content of these glass fractions was in the range of 86%-98% in all cases. Industrial glass recovery, assessed in Case Study II and III, showed tendentially lower glass shares of 86-88%.

Case Study I and III showed that the particle size fraction 8-16 mm exhibits the highest glass share. Manual sorting performed in Case Study III revealed that clear glass is the most frequent glass color, followed by green glass. These results are valid for the glass fractions directly recovered from FB-IBA but also for fractions after upgrading, investigated in Case Study III.

The most important result deduced from XRF analysis conducted in Case Study III is the content of Pb, which accounts for 520 mg/kg (FB-IBA B) and 430 mg/kg (FB-IBA C) in glass fractions prior to upgrading. Further treatment including lead glass separation can reduce the Pb content to 110-270 mg/kg.

- Is the recycling of glass from IBAs possible in the packaging glass industry? If not, what needs to be done to enable glass recycling?

The results of this thesis show that only glass from FB-IBA can potentially be recycled in the packaging glass industry. However, strict quality requirements have to be met for recycling in the packaging glass sector. The limit values concerning the content of extraneous material were clearly exceeded by glass fractions recovered from FB-IBA. Case Study III also showed that the Pb contents before upgrading surpass the recycling requirements. Direct recycling of glass recovered from FB-IBA is therefore not possible. Thus, both Case Study I and II recommended further upgrading steps to remove extraneous material and to purify the glass fractions. The upgrading investigated in Case Study III showed that the quality of the glass fractions can be significantly improved. Yet, the strict limit values for extraneous material, which are below 0.005% for CSP and metals, could not be achieved in the upgraded glass fractions. The necessity of these regulations should be discussed with potential recyclers. Furthermore, additional recycling paths for the glass fractions need to be investigated in the future, for example foam glass production. Additionally, the requirements can potentially be obtained by improved and adapted glass upgrading as this first experiment reported in Case Study III already achieved relatively clean glass fractions from FB-IBA.

5.2 Final Considerations

This thesis investigates enhanced treatment of Austrian IBAs from grate incineration and fluidized bed combustion of MSW. The scientific monitoring of the development process of IBA treatment in Austria significantly contributes to this research field as it shows the potential of improved processing of IBA regarding a more circular economy. The experiments of this thesis were not only conducted for IBAs from two different incineration technologies, but were also applied at industrial scale, which increases its practical significance. The practical applicability is also confirmed by the fact that the plant extension examined in Case Study I was implemented at the industrial treatment plant. Furthermore, glass recovery from FB-IBA is applied at several treatment plants in Austria by now and the CE marking was recently granted for the mineral fraction produced at the Brantner treatment plant (City of Vienna, 2025).

One of the key contributions of this thesis is its detailed investigation of glass recovery from different IBA types. Especially glass recovery from fluidized bed IBA has not been reported in the scientific literature before, neither have the characteristics of the glass fractions. This can be traced back to the circumstance that fluidized bed combustion is a subordinate MSWI technology. From the results of this thesis, however, it becomes clear that fluidized bed combustion has considerable advantages compared to grate incineration when it comes to recycling of IBA. In an emerging circular economy, the necessary pretreatment of MSW before fluidized bed combustion can also be beneficial since valuable material can be recovered from residual waste before incineration. This could be crucial for meeting recycling targets of the EU, especially in countries where separate collection rates are comparatively low. Considering this, a holistic comparison of fluidized bed combustion and grate incineration should be conducted in the future. Besides using the data regarding IBA recycling published in this thesis, also the waste pretreatment prior to fluidized bed combustion has to be included in this comparison. Furthermore, fly ash production needs to be evaluated since clearly higher amounts of fly ash are produced in fluidized bed combustion which need a disposal or recovery solution as well.

Even though glass recovery from G-IBA was reported to be not feasible in the present thesis, this aspect should not be disregarded in the future. As technology evolves and demand for recycled glass potentially increases, further research into optimized recovery methods remains essential. Further research should also consider glass recovery from dry discharge of grate IBA.

Nonetheless, several challenges and critical aspects of the thesis must be considered. For example, research on MSWI ashes – and waste in general – poses difficulties due to the heterogeneity and thus large sample quantities required for representative analyses. Ensuring representativeness is challenging, and the uncertainty associated with single-trial experiments needs to be addressed further. To mitigate this, investigations should be conducted regularly to establish comparative data and minimize seasonal and regional fluctuations. This thesis presents a first dataset as a basis concerning glass recovery and enhanced industrial IBA treatment in Austria.

Regarding glass recovery, while it presents opportunities, it must also be critically evaluated. Ideally, deposit-refund systems and improved separate collection methods would be more effective for recycling glass and other materials from MSW (Simon et al., 2016). Promoting high recovery effort of material from mixed MSW pretreatment and from IBA could influence consumers' participation in separate waste collection. If the public becomes aware that materials are being recovered from mixed MSW, motivation for proper waste separation might decline. Additionally, specific non-packaging glass types, like lead glass or heat resistant glass, are targeted to be disposed of in mixed MSW, as they are not suitable for packaging glass recycling. Glass recovery from IBA, however, might also recover parts of these unwanted glass types and deliver it to the packaging glass industry. Another potential hurdle for glass recovery from IBA is that the EU recycling target for glass in 2030 was already achieved in 2022. This might limit the incentive to increase glass recycling and to develop new recovery paths for glass.

Finally, while this thesis emphasizes the importance of material recovery from IBAs, it should not be overseen that waste reduction should actually have a higher priority in waste management. In the context of the circular economy, waste avoidance often receives less attention due to economic interests, yet it represents the most sustainable approach. Future research and policy efforts should balance material recovery with initiatives aimed at reducing overall waste generation.

6 References

Abbas, Z., Moghaddam, A.P., Steenari, B.-M., 2003. Release of salts from municipal solid waste combustion residues. Waste Management 23, 291–305. https://doi.org/10.1016/S0956-053X(02)00154-X.

Alam, Q., Florea, M.V.A., Schollbach, K., Brouwers, H.J.H., 2017. A two-stage treatment for Municipal Solid Waste Incineration (MSWI) bottom ash to remove agglomerated fine particles and leachable contaminants. Waste management (New York, N.Y.) 67, 181–192. https://doi.org/10.1016/j.wasman.2017.05.029.

Alderete, N.M., Joseph, A.M., van den Heede, P., Matthys, S., Belie, N. de, 2021. Effective and sustainable use of municipal solid waste incineration bottom ash in concrete regarding strength and durability. Resources, Conservation and Recycling 167, 105356. https://doi.org/10.1016/j.resconrec.2020.105356.

Aldrian, A., Pomberger, R., Schipfer, C., Gattermayer, K., 2018. Altglasrecycling - Anteil an Störstoffen im Altglas in Österreich [Waste glass recycling - share of impurities in waste glass in Austria]. [Waste glass recycling - share of impurities in waste glass in Austria], in: POSTER-Konferenzband zur 14. Recy & DepoTech-Konferenz. Recy & DepoTech, Leoben. 07.-09.11.2018. Abfallverwertungstechnik & Abfallwirtschaft Eigenverlag, pp. 193–198.

Allegrini, E., Maresca, A., Olsson, M.E., Holtze, M.S., Boldrin, A., Astrup, T.F., 2014. Quantification of the resource recovery potential of municipal solid waste incineration bottom ashes. Waste management (New York, N.Y.) 34, 1627–1636. https://doi.org/10.1016/j.wasman.2014.05.003.

Astrup, T., 2007. Pretreatment and utilization of waste incineration bottom ashes: Danish experiences. Waste Management 27, 1452–1457. https://doi.org/10.1016/j.wasman.2007.03.017.

Astrup, T., Muntoni, A., Polettini, A., Pomi, R., van Gerven, T., van Zomeren, A., 2016. Treatment and Reuse of Incineration Bottom Ash, in: Environmental Materials and Waste. Elsevier, pp. 607–645.

Austrian Standards Institute, 2011. Grundlegende Charakterisierung von Abfallhaufen oder von festen Abfällen aus Behältnissen und Transportfahrzeugen [Basic characterization of waste heaps or from solid waste from containers and transport vehicles]. Wien 13.030.01.

Back, S., Sakanakura, H., 2022. Comparison of the efficiency of metal recovery from wet- and dry-discharged municipal solid waste incineration bottom ash by air table sorting and milling. Waste management (New York, N.Y.) 154, 113–125. https://doi.org/10.1016/j.wasman.2022.08.023.

Bansal, D., Gupta, G., Ramana, G.V., Datta, M., 2024. Optimizing MSW incineration bottom ash reuse: A study on treated wastewater washing and leaching control. Waste management (New York, N.Y.) 182, 164–174. https://doi.org/10.1016/j.wasman.2024.04.035.

Barbato, P.M., Olsson, E., Rigamonti, L., 2024. Quality degradation in glass recycling: substitutability model proposal. Waste management (New York, N.Y.) 182, 124–131. https://doi.org/10.1016/j.wasman.2024.04.027.

Bawab, J., Khatib, J., Kenai, S., Sonebi, M., 2021. A Review on Cementitious Materials Including Municipal Solid Waste Incineration Bottom Ash (MSWI-BA) as Aggregates. Buildings 11, 179. https://doi.org/10.3390/buildings11050179.

Bayuseno, A.P., Schmahl, W.W., 2010. Understanding the chemical and mineralogical properties of the inorganic portion of MSWI bottom ash. Waste management (New York, N.Y.) 30, 1509–1520. https://doi.org/10.1016/j.wasman.2010.03.010.

Bernhardt, A., Brandstätter, C., Broneder, C., Gold, C., Neubauer, C., Oliva, J., Roll, M., Schaffernak, A., Stoifl, B., Tesar, M., Wankmüller-Tista, M., Walter, B., Weißenbach, T., 2024. Die Bestandsaufnahme der Abfallwirtschaft in Österreich, Statusbericht 2024. Bundesministerium für Klimaschutz, Umwelt, Energie, Mobilität, Innovation und Technologie, Wien, 274 pp. https://www.bmk.gv.at/dam/jcr:7119f610-1180-4337-8837-f5c45e73b4b5/BAWP_Statusbericht_2024.pdf (accessed 4 June 2024).

Biganzoli, L., Ilyas, A., van Praagh, M., Persson, K.M., Grosso, M., 2013. Aluminium recovery vs. hydrogen production as resource recovery options for fine MSWI bottom ash fraction. Waste management (New York, N.Y.) 33, 1174–1181. https://doi.org/10.1016/j.wasman.2013.01.037.

Blasenbauer, D., Huber, F., Lederer, J., Quina, M.J., Blanc-Biscarat, D., Bogush, A., Bontempi, E., Blondeau, J., Chimenos, J.M., Dahlbo, H., Fagerqvist, J., Giro-Paloma, J., Hjelmar, O., Hyks, J., Keaney, J., Lupsea-Toader, M., O'Caollai, C.J., Orupõld, K., Pająk, T., Simon, F.-G., Svecova, L., Šyc, M., Ulvang, R., Vaajasaari, K., van Caneghem, J., van Zomeren, A., Vasarevičius, S., Wégner, K., Fellner, J., 2020. Legal situation and current practice of waste incineration bottom ash utilisation in Europe. Waste management (New York, N.Y.) 102, 868–883. https://doi.org/10.1016/j.wasman.2019.11.031.

Blasenbauer, D., Huber, F., Mühl, J., Fellner, J., Lederer, J., 2023. Comparing the quantity and quality of glass, metals, and minerals present in waste incineration bottom ashes from a fluidized bed and a grate incinerator. Waste management (New York, N.Y.) 161, 142–155. https://doi.org/10.1016/j.wasman.2023.02.021.

Blengini, G.A., Busto, M., Fantoni, M., Fino, D., 2012. Eco-efficient waste glass recycling: Integrated waste management and green product development through LCA. Waste management (New York, N.Y.) 32, 1000–1008. https://doi.org/10.1016/j.wasman.2011.10.018.

BMK, 2023. Bundes-Abfallwirtschaftsplan 2023, Teil 1 [Austrian Federal Waste Management Plan 2023]. Bundesministerium für Klimaschutz, Umwelt, Energie, Mobilität, Innovation und Technologie, Wien, 490 pp.

BMLFUW, 2008. Verordnung des Bundesministers für Land- und Forstwirtschaft, Umwelt und Wasserwirtschaft über Deponien: Bundesministerium für Land- und Forstwirtschaft, Umwelt und Wasserwirtschaft [Austrian landfill ordinance].

BMNT, 2017. Bundes-Abfallwirtschaftsplan 2017: Teil 1 [Austrian Federal Waste Management Plan 2017]. Bundesministerium für Nachhaltigkeit und Tourismus, Wien.

Brunner, P.H., Morf, L.S., 2024. Waste to energy, indispensable cornerstone for circular economy: A mini-review. Waste management & research : the journal of the International Solid Wastes and Public Cleansing Association, ISWA, 734242X241227376. https://doi.org/10.1177/0734242X241227376.

Brunner, P.H., Rechberger, H., 2017. Handbook of material flow analysis: For environmental, resource, and waste engineers. CRC Press Taylor & Francis Group, Boca Raton, London, New York, 435 pp.

Bundesverband Glasindustrie e.V; BDE Bundesverband der Deutschen Entsorgungs-, Wasser- und Rohstoffwirtschaft e. V; bvse-Bundesverband Sekundärrohstoffe und Entsorgung e.V., 2014. Leitlinie „Qualitätsanforderungen an Glasscherben zum Einsatz in der Behälterglasindustrie“: Standardblatt T 120 [Guideline "Quality requirements for glass cullet for the use in the packaging glass industry"]. https://www.bvse.de/dateien2020/2-PDF/03-Themen_Ereignisse/FV_Glas/Standardblatt_T_120_2014-08-14_2.pdf (accessed 2 April 2025).

Bunge, R., 2016. Recovery of metals from waste incinerator bottom ash. Institut für Umwelt- und Verfahrenstechnik UMTEC.

Bunge, R., Bunge, K., 1999. Probenahme auf Altlasten: Minimal notwendige Probenmasse [Sampling for contaminated sites: Minimum required sample mass]. altlasten spektrum 3/99 1999, 174–179.

Butler, J.H., Hooper, P.D., 2019. Glass Waste, in: Waste. Elsevier, pp. 307–322.

Chen, B., Perumal, P., Illikainen, M., Ye, G., 2023. A review on the utilization of municipal solid waste incineration (MSWI) bottom ash as a mineral resource for construction materials. Journal of Building Engineering 71, 106386. https://doi.org/10.1016/j.jobe.2023.106386.

Chimenos, J., Segarra, M., Fernández, M., Espiell, F., 1999. Characterization of the bottom ash in municipal solid waste incinerator. Journal of hazardous materials 64, 211–222. https://doi.org/10.1016/S0304-3894(98)00246-5.

City of Vienna, 2025. Zertifikat der Konformität der werkseigenen Produktionskontrolle [Certificate of Conformity of the Factory Production Control]. MA 39, Prüf-, Inspektions- und Zertifizierungsstelle der Stadt Wien, Wien, 5 pp. https://www.brantner.com/green-solutions/wp-content/uploads/sites/3/2023/11/Gesteinskoernung-Zertifikat-und-Leistungserklaerungen.pdf (accessed 23 April 2025).

Costa, G., Polettini, A., Pomi, R., Spagnuolo, R., 2020. Enhanced Separation of Incinerator Bottom Ash: Composition and Environmental Behaviour of Separated Mineral and Weakly Magnetic Fractions. Waste Biomass Valor 11, 7079–7095. https://doi.org/10.1007/s12649-020-01106-1.

Del Valle-Zermeño, R., Gómez-Manrique, J., Giro-Paloma, J., Formosa, J., Chimenos, J.M., 2017. Material characterization of the MSWI bottom ash as a function of particle size. Effects of glass recycling over time. Science of The Total Environment 581-582, 897–905. https://doi.org/10.1016/j.scitotenv.2017.01.047.

Deschamps, J., Simon, B., Tagnit-Hamou, A., Amor, B., 2018. Is open-loop recycling the lowest preference in a circular economy? Answering through LCA of glass powder in concrete. Journal of Cleaner Production 185, 14–22. https://doi.org/10.1016/j.jclepro.2018.03.021.

Deutsches Institut für Normung e.V., 2020. German standard methods for the examination of water, waste water and sludge – Anions (group D) – Part 52: Photometric determination of dissolved chromium(VI) in water (D 52): DIN 38405-52 13.060.50.

Dhir, R.K., Brito, J. de, Ghataora, G.S., Lye, C.Q., 2018a. Sustainable construction materials: Glass cullet. Woodhead Publishing, Duxford, 462 pp.

Dhir, R.K., Brito, J. de, Lynn, C.J., Silva, R.V., 2018b. Sustainable Construction Materials: Municipal Incinerated Bottom Ash. Elsevier.

Dou, X., Ren, F., Nguyen, M.Q., Ahamed, A., Yin, K., Chan, W.P., Chang, V.W.-C., 2017. Review of MSWI bottom ash utilization from perspectives of collective characterization, treatment and existing application. Renewable and Sustainable Energy Reviews 79, 24–38. https://doi.org/10.1016/j.rser.2017.05.044.

EC, 2025. Regulation (EU) 2025/40 of the European Parliament and of the Council of 19 December 2024 on packaging and packaging waste, amending Regulation (EU) 2019/1020 and Directive (EU) 2019/904, and repealing Directive 94/62/EC: EU Packaging and Packaging Waste Regulation.

Energie Graz, 2024. Energiewerk Graz. https://www.holding-graz.at/wp-content/uploads/2024/10/Folder-Energiewerk-Graz-Stand-Oktober-2024.pdf (accessed 9 January 2025).

European Committee for Standardization, 2002a. Characterization of waste - Digestion for subsequent determination of aqua regia soluble portion of elements: Charakterisierung von Abfällen. Aufschluss zur anschließenden Bestimmung des in Königswasser löslichen Anteils an Elementen in Abfällen. Berlin 13.030.40.

European Committee for Standardization, 2002b. Characterization of waste - Microwave assisted digestion with hydrofluoric (HF), nitric (HNO3) and hydrochloric (HCl) acid mixture for subsequent determination of elements: ÖNORM EN 13656 13.030.40.

European Committee for Standardization, 2009. Tests for geometrical properties of aggregates: Part 11: Classification test for the constituents of coarse recycled aggregate 91.100.15.

Eusden, J., Eighmy, T., Hockert, K., Holland, E., Marsella, K., 1999. Petrogenesis of municipal solid waste combustion bottom ash. Applied Geochemistry 14, 1073–1091.

Fan, C., Wang, B., Ai, H., Liu, Z., 2022. A comparative study on characteristics and leaching toxicity of fluidized bed and grate furnace MSWI fly ash. Journal of environmental management 305, 114345. https://doi.org/10.1016/j.jenvman.2021.114345.

Feil, A., Pretz, T., Julius, J., Go, N., Bosling, M., Johnen, K., 2019. Metal Waste, in: Waste. Elsevier, pp. 211–223.

Fletcher, C.A., Dunk, R., 2023. Recovery and utilisation of municipal solid waste incineration bottom ash: implications for European waste management strategy. Detritus, 43–57. https://doi.org/10.31025/2611-4135/2023.17274.

Freyssinet, P., Piantone, P., Azaroual, M., Itard, Y., Clozel-Leloup, B., Guyonnet, D., Baubron, J., 2002. Chemical changes and leachate mass balance of municipal solid waste bottom ash submitted to weathering. Waste Management 22, 159–172. https://doi.org/10.1016/S0956-053X(01)00065-4.

Gerlach, R.W., Nocerino, J.M., 2003. Guidance for Obtaining Representative Laboratory Analytical Subsamples from Particulate Laboratory Samples. U.S. Environmental Protection Agency. https://clu-in.org/download/char/epa_subsampling_guidance.pdf (accessed 14.12.22).

German Institute for Standardization, 2003. DIN EN 12457-4: Charakterisierung von Abfällen. Auslaugung - Übereinstimmungsuntersuchung für die Auslaugung von körnigen Abfällen und Schlämmen: Teil 4: Einstufiges Schüttelverfahren mit einem Flüssigkeits-/Feststoffverhältnis von 10 l/kg für Materialien mit einer Korngröße unter 10 mm (ohne oder mit Korngrößenreduzierung) [Characterization of waste - Leaching; Compliance test for leaching of granular waste materials and sludges - Part 4: One stage batch test at a liquid to solid ratio of 10 l/kg for materials with particle size below 10 mm (without or with limited size reduction)]. Beuth Verlag GmbH, Berlin 13.030.10; 13.030.20.

German Institute for Standardization, 2012. DIN EN 16192: Charakterisierung von Abfällen – Analyse von Eluaten: Deutsche Fassung EN 16192:2011. Berlin 13.030.99.

Glauser, A., Weibel, G., Eggenberger, U., 2021. Effects of enhanced metal recovery on the recycling potential of MSWI bottom ash fractions in various legal frameworks. Waste management & research : the journal of the International Solid Wastes and Public Cleansing Association, ISWA 39, 1459–1470. https://doi.org/10.1177/0734242X211038149.

Gy, P., 1992. Sampling of heterogeneous and dynamic material systems: Theories of heterogeneity, sampling, and homogenizing. Elsevier, Amsterdam, New York, 653 pp.

Gy, P., 2004. Sampling of discrete materials—a new introduction to the theory of sampling: I. Qualitative approach. Chemometrics and Intelligent Laboratory Systems 74, 7–24. https://doi.org/10.1016/j.chemolab.2004.05.012.

Haupt, M., Vadenbo, C., Zeltner, C., Hellweg, S., 2017. Influence of Input-Scrap Quality on the Environmental Impact of Secondary Steel Production. Journal of Industrial Ecology 21, 391–401. https://doi.org/10.1111/jiec.12439.

Holm, O., Simon, F.-G., 2017. Innovative treatment trains of bottom ash (BA) from municipal solid waste incineration (MSWI) in Germany. Waste Management 59, 229–236. https://doi.org/10.1016/j.wasman.2016.09.004.

Huber, F., 2020. Modelling of material recovery from waste incineration bottom ash. Waste management (New York, N.Y.) 105, 61–72. https://doi.org/10.1016/j.wasman.2020.01.034.

Huber, F., Blasenbauer, D., Aschenbrenner, P., Fellner, J., 2020. Complete determination of the material composition of municipal solid waste incineration bottom ash. Waste management (New York, N.Y.) 102, 677–685. https://doi.org/10.1016/j.wasman.2019.11.036.

Inkaew, K., Saffarzadeh, A., Shimaoka, T., 2016. Modeling the formation of the quench product in municipal solid waste incineration (MSWI) bottom ash. Waste management (New York, N.Y.) 52, 159–168. https://doi.org/10.1016/j.wasman.2016.03.019.

Jones, F., Niklasson, F., Lindberg, D., Hupa, M., 2013. Effects of Reduced Bed Temperature in Laboratory- and Full-Scale Fluidized-Bed Boilers: Particle, Deposit, and Ash Chemistry. Energy Fuels 27, 4999–5007. https://doi.org/10.1021/ef400836e.

Kalbe, U., Simon, F.-G., 2020. Potential Use of Incineration Bottom Ash in Construction: Evaluation of the Environmental Impact. Waste Biomass Valor 11, 7055–7065. https://doi.org/10.1007/s12649-020-01086-2.

Kazmi, D., Williams, D.J., Serati, M., 2020. Waste glass in civil engineering applications—A review. Int J Applied Ceramic Tech 17, 529–554. https://doi.org/10.1111/ijac.13434.

Kellner, M., Schindler, I., Jany, A., 2022. Status report waste incineration: Reporting year 2020. Umweltbundesamt, Wien.

Keulen, A., van Zomeren, A., Harpe, P., Aarnink, W., Simons, H.A.E., Brouwers, H.J.H., 2016. High performance of treated and washed MSWI bottom ash granulates as natural aggregate replacement within earth-moist concrete. Waste management (New York, N.Y.) 49, 83–95. https://doi.org/10.1016/j.wasman.2016.01.010.

Lam, C.H.K., Ip, A.W.M., Barford, J.P., McKay, G., 2010. Use of Incineration MSW Ash: A Review. Sustainability 2, 1943–1968. https://doi.org/10.3390/su2071943.

Larsen, A.W., Merrild, H., Christensen, T.H., 2009. Recycling of glass: accounting of greenhouse gases and global warming contributions. Waste management & research : the journal of the International Solid Wastes and Public Cleansing Association, ISWA 27, 754–762. https://doi.org/10.1177/0734242X09342148.

Leckner, B., Lind, F., 2020. Combustion of municipal solid waste in fluidized bed or on grate - A comparison. Waste management (New York, N.Y.) 109, 94–108. https://doi.org/10.1016/j.wasman.2020.04.050.

Lederer, J., Schuch, D., 2024. The contribution of waste and bottom ash treatment to the circular economy of metal packaging: A case study from Austria. Resources, Conservation and Recycling 203, 107461. https://doi.org/10.1016/j.resconrec.2024.107461.

López-Delgado, A., Peña, C., López, V., López, F.A., 2003. Quality of ferrous scrap from MSW incinerators: a case study of Spain. Resources, Conservation and Recycling 40, 39–51. https://doi.org/10.1016/S0921-3449(03)00024-7.

Lu, J.-W., Zhang, S., Hai, J., Lei, M., 2017. Status and perspectives of municipal solid waste incineration in China: A comparison with developed regions. Waste management (New York, N.Y.) 69, 170–186. https://doi.org/10.1016/j.wasman.2017.04.014.

Luo, H., Cheng, Y., He, D., Yang, E.-H., 2019. Review of leaching behavior of municipal solid waste incineration (MSWI) ash. The Science of the total environment 668, 90–103. https://doi.org/10.1016/j.scitotenv.2019.03.004.

Makari, C., 2014. Optical Sorting for the Recovery of Glass from WIP Slags: – Pilot Plant in Bratislava –, in: Thomé-Kozmiensky, K.J., Thiel, S. (Eds.), Waste management. TK-Verl. Thomé-Kozmiensky, Neuruppin, pp. 345–354.

Makarichi, L., Jutidamrongphan, W., Techato, K., 2018. The evolution of waste-to-energy incineration: A review. Renewable and Sustainable Energy Reviews 91, 812–821. https://doi.org/10.1016/j.rser.2018.04.088.

Maldonado-Alameda, A., Mañosa, J., Miro-Escola, J., Quintero-Payan, A.C., Chimenos, J.M., 2023. Fluidised-bed incineration bottom ash as the sole precursor of alkali-activated binders: A comparison with bottom ash from grate incinerators. Construction and Building Materials 364, 130001. https://doi.org/10.1016/j.conbuildmat.2022.130001.

Margallo, M., Taddei, M.B.M., Hernández-Pellón, A., Aldaco, R., Irabien, Á., 2015. Environmental sustainability assessment of the management of municipal solid waste incineration residues: a review of the current situation. Clean Techn Environ Policy 17, 1333–1353. https://doi.org/10.1007/s10098-015-0961-6.

Mehr, J., Haupt, M., Skutan, S., Morf, L., Raka Adrianto, L., Weibel, G., Hellweg, S., 2021. The environmental performance of enhanced metal recovery from dry municipal solid waste incineration bottom ash. Waste management (New York, N.Y.) 119, 330–341. https://doi.org/10.1016/j.wasman.2020.09.001.

Mohajerani, A., Vajna, J., Cheung, T.H.H., Kurmus, H., Arulrajah, A., Horpibulsuk, S., 2017. Practical recycling applications of crushed waste glass in construction materials: A review. Construction and Building Materials 156, 443–467. https://doi.org/10.1016/j.conbuildmat.2017.09.005.

Mühl, J., Hofer, S., Blasenbauer, D., Lederer, J., 2024. Recovery of aluminum, magnetic ferrous metals and glass through enhanced industrial-scale treatment of different MSWI bottom ashes. Waste management (New York, N.Y.) 190, 557–568. https://doi.org/10.1016/j.wasman.2024.10.025.

Mühl, J., Mika, S., Tischberger-Aldrian, A., Lederer, J., 2025. Upgrading and Characterization of Glass Recovered from MSWI Bottom Ashes from Fluidized Bed Combustion. Recycling 10, 63. https://doi.org/10.3390/recycling10020063.

Mühl, J., Skutan, S., Stockinger, G., Blasenbauer, D., Lederer, J., 2023. Glass recovery and production of manufactured aggregate from MSWI bottom ashes from fluidized bed and grate incineration by means of enhanced treatment. Waste Management 168, 321–333. https://doi.org/10.1016/j.wasman.2023.05.048.

Muñiz Sierra, H., Šyc, M., Korotenko, E., 2023. Wet shaking table operating parameters optimization for maximizing metal recovery from incineration bottom ash fine fraction. Waste management (New York, N.Y.) 174, 539–548. https://doi.org/10.1016/j.wasman.2023.12.030.

Neuwahl, F., Cusano, G., Benavides, J.G., Holbrook, S., 2019. Best Available Techniques (BAT) Reference Document for Waste Incineration: EUR 29971 EN. Europäische Union, Luxemburg. https://eippcb.jrc.ec.europa.eu/sites/default/files/2020-01/JRC118637_WI_Bref_2019_published_0.pdf (accessed 6 April 2023).

Perrin, M., Svecova, L., Deseure, J., 2023. Closed-loop process for Zn and Cu selective recovery from MSWI bottom ash fine fraction. Minerals Engineering 203, 108353. https://doi.org/10.1016/j.mineng.2023.108353.

Pfandl, K., Küppers, B., Scheiber, S., Stockinger, G., Holzer, J., Pomberger, R., Antrekowitsch, H., Vollprecht, D., 2020. X-ray fluorescence sorting of non-ferrous metal fractions from municipal solid waste incineration bottom ash processing depending on particle surface properties. Waste management & research : the journal of the International Solid Wastes and Public Cleansing Association, ISWA 38, 111–121. https://doi.org/10.1177/0734242X19879225.

Pienkoß, F., Abis, M., Bruno, M., Grönholm, R., Hoppe, M., Kuchta, K., Fiore, S., Simon, F.-G., 2022. Heavy metal recovery from the fine fraction of solid waste incineration bottom ash by wet density separation. J Mater Cycles Waste Manag 24, 364–377. https://doi.org/10.1007/s10163-021-01325-1.

Pomberger, R., Sarc, R., Lorber, K.E., 2017. Dynamic visualisation of municipal waste management performance in the EU using Ternary Diagram method.

Waste management (New York, N.Y.) 61, 558–571. https://doi.org/10.1016/j.wasman.2017.01.018.
Qi, W., Geng, C., Zhu, F., Zhang, C., Du, B., Ji, Y., Wang, F., Zhang, S., Liu, J., 2024. Complementary vitrification of municipal solid waste incineration fly ash from grate furnaces and fluidised bed incinerators via a co-reduction process. Waste management (New York, N.Y.) 184, 92–100. https://doi.org/10.1016/j.wasman.2024.05.033.
Rübner, K., Haamkens, F., Linde, O., 2008. Use of municipal solid waste incinerator bottom ash as aggregate in concrete. Quarterly Journal of Engineering Geology and Hydrogeology 41, 459–464. https://doi.org/10.1144/1470-9236/07-036.
Saikia, N., Cornelis, G., Mertens, G., Elsen, J., van Balen, K., van Gerven, T., Vandecasteele, C., 2008. Assessment of Pb-slag, MSWI bottom ash and boiler and fly ash for using as a fine aggregate in cement mortar. Journal of hazardous materials 154, 766–777. https://doi.org/10.1016/j.jhazmat.2007.10.093.
Saqib, N., Bäckström, M., 2014. Trace element partitioning in ashes from boilers firing pure wood or mixtures of solid waste with respect to fuel composition, chlorine content and temperature. Waste management (New York, N.Y.) 34, 2505–2519. https://doi.org/10.1016/j.wasman.2014.08.025.
Scalet, B.M., Garcia Munoz, M., Sissa, A.Q., Roudier, S., Delgado Sancho, L., 2013. Best Available Techniques (BAT) Reference Document for The Manufacture of Glass: Industrial Emissions Directive 2010/75/EU Integrated Pollution Prevention and Control. EUR 25786 EN, Luxemburg. https://eippcb.jrc.ec.europa.eu/sites/default/files/2019-11/GLS_Adopted_03_2012_0.pdf (accessed 14.01.22).
Schaeffer, H.A., Langfeld, R., 2020. Werkstoff Glas: Alter Werkstoff mit großer Zukunft, 2nd ed. Springer Berlin Heidelberg; Imprint: Springer, Berlin, Heidelberg, 230).
Sepúlveda Olea, F.E., Burke, I.T., Mohammad, A., Stewart, D.I., 2024. Reuse potential of municipal solid waste incinerator bottom ash as secondary aggregate: Material characteristics, persistent organic pollutant content and effects of pH and selected environmental lixiviants on leaching behaviour. Waste management (New York, N.Y.) 187, 262–274. https://doi.org/10.1016/j.wasman.2024.07.026.
Silva, R.V., Brito, J. de, Lynn, C.J., Dhir, R.K., 2019. Environmental impacts of the use of bottom ashes from municipal solid waste incineration: A review. Resources, Conservation and Recycling 140, 23–35. https://doi.org/10.1016/j.resconrec.2018.09.011.
Simon, B., Amor, M.B., Földényi, R., 2016. Life cycle impact assessment of beverage packaging systems: focus on the collection of post-consumer bottles. Journal of Cleaner Production 112, 238–248. https://doi.org/10.1016/j.jclepro.2015.06.008.

Simon, F.-G., Kalbe, U., 2023. Case Study on Secondary Building Materials for a Greener Economy. Applied Sciences 13, 6010. https://doi.org/10.3390/app13106010.

Skutan, S., Brunner, P.H., 2005. Stoffbilanzen mechanisch-biologischer Anlagen zur Behandlung von Restmüll (SEMBA): Endbericht [Material Balances of Mechanical-Biological Treatment Plants for Residual Waste]. Technische Universität Wien Institut für Wassergüte, Ressourcenmanagement und Abfallwirtschaft, Wien.

Skutan, S., Brunner, P.H., 2012. Metals in RDF and other high calorific value fractions from mechanical treatment of MSW: analysis and sampling errors. Waste management & research : the journal of the International Solid Wastes and Public Cleansing Association, ISWA 30, 645–655. https://doi.org/10.1177/0734242X12442740.

Skutan, S., Gloor, R., Morf, L., 2018. Methods report: Sampling, sample preparation and analysis of solid residues from thermal waste treatment and its processing products. AWEL Zurich, ZAR.

Sorlini, S., Collivignarelli, M.C., Abbà, A., 2017. Leaching behaviour of municipal solid waste incineration bottom ash: From granular material to monolithic concrete. Waste management & research : the journal of the International Solid Wastes and Public Cleansing Association, ISWA 35, 978–990. https://doi.org/10.1177/0734242X17721340.

Šyc, M., Krausová, A., Kameníková, P., Šomplák, R., Pavlas, M., Zach, B., Pohořelý, M., Svoboda, K., Punčochář, M., 2018. Material analysis of Bottom ash from waste-to-energy plants. Waste management (New York, N.Y.) 73, 360–366. https://doi.org/10.1016/j.wasman.2017.10.045.

Šyc, M., Simon, F.G., Hykš, J., Braga, R., Biganzoli, L., Costa, G., Funari, V., Grosso, M., 2020. Metal recovery from incineration bottom ash: State-of-the-art and recent developments. Journal of hazardous materials 393, 122433. https://doi.org/10.1016/j.jhazmat.2020.122433.

Šyc, M., Výravský, J., Muñiz Sierra, H., Korotenko, E., Kameníková, P., 2024. Resource recovery potential of incineration bottom ash fine fraction. Waste management (New York, N.Y.) 190, 569–577. https://doi.org/10.1016/j.wasman.2024.10.020.

Tayibi, H., Peña, C., López, F.A., López-Delgado, A., 2007. Management of MSW in Spain and recovery of packaging steel scrap. Waste Management 27, 1655–1665. https://doi.org/10.1016/j.wasman.2006.09.012.

Tian, Y., Themelis, N.J., Bourtsalas, A.C., 2024. Effects of water, acid, or alkali washing on Waste-to-Energy (WTE) bottom ash, fly ash, and combined ash. Journal of Environmental Chemical Engineering 12, 111936. https://doi.org/10.1016/j.jece.2024.111936.

Turner, A., 2019. Heavy Metals in the Glass and Enamels of Consumer Container Bottles. Environmental science & technology 53, 8398–8404. https://doi.org/10.1021/acs.est.9b01726.

van Caneghem, J., Brems, A., Lievens, P., Block, C., Billen, P., Vermeulen, I., Dewil, R., Baeyens, J., Vandecasteele, C., 2012. Fluidized bed waste incinerators: Design, operational and environmental issues. Progress in Energy and Combustion Science 38, 551–582. https://doi.org/10.1016/j.pecs.2012.03.001.

van Caneghem, J., Coster, E. de, Vandenbergh, K., Broyer, S. de, Lambrix, N., Weemaels, L., 2019a. Closing the household metal packaging cycle through recovery of scrap from waste-to-energy bottom ash: The case study of Flanders. Resources, Conservation and Recycling 144, 115–122. https://doi.org/10.1016/j.resconrec.2019.01.028.

van Caneghem, J., van Acker, K., Greef, J. de, Wauters, G., Vandecasteele, C., 2019b. Waste-to-energy is compatible and complementary with recycling in the circular economy. Clean Techn Environ Policy 21, 925–939. https://doi.org/10.1007/s10098-019-01686-0.

van de Wouw, P.M.F., Loginova, E., Florea, M.V.A., Brouwers, H.J.H., 2020. Compositional modelling and crushing behaviour of MSWI bottom ash material classes. Waste management (New York, N.Y.) 101, 268–282. https://doi.org/10.1016/j.wasman.2019.10.013.

Vateva, I., Laabs, M., Middendorf, B., Laner, D., 2025. Treatment of fine and medium fractions of MSWI bottom ash for use in concrete: A German case study. Waste management (New York, N.Y.) 198, 117–127. https://doi.org/10.1016/j.wasman.2025.02.050.

Vateva, I., Laner, D., 2020. Grain-Size Specific Characterisation and Resource Potentials of Municipal Solid Waste Incineration (MSWI) Bottom Ash: A German Case Study. Resources 9, 66. https://doi.org/10.3390/resources9060066.

Verbinnen, B., Billen, P., van Caneghem, J., Vandecasteele, C., 2017. Recycling of MSWI Bottom Ash: A Review of Chemical Barriers, Engineering Applications and Treatment Technologies. Waste Biomass Valor 8, 1453–1466. https://doi.org/10.1007/s12649-016-9704-0.

Vermeulen, I., van Caneghem, J., Block, C., van Brecht, A., Wauters, G., Vandecasteele, C., 2012. Sustainable waste processing in a grate furnace and in a fluidized bed incinerator: WtE, recycling and environmental concerns, in: Waste Management and the Environment VI. WASTE MANAGEMENT 2012, New Forest, UK. 04.07.2012 - 06.07.2012. WIT PressSouthampton, UK, pp. 167–176.

Xuan, D., Tang, P., Poon, C.S., 2018. Limitations and quality upgrading techniques for utilization of MSW incineration bottom ash in engineering applications – A review. Construction and Building Materials 190, 1091–1102. https://doi.org/10.1016/j.conbuildmat.2018.09.174.

Yeo, R.J., Sng, A., Wang, C., Tao, L., Zhu, Q., Bu, J., 2024. Strategies for heavy metals immobilization in municipal solid waste incineration bottom ash: a critical review. Rev Environ Sci Biotechnol. https://doi.org/10.1007/s11157-024-09694-3.

7 List of Figures

8 List of Tables

Appendix I

Paper I:

Glass recovery and production of manufactured aggregate from MSWI bottom ashes from fluidized bed and grate incineration by means of enhanced treatment

Mühl, J.; Skutan, S.; Stockinger, G.; Blasenbauer, D.; Lederer, J.

Waste Management 168 (2023), 321–333.
Available online: June, 17th 2023
DOI: https://doi.org/10.1016/j.wasman.2023.05.048

Waste Management 168 (2023) 321–333

Contents lists available at ScienceDirect

Waste Management

journal homepage: www.elsevier.com/locate/wasman

Research Paper

Glass recovery and production of manufactured aggregate from MSWI bottom ashes from fluidized bed and grate incineration by means of enhanced treatment

Julia Mühl [a,*], Stefan Skutan [a,b], Gerhard Stockinger [c], Dominik Blasenbauer [a], Jakob Lederer [a]

[a] Christian Doppler Laboratory for a Recycling-based Circular Economy, Institute of Chemical, Environmental and Bioscience Engineering, TU Wien, Getreidemarkt 9/166, 1060 Vienna, Austria

[b] Ingenieurbüro Stefan Skutan e.U., Fritz-Weigl-Gasse 1a, 3423 St. Andrä-Wördern, Austria

[c] Brantner Österreich GmbH, Dr.-Franz-Wilhelm-Straße 2a, 3500 Krems an der Donau, Austria

ARTICLE INFO

Keywords:
Circular economy
Municipal solid waste incineration
Incineration bottom ash
Fluidized bed combustion
Grate incineration
Waste glass
Glass recycling
Manufactured aggregate
Concrete production

ABSTRACT

Enhanced treatment of incineration bottom ashes (IBA) from municipal solid waste incineration can contribute to a circular economy since not only metals can be recovered but also glass for recycling. Moreover, the remaining mineral fraction can be utilized in concrete as manufactured aggregate. To evaluate the effects of an enhanced treatment, three IBAs from fluidized bed combustion (FB-IBAs) and three grate incineration bottom ashes (G-IBAs) were standardly treated in a jig and further processed on a pilot scale, including improved metal recovery and sensor-based glass separation. The removed glass fractions were weighed and their composition was assessed by means of manual sorting. The manufactured aggregate was also sorted manually and its total and leachate contents were determined before and after aging. Results showed general differences between FB-IBAs and G-IBAs. For G-IBAs, higher contents of heavy metals and residual metal pieces were determined, while the share of glass removed was low compared to FB-IBA. The treated mineral fractions from G-IBA contained more mineral agglomerates, whereas FB-IBAs contained more glass. However, the glass-fractions removed from FB-IBAs need further treatment to be accepted in glass recycling. Austrian limit values for utilization in concrete were met by all manufactured aggregates produced from FB-IBA, but only by one from G-IBA. Overall, the enhanced treatment in the study performed well compared to the literature. Nevertheless, further investigations are necessary to improve the recyclability of the recovered glass fractions and to determine the technical suitability of manufactured aggregates produced from IBAs.

1. Introduction

Municipal solid waste incineration (MSWI) with energy recovery (waste-to-energy) is a widespread and indispensable technology to reduce landfill volumes and recover energy from waste that cannot be recycled (van Caneghem et al., 2019). For a circular economy, however, material loops from municipal solid waste (MSW) management must be closed in order to save natural resources and raw materials (Abis et al., 2020; Lederer et al., 2022). Thus, the utilization of incineration bottom ash (IBA) has received much attention in policy, practice and research as it promotes circularity and the sustainability of MSWI (Bruno et al., 2021). For the most commonly applied grate incineration (GI) technology, IBA makes up the bulk of solid MSWI residues, with about 20–25% of the incinerated MSW (Dhir et al., 2018). For fluidized bed combustion (FBC) lower IBA amounts of around 10% of the incinerated MSW have been reported (Blasenbauer et al., 2023; Fan et al., 2022; Purgar et al., 2016; Saqib and Bäckström, 2015). This is due to higher shares of solids transferred to the fly ash. FBC is a secondary incineration technology in the EU, but plays an important role in particular countries such as Austria, Sweden, China, or USA (Leckner and Lind, 2020; Saqib and Bäckström, 2015). This type of firing technology requires pre-treatment of the MSW before incineration, including metal separation and particle size reduction (Leckner and Lind, 2020; Maldonado-Alameda et al., 2023). Due to the different firing conditions, IBA from FBC differs from IBA from GI, e.g. regarding its share and composition of glass and mineral fraction (Blasenbauer et al., 2023). Another aspect that influences IBA properties, is the IBA discharge, which can be realized in wet or dry form (Back and Sakanakura, 2022; Inkaew et al., 2016).

* Corresponding author.
E-mail address: julia.muehl@tuwien.ac.at (J. Mühl).

https://doi.org/10.1016/j.wasman.2023.05.048
Received 6 February 2023; Received in revised form 28 April 2023; Accepted 28 May 2023
Available online 17 June 2023

Abbreviations

Chemical elements and compounds

As	Arsenic
Cd	Cadmium
Cr	Chromium
Cu	Copper
Mo	Molybdenum
Ni	Nickel
Pb	Lead
Sb	Antimony
TOC	Total Organic Carbon

Acronyms

dm	Dry matter
ECS	eddy current separation
EN	European Standards
FB-IBA	fluidized bed incineration bottom ash
FBC	fluidized bed combustion
Fe	ferrous
G-IBA	grate incineration bottom ash
GI	grate incineration
IBA	incineration bottom ash
ICP-OES	inductively coupled plasma optical emission spectrometry
ICW	industrial & commercial waste
MAG	manufactured aggregate
MF	mineral fraction
MSW	municipal solid waste
MSWI	municipal solid waste incineration
NFe	non-ferrous
OW	other waste
SS	sewage sludge
stMF	standardly-treated-mineral-fraction
TEQ	toxic equivalence
VIS	Visible spectrum
WHO	World Health Organization
w-%	weight-percent

The main focus of efforts to recover recyclable material from IBA are metals due to their high economic value and the fact that their recycling mitigates negative environmental impact (Mehr et al., 2021; Šyc et al., 2020; Turner et al., 2015). Thus, most IBA treatment plants are primarily designed for metal extraction (Huber, 2020; Neuwahl et al., 2019). The remaining fraction after metal removal, which is about 90% of the IBA, mainly consists of mineral material such as mineral agglomerates, ceramics, construction material, porcelain as well as substantial amounts of glass (Bunge, 2018; Chimenos et al., 1999; Del Valle-Zermeño et al., 2017; Huber et al., 2020; Šyc et al., 2018; Vateva and Laner, 2020). As this fraction is currently landfilled to a large extent, enhanced efforts are being made to find utilization paths for this material (Bruno et al., 2021; Holm and Simon, 2017; Huber, 2020). In some European countries, this fraction is used as mineral construction material, particularly in road construction, but rarely as manufactured aggregate (*MAG*) in concrete (Astrup et al., 2016; Blasenbauer et al., 2020; Verbinnen et al., 2017). Since the potential of using secondary raw material in concrete would be environmentally beneficial but is not yet fully utilized (Dhir et al., 2018; Lederer et al., 2020), there is an increasing interest in producing *MAG* from IBA (Alderete et al., 2021; Verbinnen et al., 2017).

However, the use of *MAG* generated from standardly treated IBA is impeded by factors such as residual metals, glass and other substances (e.g. soluble salts) contained therein (Alderete et al., 2021; Rübner et al., 2008; Saikia et al., 2008; Xuan et al., 2018). Technical requirements may, therefore, not be met by *MAG* generated from IBA. From an environmental, hence legal, point of view, leachable heavy metals also represent limiting factors (Blasenbauer et al., 2020; Neuwahl et al., 2019). This means that enhanced treatment of standard-processed IBA is required to produce *MAG*. Therefore, various treatment processes for advanced processing of IBA have been developed in recent years (Holm and Simon, 2017; Šyc et al., 2020). Crushing, multi-step sieving and metal separation are widely used to reduce the metal content (Šyc et al., 2020). Aging or accelerated carbonation and contact with water are also established treatment steps to decrease the leachability of heavy metals as well as the content of metallic aluminum and soluble salts (Dou et al., 2017; Holm and Simon, 2017; Hykš and Astrup, 2009; Keulen et al., 2016; Nørgaard et al., 2019; Santos et al., 2013). Concerning the removal of glass from IBA, hitherto few attempts have been made (Hauer et al., 2014; Makari, 2014), although the glass amount is reported to constitute 5–30% of IBA from GI and is potentially even higher in IBA from FBC (Blasenbauer et al., 2023; Del Valle-Zermeño et al., 2017; Šyc et al., 2020; Vateva and Laner, 2020). The contained glass may not only be recycled, but the separation could also be beneficial for *MAG* production (Blasenbauer et al., 2023; Müller and Rübner, 2006).

Hence, this study aimed to apply and evaluate enhanced treatment, including glass removal of standardly treated mineral fractions of IBA. Thereby, *MAG* was produced from the remaining mineral fraction and analyzed. The results of the analysis were compared to novel Austrian legal requirements for use in concrete production, which are valid as of 2023. Moreover, two hitherto poorly investigated issues concerning IBAs were examined more closely, namely the removal of glass from IBA as well as the processing of IBAs by means of different firing technologies. The latter topic focuses on differences in composition and properties between treated fluidized bed incineration bottom ashes (FB-IBAs) and grate incineration bottom ashes (G-IBAs). This information is essential for comparing different MSWI technologies regarding the circularity potential of their remaining solid residues. Furthermore, the findings of this paper can contribute to improving the recovery rate of MSW by examining opportunities to recycle the mineral fraction and glass cullet from IBAs.

In order to close these research gaps, three G-IBAs from GI and three FB-IBAs from FBC plants in Austria were processed in an industrial-scale standard IBA treatment plant. The standardly treated mineral fractions of the six IBAs then underwent an experimental enhanced treatment on a pilot scale, producing glass fractions and *MAG*. These outputs were analyzed through single-grain characterization based on hand-sorting. Additionally, the content of residual metal pieces was determined in the mineral fraction and the *MAG* was chemically analyzed before and after aging.

2. Material and methods

2.1. MSWI plants and IBAs considered

The six IBAs treated within this large-scale experiment derive from six Austrian MSWI plants, three with GI and three with FBC. GI mainly uses untreated MSW as well as different amounts of bulky and commercial waste as fuel. The FBC plants primarily incinerate mechanically pretreated mixed MSW, but also sewage sludge. The discharge type for the three GI plants is quenching in a water bath, whereas the FBC plants are equipped with dry discharge. An overview of the MSWI plants considered, their firing technology and their MSW input composition are shown in Table 1.

Austria's total capacity of MSWI plants is 2.6 Mt/a (BMK, 2023). FBC makes up 0.8 Mt/a and, therefore, 30% of the installed capacities. The

Table 1
Overview of the incineration plants of the IBAs investigated. Data obtained from plant operators and ISWA (2012), respectively. GI: grate incineration, FBC: fluidized bed combustion, ICW: industrial & commercial waste, OW: other waste, SS: sewage sludge.

MSWI plant	Furnace type	Input material [w-%]
FB-IBA A	FBC	13% pretreated MSW, 50% ICW, 17% SS, 20% OW
FB-IBA B	FBC	33% mixed MSW, 16% pretreated MSW, 51% ICW, OW and bulky waste
FB-IBA C	FBC	98% pretreated MSW, 1% ICW, 1% SS
G-IBA X	GI	27% mixed MSW, 73% ICW
G-IBA Y	GI	13% pretreated & 40% mixed MSW, 18% ICW, 3% SS, 24% bulky waste, 2% OW
G-IBA Z	GI	14% pretreated & 65% mixed MSW, 15% ICW, 2% bulky waste, 3% OW

remaining 1.8 Mt/a are GI plants (BMK, 2023). This experiment examined three GI and three FBC plants with a total capacity of 670,000 t/a and 677,000 t/a, respectively. Hence, this study covers 84% of the installed capacity of FBC and 37% of GI, which underlines the high relevance of this study for Austrian MSWI (Mühl et al., 2022).

2.2. *Experimental setup of standard and enhanced treatment of IBA*

In the experimental setup, each IBA underwent a standard wet treatment on an industrial scale (see 2.2.1). Samples from each resulting standardly treated mineral fraction (MF) were taken for subsequent enhanced treatment on a pilot scale. The enhanced treatment steps aimed at recovering a glass fraction from the *standardly-treated-MFs 8–35 mm* and producing a *MAG* with a grain size of 0–8 mm out of the enhanced treated MFs. These products were further analyzed. Fig. 1 gives an overview of the subsequently described experimental setup.

Sample division for reduction of the IBA amounts handled was primarily carried out by fractional or alternate shoveling (Gerlach and Nocerino, 2003). To ensure good representativity, each subsample contained at least ten increments per pile, as recommended by Gerlach and Nocerino (2003).

The characterization of the metal flows was not within the scope of this experiment. Therefore, removed metal fractions were not further analyzed, with the exception of metals remaining in glass, the treated MF and *MAG*, respectively.

2.2.1. *Standard IBA treatment*

As standard treatment for the six IBAs, the industrial-scale treatment plant of *Brantner Österreich GmbH* was chosen. This plant for wet processing of G-IBA and FB-IBA is considered state of the art (Neuwahl et al., 2019). Its primary goal is to maximize the metal yield from the IBAs. As reported by Huber (2020), the plant (Plant B) performs very well in this respect, achieving the highest metal recovery rates, with the exception of Al, compared to other plants. The plant is only briefly described in the next paragraph as its design has already been reported several times in the literature (Pfandl et al., 2020; Stockinger, 2016; Šyc et al., 2020).

In the experiment, 100–150 t of each IBA was treated in the standard IBA treatment plant, where the input material was first sieved with a 50 mm screen. The retained material > 50 mm was not considered further due to its negligible quantity (Huber et al., 2020). After separation of magnetic, ferrous (Fe) metals (magnetic separator from *IFE Aufbereitungstechnik GmbH*, Austria), particles < 50 mm were fed into the jig (*Siebtechnik GmbH*, Germany), which separates metals based on their density. Output streams of the jig were a high-density fraction of 4–50 mm rich in heavy metals, a fine fraction < 4 mm and a lighter fraction of 4–50 mm, primarily containing lighter metals and minerals. A specific process for fines splits the fine fraction of < 4 mm into metals < 4 mm, mineral constituents < 4 mm and sludge. The remaining mineral constituents < 4 mm were mixed with the lighter fraction of 4–50 mm and these fractions underwent an eddy current separation (ECS) (*IMRO Maschinenbau GmbH*, Germany) for non-ferrous (NFe) metal-removal. The thereby resulting *standardly-treated-MFs < 50 mm* of the six IBAs were used for enhanced treatment.

2.2.2. *Sample collection, screening and crushing*

A subset of each *standardly-treated-MF < 50 mm* was collected during standard treatment and used for enhanced treatment on a pilot scale. The sampling took place every five minutes from the falling stream at the head of the conveyor belt with a wheel loader. In total, 30 samples of about 50 kg each amounted to about 1.5–2 t of every *standardly-treated-MF < 50 mm* for the enhanced treatment.

Since narrower particle size fractions are beneficial for the following experimental separation steps (Holm and Simon, 2017; Šyc et al., 2020), the primary samples of the *standardly-treated-MFs < 50 mm* were sieved and crushed. First, every sample was sieved with a circular motion vibrating screen (*Keestrack*, Belgium) into the particle size fractions of 0–8 mm, 8–35 mm and > 35 mm. Coarse metal pieces of the fraction > 35 mm were separated manually in this and the following sieving runs since it can be expected that they will be removed in industrial-scale enhanced treatment as well (Šyc et al., 2020). Subsequently, the *standardly-treated-MFs 8–35 mm* and *> 35 mm* of the G-IBAs were fed into a mobile jaw crusher (*Rubble Master HMH GmbH*, Austria) and crushed in three consecutive runs. This step was essential to comminute mineral agglomerates and expose embedded metal pieces (Šyc et al., 2020). The crushed G-IBA material was again fed into the circular motion vibrating screen, producing two *standardly-treated-MFs* of particle size *0–8 mm* and *8–35 mm*. The small remaining amount of > 35 mm was crushed again in a roll crusher after another manual metal-separation step and manually sieved with an 8 mm mesh. The sieved fractions also were accordingly added to the *standardly-treated-MFs 0–8 mm* and *8–35 mm*, respectively.

As FB-IBAs contain barely any mineral agglomerates, the crushing was not applied to the *standardly-treated-MFs < 50 mm* of FB-IBAs. These were directly fed into the circular motion vibrating screen, producing *standardly-treated-MFs* of particle size *0–8 mm* and *8–35 mm*. Only material > 35 mm from FB-IBAs was crushed in a roll crusher after manual metal separation. As for G-IBA, the crushed material was manually sieved and accordingly added to the *standardly-treated-MFs 0–8 mm* and *8–35 mm*, respectively. The results were two *standardly-treated-MFs* per IBA, one with 0–8 mm and one with 8–35 mm. Hence, twelve fractions were available for the enhanced treatment, all of which were divided into two halves for further processing.

2.2.3. *Metal separation*

After sample division, half of the material of each *standardly-treated-MF 0–8 mm* and *8–35 mm* was used for advanced metal separation in a pilot plant of *IFE Aufbereitungstechnik GmbH* (Austria). This included a magnetic sorter (barium-ferrite, HPG 500x650/13, *IFE Aufbereitungstechnik GmbH*, Austria) followed by an ECS (INPXS 650x500/J36, *IFE Aufbereitungstechnik GmbH*, Austria). The additional metal separation was expected to be more efficient than the first metal removal at the standard IBA treatment plant for several reasons: magnetic separation prior to an ECS improves the efficiency of the ECS; the size range of the IBAs was narrower compared to the first ECS at the standard IBA treatment; and in this run, the splitter of the ECS was placed in such a manner that also weakly-conductive material was removed, accepting a certain associated removal of non-conductive material (Bunge, 2018; Holm and Simon, 2017; Šyc et al., 2020). The result of the metal removal were *metal-depleted-MFs*, six of 0–8 mm and six of 8–35 mm particle size, as well as the corresponding metal fractions removed. All of these were weighed.

2.2.4. *Glass separation*

The six coarser *metal-depleted-MFs 8–35 mm* passed through the sensor-based sorting device CLARITY® (*Binder + Co AG*, Austria). The

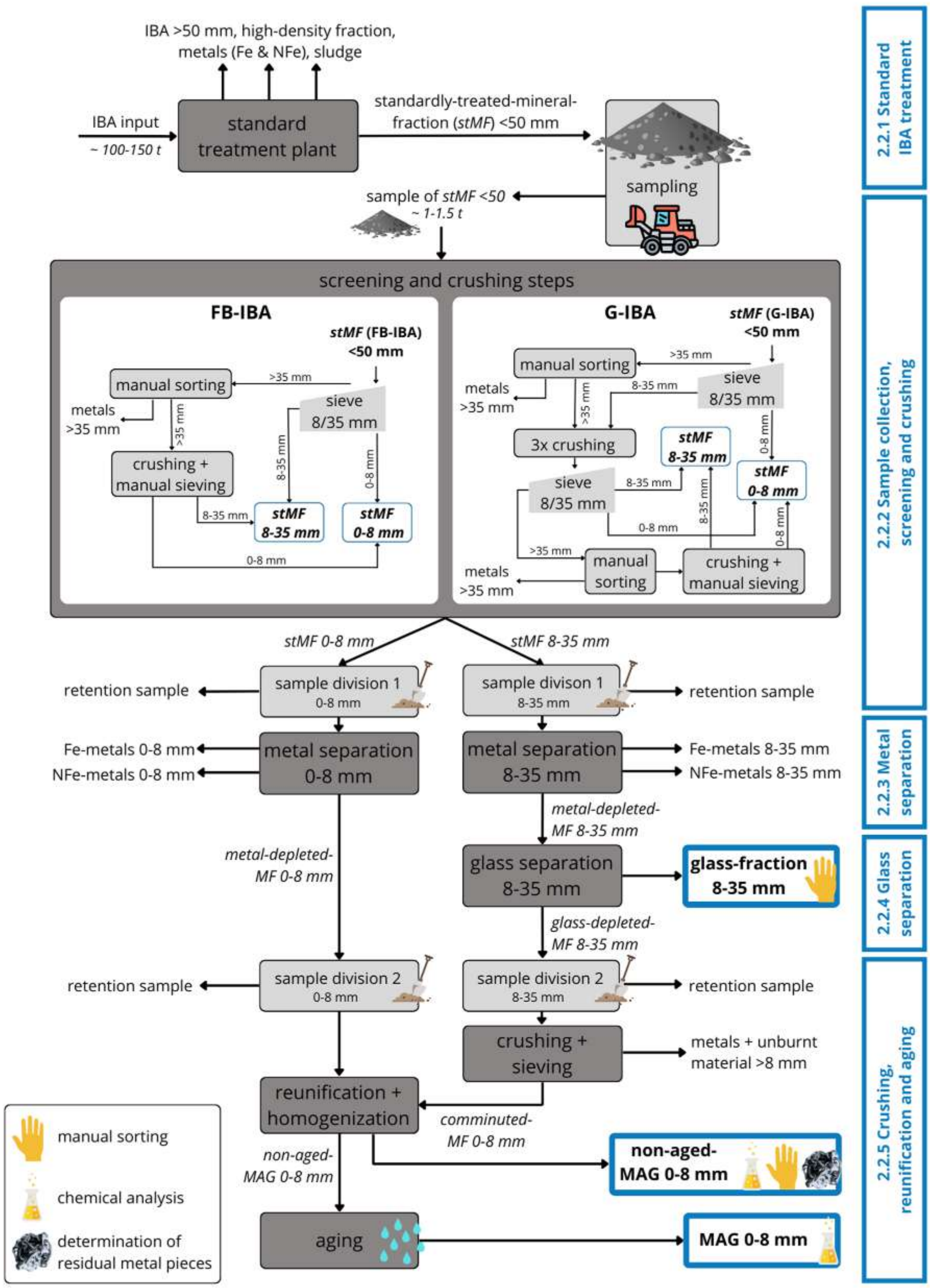

Fig. 1. Treatment steps of the IBA processing. MF: mineral fraction, stMF: standardly-treated-mineral-fraction, FB-IBA: fluidized bed incineration bottom ash, G-IBA: grate incineration bottom ash, Fe: ferrous, NFe: non-ferrous, MAG: manufactured aggregate.

inlet conveyor was manually fed with the six fractions. Glass detected by the VIS-based sensor unit was ejected via compressed air, splitting the input streams into *glass-depleted-MFs 8–35 mm* and *glass-fractions 8–35 mm*. Both outputs were weighed. As there was no additional removal of extraneous material from the *glass-fractions 8–35 mm*, these fractions do not contain solely glass but also contaminants like metals or ceramics. The *glass-depleted-MFs 8–35 mm* were used for further processing.

2.2.5. Crushing, reunification and aging

The *metal-depleted-MFs 0–8 mm* and the *glass-depleted-MFs* 8–35 mm were divided again to produce *MAG*. In order to receive a homogenous *MAG* with a particle size of 0–8 mm, the *glass-depleted-MFs* 8–35 mm were comminuted batch-wise to < 8 mm by a vibratory roller (BOMAG 65S). Afterward, the material was manually screened at 8 mm and unbreakable particles > 8 mm, such as metals or unburnt material, were removed. This treatment step should simulate a crusher and a screen that could be used in enhanced treatment on an industrial scale. The result was a *comminuted-MF* 0–8 mm.

Subsequently, the *metal-depleted-MFs 0–8 mm* and the *comminuted-MFs 0–8 mm* were reunified with the respective share of each fraction and homogenized, thereby obtaining six *non-aged-MAGs* with a particle size of 0–8 mm. Samples of each *non-aged-MAG* were taken for analysis before aging. The remaining amount was filled into purpose-built aging boxes made from standard Euro-pallets (see Appendix, Figures S1, S2). The layer thickness of the *non-aged-MAGs* in each box was between 100 and 140 mm, accounting for at least 0,1 m^3 of material in each aging box. In those wooden boxes with a permeable fleece base layer, the material was aged for eight weeks indoors under controlled conditions, applying 25 L of regular tap water per m^2 in the beginning, followed by ten liters per m^2 every two weeks. The material was watered cautiously and mixed during the water application. This should ensure good contact with water and that all water was absorbed by the ash, preventing soluble compounds from being washed out with leaking water. This amount was calculated based on the annual precipitation at the plant location (Hohenruppersdorf, Austria) (Land Niederösterreich, 2022). After aging, the *non-aged-MAG* is referred to as *MAG*.

2.3. Mass flows of the enhanced treatment steps

Mass flow calculations were conducted for the experimentally enhanced treatment steps using the software STAN 2.6 (Cencic and Rechberger, 2008). Thereby, the proportions of *glass-fractions*, *metal-depleted-MFs* 0–8 mm and *glass-depleted-MFs* 8–35 mm were displayed for each IBA.

2.4. Evaluation of the glass removal and glass quality

After sensor-based glass sorting, the separated *glass-fractions 8–35 mm*, as well as the remaining *glass-depleted-MFs 8–35 mm*, were weighed. A visual control led to the decision to further process only the *glass-fractions 8–35 mm* from FB-IBA. The glass-fractions from G-IBA were obviously not suitable for high-quality glass recycling. A comparison of glass-fractions from both IBAs is shown in Fig. 3.

The *glass-fractions 8–35 mm* derived from the FB-IBA were sieved into the fractions 0–4 mm, 4–8 mm, 8–16 mm and 16–35 mm. As sieving, especially for flat particles, is imprecise and glass cullet can break during treatment, material < 8 mm was also found in the fraction 8–35 mm. All particle size fractions were weighed. The fractions > 4 mm were then divided to receive at least 1,000 particles in accordance with EN 933–11 (European Committee for Standardization, 2009). Finally, the particles were manually sorted according to their visual appearance into glass, other mineral material (e.g. ceramic, stones, porcelain) and metals. The latter two constituents deteriorate glass recycling and are thus limited in guidelines concerning glass production (Bundesverband Glasindustrie e. V, 2014; Friedrich et al., 2020). The composition of the total *glass-fractions 8–35 mm* was calculated, using the results gained from sieving and manual sorting. The share $x_{c,tot}$ of a component *c* (glass, metal, other mineral material) in the fraction 4–35 mm was calculated with the following equation:

$$x_{c,tot} = \frac{1}{m_{s,4-35}} \sum_f \frac{m_{c,f} * m_{f,s}}{m_{f,ms}}$$

$x_{c,tot}$... *mass fraction of component c in glass-fraction (4–35 mm).*

$m_{c,f}$... *mass of component c in particle size fraction f (result from manual sorting).*

$m_{f,ms}$... *mass of manually sorted material of particle size fraction f.*

$m_{f,s}$... *total mass of particle size fraction f (result from sieving).*

$m_{s,4-35}$... *mass of particle size fractions 4–8 mm, 8–16 mm and 16–35 mm (result from sieving).*

2.5. Evaluation of the MAGs

To evaluate the *MAGs*, relevant parameters of extraneous material and substance contents were determined. The materials used for the evaluation were the *non-aged-MAGs* and the *MAGs* after aging. The results were compared to available literature data.

2.5.1. Manual sorting of the non-aged-MAGs 4–8 mm

The *non-aged-MAGs* (0–8 mm) were sieved through a 4 mm sieve. After sample division, >1,000 particles of the fraction 4–8 mm were manually sorted into the fractions metals, unburnt material, mineral agglomerates (sintered / vitrified compounds), glass and other inert material (i.e. ceramics, stones, porcelain, building material) based on optical appearance. The aim was to assess the content of glass and metals in the *MAGs*, as this should be limited in concrete production (Müller and Rübner, 2006). Furthermore, differences between G-IBA and FB-IBA regarding their constituents could be evaluated.

2.5.2. Determination of the residual metal pieces of the non-aged-MAGs

The share of residual metal pieces (pure metals or alloys) in *MAG* produced from IBA was determined as it is limited in Austrian waste management legislation (BMK, 2023). Based on BMK (2023), about 15 kg of each *non-aged-MAG* were dried, weighed and then comminuted to <4 mm by a vibratory roller (BOMAG 65S). After crushing, the material was sieved to manually remove metals and unburnt material > 4 mm that remained on the sieve. Mineral material > 4 mm was crushed and sieved several times again until only metals and unburnt material remained after sieving. Received metals of each fraction were separated into magnetic (Fe) and non-magnetic (NFe) metals by a hand magnet and weighed. The content of residual metal pieces $x_{Fe,i}$ and $x_{NFe,i}$ was calculated using the equations $x_{Fe,i} = m_{Fe,i}/m_{tot}$ and $x_{NFe,i} = m_{NFe,i}/m_{tot}$, respectively, using the weighed masses of remaining metal pieces ($m_{Fe,i}$, $m_{NFe,i}$) in the respective grain-size fraction *i* (e.g. > 4 mm) and the total mass of the dry sample before crushing (m_{tot}).

In addition to the requirements of Austrian legislation, residual metal pieces > 2 mm and > 1 mm were determined to show the remaining metal piece potential in the fractions 2–4 mm and 1–2 mm. Therefore, the crushed *non-aged-MAG* < 4 mm, which remained after examining residual metal pieces > 4 mm, was sieved with a 2 mm and 1 mm mesh. The fraction 2–4 mm was treated like the fraction > 4 mm previously: the material was consecutively crushed and sieved with a 2 mm mesh until only metal pieces > 2 mm were left. The same procedure was applied to the remaining material 1–2 mm. In the end, residual metal pieces > 4 mm, 2–4 mm and 1–2 mm and a mineral fraction crushed to < 1 mm were obtained. The metal pieces in each fraction were separated into Fe- and NFe-metals with a hand magnet and weighed. The weighed masses were used for calculation.

2.5.3. Chemical analysis of the non-aged-MAGs and MAGs

Chemical analysis included the determination of total and leaching contents of the *MAGs*. Leaching contents were also assessed for the *non-aged-MAGs* in order to evaluate the effects of aging. All parameters defined in BMK, section 4.10.1 (2023) and the Austrian landfill ordinance (DVO, 2008, Appendix 1, table 7 and 8: residual materials landfill) were determined. In section 3, only selected parameters are displayed and discussed as they are required for *MAGs* according to BMK (2023); i.e. total contents of Cd, Cr, Ni, Pb, TOC and leaching contents of pH, As, Cr, Cu, Mo, Ni, Pb, Sb, chloride and sulfate. For each parameter, two limit values are defined by BMK (2023), depending on the different levels of *MAG* addition in concrete production (10% and 20% *MAG* of the total concrete, respectively). All measurements were performed in duplicate.

The total contents of Cd, Cr, Ni and Pb were determined by means of inductively coupled plasma optical emission spectrometry (ICP-OES) (Spectroblue) after an aqua regia-digestion following the standard ÖNORM EN 13657 (European Committee for Standardization, 2002). TOC in the solid samples was measured in accordance with EN 1484 (German Institute for Standardization, 1997). Leaching tests were performed according to EN 16192:2011 (German Institute for Standardization, 2012) and EN 12457–4 (German Institute for Standardization, 2003) with a liquid-to-solid ratio of 1:10 l/kg. Contents of chloride and sulfate in the leachates were detected with ion chromatography (IC Dionex Aquion). The other leachate contents were also analyzed by ICP-OES. The pH value was determined according to DIN 38404 (German Institute for Standardization, 2009).

3. Results

3.1. *Mass flows of the enhanced treatment steps*

Fig. 2 shows the graphical model of the enhanced treatment steps. The values for the mass flows and a pie chart of the proportions of the *glass-fraction 8–35 mm*, the *metal-depleted-MF 0–8 mm* and the *glass-depleted-MF 8–35 mm* are also given for each IBA. The latter two fractions (after removal of minor amounts of metal and unburnt material from *glass-depleted-MFs* 8–35 mm) were reunified to the *non-aged-MAGs*. For the mass flows of the experimental enhanced treatment steps of all IBAs, see Appendix, Figures S3-S8.

These results show that higher shares of *metal-depleted-MFs 0–8 mm* were received from the treatment of G-IBA. This is likely due to the repeated crushing of the particle size fractions > 8 mm of G-IBAs before enhanced treatment and the lower amount of fine fraction that is removed with the fly ash in GI (Blasenbauer et al., 2023; Saqib and Bäckström, 2015). Moreover, FB-IBAs contain a significant amount of *glass-fraction 8–35 mm*, contrary to G-IBAs.

3.2. *Evaluation of the separated glass-fractions 8–35 mm*

The share of *glass-fractions 8–35 mm* removed by sensor-based glass separation was 59% for FB-IBA A, 64% for FB-IBA B, and 73% for FB-IBA C from the input into the sorter (*metal-depleted-MFs 8–35 mm*). Contrary to that, the share of *glass-fractions 8–35 mm* removed from G-IBAs X, Y and Z was 5%, 11% and 26%, respectively. Fig. 3 shows the glass fractions obtained, indicating an apparent optical difference between these.

The calculated results of the manual sorting of the *glass fractions 8–35 mm* of FB-IBAs are shown in Fig. 4.

Manual sorting of the *glass-fractions 8–35 mm* from FB-IBA showed that all of them consist of>80% glass, with variations between 86% and 98%. What also stands out in Fig. 4 is that the particle size fraction 8–16 mm dominates with 71–76%. This finding aligns with data from Huber et al. (2020) and Šyc et al. (2018), who also report the most glass in this fraction.

3.3. *Evaluation of the MAGs*

3.3.1. *Composition of the non-aged-MAGs*

Fig. 5 shows *MAG* from an FB-IBA and a G-IBA, indicating clear differences in the composition of *MAGs* from different firing technologies.

The results of sieving at 4 mm particle size and the subsequent manual sorting of particle sizes 4–8 mm of the *non-aged-MAGs* can be found in Fig. 6.

The shares of metal and unburnt material are relatively low (all <

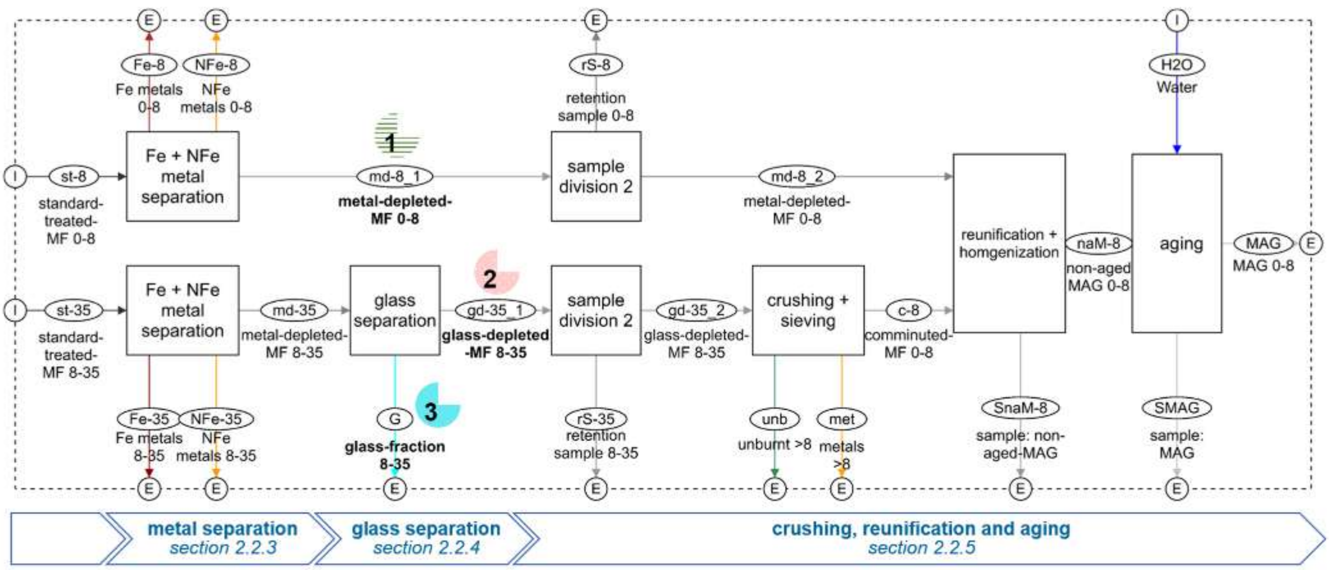

fraction	unit	no.	FB-IBA A	FB-IBA B	FB-IBA C	G-IBA X	G-IBA Y	G-IBA Z
metal-depleted-MF 0-8	kg	1	562	378	266	397	345	343
glass-depleted-MF 8-35	kg	2	146	207	150	179	111	66
glass-fraction 8-35	kg	3	211	364	406	10	14	23

share of remaining IBA fractions after enhanced IBA treatment

Fig. 2. Model of the enhanced treatment and mass flow results for the glass-fraction 8–35 mm, metal-depleted-MF 0–8 mm and glass-depleted-MF 8–35 mm. (Note that the glass-fraction 8–35 mm contains extraneous material, as described in section 3.2.). E: export flow of the system, I: import flow into the system, MAG: manufactured aggregate, MF: mineral fraction.

Fig. 3. Sensor-based separated glass-fractions 8–35 mm from incineration bottom ashes from fluidized bed (top) and from grate (bottom).

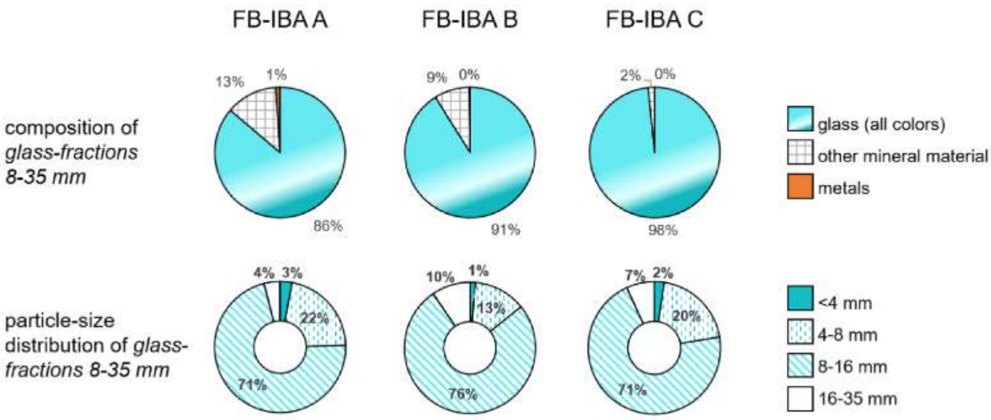

Fig. 4. Results from manual sorting of the FB-IBA glass-fractions 8–35 mm and their particle size distribution.

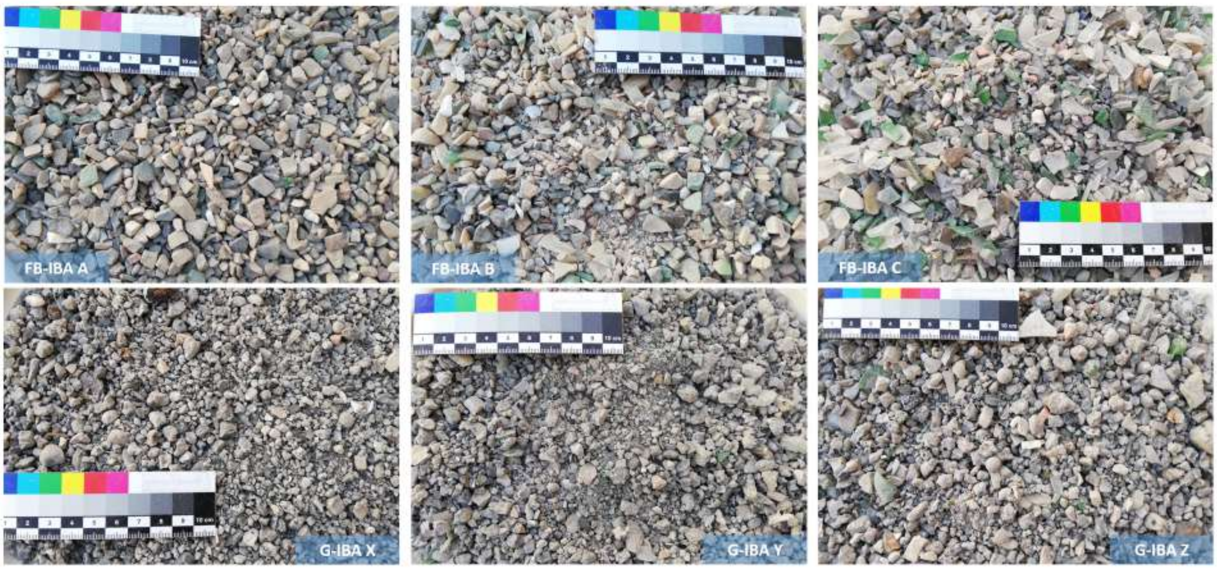

Fig. 5. MAG from incineration bottom ashes from fluidized bed (top) and grate (bottom).

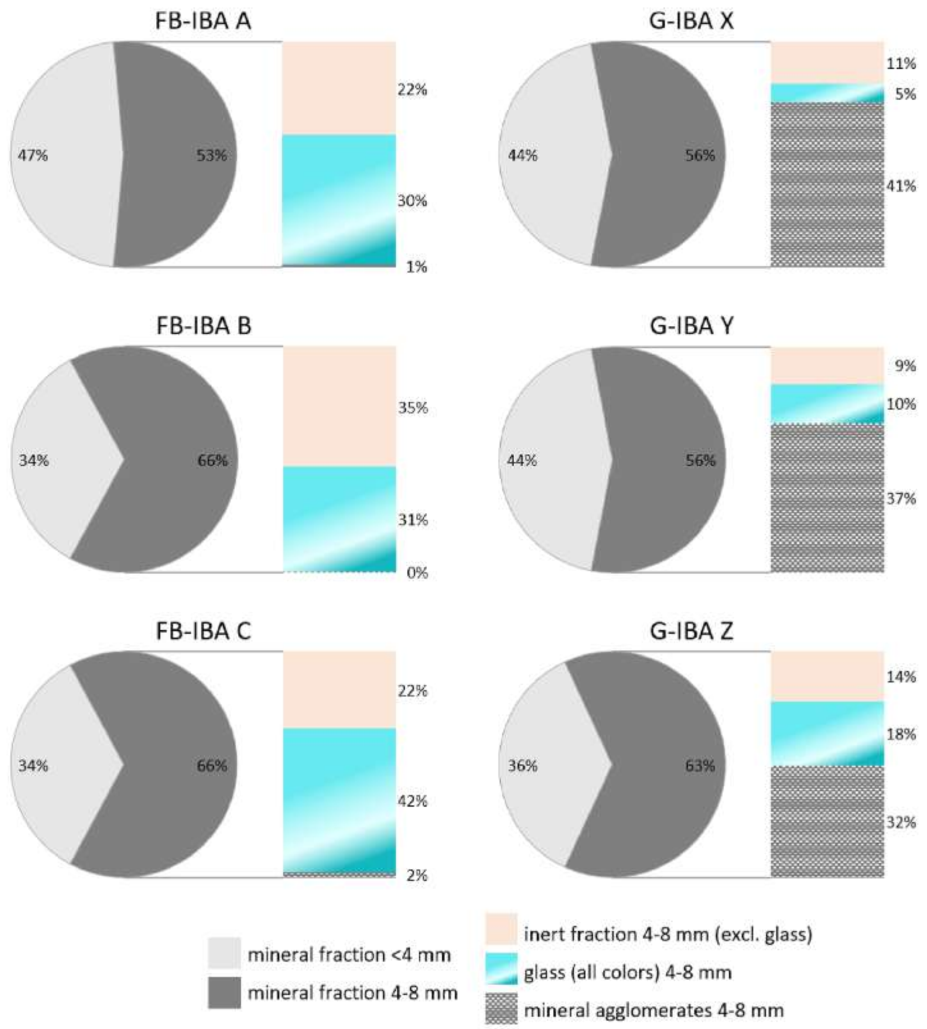

Fig. 6. Composition of the non-aged-MAGs made from incineration bottom ashes from fluidized bed (left) and from grate (right). Only fractions > 1% are shown. All values are shown in the Appendix, Table S1.

Table 2
Residual metal piece contents, total and leaching contents. Dm: dry matter, FBC: fluidized bed combustion, GI: grate incineration, MAG: manufactured aggregate.

Parameter	Unit (dm)	Limit value (% *MAG* in concrete)		*MAG* 0–8 mm from IBA of different FBC and GI MSWI plants					
		≤10%	≤20%	FB-IBA A	FB-IBA B	FB-IBA C	G-IBA X	G-IBA Y	G-IBA Z
Residual metal piece contents									
Fe > 4 mm	%	0.5	0.5	0.00	0.00	0.00	0.02	0.03	0.00
Fe > 2 mm	%	–	–	0.00	0.00	0.00	0.03	0.05	0.02
NFe > 4 mm	%	0.4	0.4	0.11	0.03	0.04	0.17	0.21	0.14
NFe > 2 mm	%	–	–	0.18	0.04	0.08	0.39	0.50	0.43
Total contents									
Cd	mg/kg	4	3	0.63	1.52	1.98	2.34	2.44	2.19
Cr	mg/kg	500	400	62	44	51	610**	186	177
Ni	mg/kg	200	200	38	13	25	162	123	82
Pb	mg/kg	600	500	125	208	229	248	426	576*
TOC	%	1.0	1.0	0.47	0.54	0.48	0.81	1.41**	0.99
Leaching contents									
pH		12	12	10.2	10.0	9.0	10.7	9.1	9.5
As	mg/kg	0.5	0.5	<0.007	<0.007	<0.007	<0.007	<0.007	<0.007
Cr	mg/kg	0.5	0.5	<0.001	0.10	<0.001	1.99**	<0.001	0.09
Cu	mg/kg	2.0	2.0	<0.03	<0.03	<0.03	<0.03	<0.03	<0.03
Mo	mg/kg	0.8	0.8	0.18	0.10	0.13	0.52	0.69	0.28
Ni	mg/kg	0.4	0.4	<0.004	<0.004	<0.004	<0.004	<0.004	<0.004
Pb	mg/kg	0.5	0.5	<0.02	<0.02	<0.02	<0.02	<0.02	<0.02
Sb	mg/kg	0.6	0.6	0.04	0.05	<0.02	0.03	0.03	0.03
Chloride	mg/kg	2,500	2,000	670	850	1,000	2,200*	1,900	1,900
Sulfate	mg/kg	5,000	3,000	4,000*	1,500	3,000	3,100*	1,600	2,100

* Exceedance of limit value for 20% MAG-addition.
** Exceedance of limit value for 10% MAG-addition.

1%), which demonstrates the good performance of the treatment conducted. The fraction 4–8 mm makes up 34–47% of the *non-aged-MAGs*. Regarding this, no significant differences between G-IBA and FB-IBA were observed, although the fraction 8–35 mm of G-IBA was crushed three times during the processing and more fine fraction is transferred to fly ash in FBC and can therefore not be found in the FB-IBA.

Obvious differences in the composition of FB-IBAs and G-IBAs appear for the other constituents. The glass rates in the *non-aged-MAGs* from FB-IBAs range from 30 to 42%, whereas for *MAGs* from GI, the maximum glass share was 18%. The remaining glass in the *MAGs* mainly derives from glass in the *metal-depleted-MF 0–8 mm* and should not be misinterpreted as poor glass separation as this fraction did not undergo glass separation.

What is also apparent from Fig. 6 is that the *non-aged-MAGs* from G-IBAs contain an additional type of particle. These particles can be described as mineral agglomerates, comprising sintered and vitrified ash compounds, respectively, that cannot originally be found in MSW in this form (Joseph et al., 2018; Quicker and Stockschläder, 2018), but are built during the firing or quenching process (Bayuseno and Schmahl, 2010). This fraction constitutes 32–41% of the *non-aged-MAG* from G-IBA and scarcely appears in FB-IBA.

3.3.2. *Residual metal piece content of the non-aged-MAGs*

The content of residual metal pieces is shown in Table 2 for magnetic (Fe) and non-magnetic (NFe) metals determined in the *non-aged-MAGs* > 4 mm and > 2 mm. Results for the fraction > 1 mm are given in the Appendix, Table S2. The content of Fe-metals is significantly lower than NFe-metals for all MSWI plants. Although more Fe-metals than NFe-metals can be found in MSW and its corresponding IBA, this shows that removing Fe-metals in IBA processing is more effective (Bruno et al., 2021; Dou et al., 2017). Another ascertainment is that higher rates of both magnetic and non-magnetic metals were found in the *non-aged-MAGs* from G-IBAs. Moreover, the comparison of residual metal pieces > 4 mm and > 2 mm shows that there is still some metal recovery potential in the fine fraction, especially for G-IBA, as metal separation from finer particle size fractions is more complex (Bunge, 2018).

3.3.3. *Chemical composition of the MAGs*

Chemical analysis delivered the total and leaching contents of the *MAGs* given in Table 2 for the relevant parameters according to BMK (2023). Additional values of total and leaching contents according to the Austrian landfill ordinance (DVO, 2008), as well as leaching contents of the *non-aged-MAGs* according to BMK (2023), are shown in the Appendix (Table S3, S4).

It is apparent that nearly all total contents measured show higher values for *MAG* from G-IBAs than from FB-IBAs. The comparison of the leachate contents of the *MAGs* and the *non-aged-MAGs* (see Appendix, Table S4) reveals some common tendencies with regard to the results in the literature (Hykš and Astrup, 2009; Luo et al., 2019). Through carbonatization reactions, aging leads to decreasing pH values and lower leaching rates, especially for elements like Cu, Pb and to some extent Cr, which was also shown in the present experiment. Contrary to these, increasing values for sulfate were found, which were also reported by Astrup (2007), Grosso et al. (2011) and Polettini and Pomi (2004). For Sb, a decrease after aging was observed. It would go beyond the scope of this paper to find an exact explanation for this result as the leaching behavior of Sb in IBA is very complex and discussed ambiguously in the literature (Blasenbauer et al., 2023; Santos et al., 2013; Simon et al., 2021; Todorovic and Ecke, 2006; van Caneghem et al., 2016; Verbinnen et al., 2017).

4. Discussion

4.1. *Assessment of the enhanced treatment*

Both the manual sorting of the *non-aged-MAGs* and the determination of residual metal pieces indicate an extensive removal of metal pieces in the enhanced treatment compared to the input metal content of IBAs.

Regarding total contents of Cd, Cr, Pb and Ni, generally lower values were achieved through the enhanced IBA treatment investigated than in comparable studies, which conducted wet or dry IBA treatment (Allegrini et al., 2014; Glauser et al., 2021; Huber, 2020; Kalbe and Simon, 2020). Comparison with Huber (2020) also indicates that modeled results for “plant B”, which corresponds to the standard treatment in the present study, showed higher total contents for the parameters selected, except for Ni in G-IBAs. This demonstrates an improvement through the enhanced treatment. Especially the additional metal separation step (see section 2.2.3) is presumably causing lower total contents of the heavy metals mentioned, as this is only applied in the present study. Nevertheless, it has to be mentioned that the enhanced treatment in this study was conducted on a pilot scale and aging was performed indoors under controlled circumstances. These conditions can possibly lead to better results. Hence, large-scale experiments should be conducted to determine the performance of an industrial enhanced treatment. A more detailed examination of the enhanced treatment is also necessary to demonstrate that heavy metals are enriched in other output flows (e.g. metal fractions or heavy fine fractions). Thereby, it can be excluded that the lower heavy metal contents in the mineral fraction of this study are caused by MSWI input with little metal contamination.

Additionally, similar or better results for processed IBA were reported with respect to the wet IBA treatment investigated by Sorlini et al. (2017), who performed intense washing of sieved IBA fractions after metal separation. Particularly, leachate values of chloride and sulfate were clearly lower than in the present enhanced treatment. This is also the case for the work of Keulen et al. (2016), who applied aging, washing and multiple metal separation to the IBAs. Therefore, additional washing of aged and enhanced-treated IBAs should be further examined to remove soluble salts (Abbas et al., 2003).

Regarding glass separation as part of the enhanced treatment, it could be shown that recovery of the high amount of glass cullet from the mineral fraction of FB-IBA is technically feasible and could contribute to resource conservation.

4.2. *Suitability of the MAGs for concrete production in Austria*

Austrian threshold limits for residual metal pieces, as defined in BMK (2023) for utilization as *MAG* in concrete, can easily be achieved by applying the enhanced treatment (3.3.3). Concerning pollutant contents, chemical analysis showed that *MAGs* derived from FBC maintain all limit values for their use at 10% in concrete. The limit values for using 20% *MAG* in concrete are only exceeded by sulfate in FB-IBA A. A few more exceedances can be seen for *MAG* from GI. G-IBA Y surpasses the limit value for TOC and would, therefore, not be allowed as an aggregate in concrete. G-IBA X would also be excluded from its use as an aggregate due to high contents of Cr (total and leaching content). A possible explanation for this exceedance of G-IBA X is the high share of industrial and commercial waste incinerated in this GI plant (see Table 1). Furthermore, information from the plant operator suggests that the high Cr content in this *MAG* could be traced back to waste from the leather industry, which is incinerated in this plant and a potential source of Cr in MSW (Viczek et al., 2020).

Considering that none of the standard IBA treatment plants investigated by Huber (2020) can produce *MAG* suitable for standard concrete in Austria (only “plant B” and “plant C” comply with the stipulated total content for Ni), the results obtained are remarkable, especially for *MAGs* from FBC.

Nevertheless, the technical suitability of the *MAGs* produced has to be investigated. For example, further reduction of soluble salts is essential as this is required by concrete standards for technical reasons (Alderete et al., 2021; Austrian Standards Institute, 2018). As mentioned in section 4.1, this could be achieved by additional and intense washing, as also suggested by Abbas et al. (2003), Alderete et al. (2021) and

Sorlini et al. (2017). Furthermore, removing the fine fraction could improve the MAG's quality, as leachable Cl and heavy metals like Cd, Pb, Sb or Zn are enriched in the fine fraction (Glauser et al., 2021; Vateva and Laner, 2020). Reducing the content of soluble salts by means of treatment with sodium compounds could also be beneficial, hence more complex and material-consuming (Rübner et al., 2008; Saikia et al., 2015).

4.3. Assessment of the glass-fractions from FB-IBAs

In section 3.2, different contaminant rates were observed for the *glass-fractions 8–35 mm* from FB-IBAs. The highest share of extraneous material was found for FB-IBA A. The corresponding FBC plant incinerates the highest share of industrial and commercial waste. Conversely, FB-IBA C, which shows the lowest share of contaminants, originates from a plant that primarily incinerates pretreated MSW. MSW contains higher packaging glass amounts than industrial and commercial waste. This leads to the assumption that the input waste of FBC is decisive regarding the glass recycling potential of IBAs. Considering that lower separate collection rates are reported for densely populated areas (Lederer et al., 2022; Schuch et al., 2023) and that four times more glass per capita is found in mixed MSW from urban than from rural areas (Beigl, 2020), this can be an important factor for glass removal from FB-IBAs.

The manual sorting of the *non-aged-MAG* of FB-IBAs (Fig. 6) shows that large amounts of glass can still be found in the *MAG* if glass is not removed from the *metal-depleted-MF 0–8 mm*. It can thus be suggested that glass removal from the mineral fractions 4–8 mm could be considered to further increase the recovered amounts.

Nevertheless, the amount of contaminants in the *glass-fractions 8–35 mm* is high compared to the strict regulations of the glass packaging industry for glass cullet (Bundesverband Glasindustrie e.V, 2014). Relevant limit values are, for instance, 2 and 3 g/t for Fe- and NFe-metals, respectively, and 20 g/t for ceramic (Friedrich et al., 2020). Still, this result should not be misleading as several processing steps are usually necessary for post-consumer glass cullet to meet the regulations (Scalet et al., 2013). Therefore, further treatment of the separated *glass-fraction 8–35 mm* should be subject to future investigations. Additional removal of contaminants from the glass-fractions, including lead glass and glass ceramics, could deliver improved results.

4.4. Differences between FB-IBA and G-IBA

Various differences between FB-IBAs and G-IBAs were observed. This was expected, considering the different firing conditions and discharge types in FBC and GI and related findings in the literature. As all MSWI plants considered primarily use Austrian MSW in untreated or pre-treated form, the waste composition cannot be expected to be the predominant cause for these tendencies observed. For FBC, lower temperature and retention time as well as a higher incineration efficiency and turbulence, are reported (Blasenbauer et al., 2023; Jung et al., 2004; Nedkvitne et al., 2021; Saqib and Bäckström, 2014; van Caneghem et al., 2012). This, on the one hand, leads to better conversion of the waste and, in combination with dry IBA discharge, to cleaner outputs such as glass and metals. Still, on the other hand, higher shares of fly ash per unit of incinerated MSW compared to GI are produced. As many trace metals accumulate in the fly ash, G-IBAs show higher total and leachate values than FB-IBAs (Jung et al., 2004; Nedkvitne et al., 2021; Saqib and Bäckström, 2015, 2014), which could also be seen in the present study. Moreover, a higher content of residual metal pieces was found in G-IBAs compared to FB-IBAs. These results might be attributed to the mineral agglomerates inherent to the G-IBAs, which contain enclosed metal pieces which are unavailable for separation. This is also shown through a comparison of the results of residual metal pieces for > 4 mm, >2mm and >1 mm: in the G-IBAs of the latter two, there is still some metal potential, particularly of NFe.

For G-IBAs, also the share of glass is clearly lower. This counts for the *glass-fractions 8–35 mm*. Also, the *standardly-treated-MFs 0–8 mm* from G-IBAs contain less glass than those from FB-IBAs (Fig. 6). This contradicts the assumption that glass from G-IBA is comminuted during the additional crushing in the pre-treatment stage, thus accumulating in the *standardly-treated-MFs 0–8 mm*, which could be concluded from Fig. 2. Hence, a generally lower glass content in G-IBAs can be claimed. This may primarily be explained by melting and merging of glass cullet together with other IBA constituents to mineral agglomerates in GI, as also reported by Blasenbauer et al. (2023) and Bayuseno and Schmahl (2010). Further reasons for the lower glass amounts removed from G-IBA can be assumed to be due to the higher surface contamination of glass from GI (see Fig. 3), which impedes the sensor-based sorting of glass (Makari, 2014). Furthermore, the higher share of fly ash produced in FBC leads to a higher relative glass content in FB-IBAs as all glass from MSWI is assumed to end up in the IBA (Blasenbauer et al., 2023).

5. Conclusions

IBA from MSWI is an important source of secondary raw material. The present study shows that through enhanced treatment of IBAs not only large amounts of metals, but also glass can be recovered and the mineral fraction can potentially be used as *MAG* in concrete. In general, significant differences between FB-IBAs and G-IBAs were observed in this study.

The findings of this study indicate that FB-IBAs show some advantages regarding their recyclability compared to G-IBAs. Higher rates of glass can be separated and potentially be recycled. Moreover, the *MAGs* from enhanced IBA treatment are more suitable for utilization in concrete from a legal point of view. However, the higher sulfate content of FB-IBAs can be challenging for concrete production from a technical perspective (Alderete et al., 2021). Moreover, the higher amount of fly ash produced by FBC has to be considered as it also needs to be disposed of or utilized (Saqib and Bäckström, 2014).

The results presented are fundamental to assess, whether FBC or GI is environmentally and economically more beneficial. For an encompassing determination, an LCA study, including MSW pretreatment, bottom and fly ash disposal as well as resource savings through the recyclability of the glass and mineral fraction from IBA of the two firing technologies could be suitable. For a comprehensive comparison, also dry discharge of G-IBA should be evaluated, as this is reported to be beneficial for metal recovery from G-IBA (Back and Sakanakura, 2022; Lamers, 2015). To include economic aspects of FBC and GI, also an eco-efficiency analysis could be conducted.

However, additional research has to be done in order to use the full potential of glass and minerals in IBAs. Further investigations should focus on reducing extraneous material in glass fractions through enhanced glass treatment. Additionally, upscaled experiments with an enhanced IBA treatment on an industrial scale could be conducted. Since the treatment plant of *Brantner Österreich GmbH* was recently extended by the enhanced treatment steps assessed in this study, such upscaled investigations are in implementation. Combined with subsequent concrete production tests, it can be determined whether technical requirements for *MAG* as defined in concrete standards can be met.

Declaration of Competing Interest

The authors declare that they have no known competing financial interests or personal relationships that could have appeared to influence the work reported in this paper.

Data availability

Data will be made available on request.

Acknowledgments

The financial support by the Austrian Federal Ministry for Digital and Economic Affairs, the National Foundation for Research, Technology and Development and the Christian Doppler Research Association is gratefully acknowledged. Furthermore, we thankfully acknowledge the financial and non-financial support of our company partners Brantner Österreich GmbH, Linz Service GmbH, Wien Energie GmbH, and Wopfinger Transportbeton Ges.m.b.H. In addition, we thank Magistratsabteilung MA48, the public Waste Management provider of Vienna, for its non-financial support, Binder + Co AG and IFE Aufbereitungstechnik GmbH for their experimental support and Felix Feher for his hard work. The TU Wien Bibliothek is thanked for financial support through its Open Access Funding Program.

Appendix A. Supplementary data

Supplementary data to this article can be found online at https://doi.org/10.1016/j.wasman.2023.05.048.

References

Abbas, Z., Moghaddam, A.P., Steenari, B.-M., 2003. Release of salts from municipal solid waste combustion residues. Waste Management 23, 291–305. https://doi.org/10.1016/S0956-053X(02)00154-X.

Abis, M., Bruno, M., Kuchta, K., Simon, F.-G., Grönholm, R., Hoppe, M., Fiore, S., 2020. Assessment of the Synergy between Recycling and Thermal Treatments in Municipal Solid Waste Management in Europe. Energies 13, 6412. https://doi.org/10.3390/en13236412.

Alderete, N.M., Joseph, A.M., van den Heede, P., Matthys, S., de Belie, N., 2021. Effective and sustainable use of municipal solid waste incineration bottom ash in concrete regarding strength and durability. Resources, Conservation and Recycling 167, 105356. https://doi.org/10.1016/j.resconrec.2020.105356.

Allegrini, E., Maresca, A., Olsson, M.E., Holtze, M.S., Boldrin, A., Astrup, T.F., 2014. Quantification of the resource recovery potential of municipal solid waste incineration bottom ashes. Waste management (New York N.Y.) 34, 1627–1636. https://doi.org/10.1016/j.wasman.2014.05.003.

Astrup, T., 2007. Pretreatment and utilization of waste incineration bottom ashes: Danish experiences. Waste Management 27, 1452–1457. https://doi.org/10.1016/j.wasman.2007.03.017.

Astrup, T., Muntoni, A., Polettini, A., Pomi, R., van Gerven, T., van Zomeren, A., 2016. Treatment and Reuse of Incineration Bottom Ash. Environmental Materials and Waste. Elsevier 607–645.

ÖNORM B4710-1: Beton — Festlegung, Eigenschaften, Herstellung, Verwendung und Konformität: Teil 1: Regeln zur Umsetzung der ÖNORM EN 206 für Normal- und Schwerbeton [Concrete — Specification, performance, production, use and conformity — Part 1: Rules for the implementation of ÖNORM EN 206 for normal and heavy concrete] 91.100.30.

Back, S., Sakanakura, H., 2022. Comparison of the efficiency of metal recovery from wet- and dry-discharged municipal solid waste incineration bottom ash by air table sorting and milling. Waste management (New York N.Y.) 154, 113–125. https://doi.org/10.1016/j.wasman.2022.08.023.

Bayuseno, A.P., Schmahl, W.W., 2010. Understanding the chemical and mineralogical properties of the inorganic portion of MSWI bottom ash. Waste management (New York N.Y.) 30, 1509–1520. https://doi.org/10.1016/j.wasman.2010.03.010.

Beigl, P., 2020. Auswertung der Restmüllzusammensetzung in Österreich 2018/2019: Ergebnisbericht [Evaluation of the residual waste composition in Austria 2018/2019]. Institut für Abfallwirtschaft, Universität für Bodenkultur Wien, Wien. https://www.bmk.gv.at/dam/jcr:c034808f-c67d-4eab-b2a3-30a6bcd6d0eb/Restmuell-Zusammensetzung-2018-19.pdf (accessed 07.06.22).

Blasenbauer, D., Huber, F., Lederer, J., Quina, M.J., Blanc-Biscarat, D., Bogush, A., Bontempi, E., Blondeau, J., Chimenos, J.M., Dahlbo, H., Fagerqvist, J., Giro-Paloma, J., Hjelmar, O., Hyks, J., Keaney, J., Lupsea-Toader, M., O'Caollai, C.J., Orupõld, K., Pająk, T., Simon, F.-G., Svecova, L., Šyc, M., Ulvang, R., Vaajasaari, K., Van Caneghem, J.o., van Zomeren, A., Vasarevičius, S., Wégner, K., Fellner, J., 2020. Legal situation and current practice of waste incineration bottom ash utilisation in Europe. Waste management (New York N.Y.) 102, 868–883. https://doi.org/10.1016/j.wasman.2019.11.031.

Blasenbauer, D., Huber, F., Mühl, J., Fellner, J., Lederer, J., 2023. Comparing the quantity and quality of glass, metals, and minerals present in waste incineration bottom ashes from a fluidized bed and a grate incinerator. Waste management (New York, N.Y.) 161, 142–155. https://doi.org/10.1016/j.wasman.2023.02.021.

BMK, 2023. Bundes-Abfallwirtschaftsplan 2023, Teil 1 [Austrian Federal Waste Management Plan]. Bundesministerium für Klimaschutz, Umwelt, Energie, Mobilität, Innovation und Technologie, Wien, 490 pp.

Bruno, M., Abis, M., Kuchta, K., Simon, F.-G., Grönholm, R., Hoppe, M., Fiore, S., 2021. Material flow, economic and environmental assessment of municipal solid waste incineration bottom ash recycling potential in Europe. Journal of Cleaner Production 317, 128511. https://doi.org/10.1016/j.jclepro.2021.128511.

Bundesverband Glasindustrie e.V; BDE Bundesverband der Deutschen Entsorgungs-, Wasser- und Rohstoffwirtschaft e. V; bvse-Bundesverband Sekundärrohstoffe und Entsorgung e.V., 2014. Leitlinie „Qualitätsanforderungen an Glasscherben zum Einsatz in der Behälterglasindustrie": Standardblatt T 120.

Bunge, R., 2018. Recovery of Metals from Waste Incineration Bottom Ash. In: Holm, O., Thomé-Kozmiensky, E. (Eds.), Removal, treatment and utilisation of waste incineration bottom ash. Thomé-Kozmiensky Verlag GmbH, Nietwerder, pp. 63–143.

Cencic, O., Rechberger, H., 2008. Material flow analysis with software STAN. J. Environ. Eng. Manage. 2008, 3–7.

Chimenos, J., Segarra, M., Fernández, M., Espiell, F., 1999. Characterization of the bottom ash in municipal solid waste incinerator. Journal of hazardous materials 64, 211–222. https://doi.org/10.1016/S0304-3894(98)00246-5.

Del Valle-Zermeño, R., Gómez-Manrique, J., Giro-Paloma, J., Formosa, J., Chimenos, J. M., 2017. Material characterization of the MSWI bottom ash as a function of particle size. Effects of glass recycling over time. Science of The Total Environment 581–582, 897–905. https://doi.org/10.1016/j.scitotenv.2017.01.047.

Dhir, R.K., de Brito, J., Lynn, C.J., Silva, R.V., 2018. Sustainable Construction Materials: Municipal Incinerated Bottom Ash. Elsevier.

Dou, X., Ren, F., Nguyen, M.Q., Ahamed, A., Yin, K., Chan, W.P., Chang, V.-W.-C., 2017. Review of MSWI bottom ash utilization from perspectives of collective characterization, treatment and existing application. Renewable and Sustainable Energy Reviews 79, 24–38. https://doi.org/10.1016/j.rser.2017.05.044.

DVO, 2008. Verordnung des Bundesministers für Land- und Forstwirtschaft, Umwelt und Wasserwirtschaft über Deponien: DVO 2008 [Austrian landfill ordinance].

European Committee for Standardization, 2002. Characterization of waste - Digestion for subsequent determination of aqua regia soluble portion of elements: Charakterisierung von Abfällen. Aufschluss zur anschließenden Bestimmung des in Königswasser löslichen Anteils an Elementen in Abfällen. Berlin 13.030.40.

European Committee for Standardization, 2009. Tests for geometrical properties of aggregates: Part 11: Classification test for the constituents of coarse recycled aggregate 91.100.15.

Fan, C., Wang, B., Ai, H., Liu, Z., 2022. A comparative study on characteristics and leaching toxicity of fluidized bed and grate furnace MSWI fly ash. Journal of environmental management 305, 114345. https://doi.org/10.1016/j.jenvman.2021.114345.

Friedrich, K., Holzschuster, S., Fritz, T., Pomberger, R., Aldrian, A., 2020. Benchmark Analysis for Recycled Glass in Austrian Waste Management. Detritus 87–98. https://doi.org/10.31025/2611-4135/2020.14038.

Gerlach, R.W., Nocerino, J.M., 2003. Guidance for Obtaining Representative Laboratory Analytical Subsamples from Particulate Laboratory Samples. Environmental Protection Agency, U.S https://clu-in.org/download/char/epa_subsampling_guidance.pdf (accessed 14.12.22).

German Institute for Standardization, 1997. DIN EN 1484: Water analysis - Guidelines for the determination of total organic carbon (TOC) and dissolved organic carbon (DOC) 13.060.01.

German Institute for Standardization, 2003. DIN EN 12457-4: Charakterisierung von Abfällen. Auslaugung - Übereinstimmungsuntersuchung für die Auslaugung von körnigen Abfällen und Schlämmen: Teil 4: Einstufiges Schüttelverfahren mit einem Flüssigkeits-/Feststoffverhältnis von 10 l/kg für Materialien mit einer Korngröße unter 10 mm (ohne oder mit Korngrößenreduzierung) [Characterization of waste - Leaching; Compliance test for leaching of granular waste materials and sludges - Part 4: One stage batch test at a liquid to solid ratio of 10 l/kg for materials with particle size below 10 mm (without or with limited size reduction)]. Beuth Verlag GmbH, Berlin 13.030.10; 13.030.20.

German Institute for Standardization, 2009. DIN 38404-5: German standard methods for the examination of water, waste water and sludge - Physical and physico-chemical characteristics (group C) - Part 5: Determination of pH value (C 5), 07th ed. 13.060.60.

German Institute for Standardization, 2012. DIN EN 16192: Charakterisierung von Abfällen – Analyse von Eluaten: Deutsche Fassung EN 16192:2011. Berlin 13.030.99.

Glauser, A., Weibel, G., Eggenberger, U., 2021. Effects of enhanced metal recovery on the recycling potential of MSWI bottom ash fractions in various legal frameworks. Waste management & research : the journal of the International Solid Wastes and Public Cleansing Association, ISWA 39, 1459–1470. https://doi.org/10.1177/0734242X211038149.

Grosso, M., Biganzoli, L., Rigamonti, L., 2011. A quantitative estimate of potential aluminium recovery from incineration bottom ashes. Resources, Conservation and Recycling 55, 1178–1184. https://doi.org/10.1016/j.resconrec.2011.08.001.

Hauer, W., Zerz, H.-J., Schöner, H., 2014. Abtrennung und Verwertung von Glas aus Wirbelschicht-Bettasche, in: Pomberger, R. (Ed.), Abfallwirtschaft, Abfallverwertung und Recycling, Deponietechnik und Altlasten: DepoTech 2014; Tagungsband zur 12. DepoTech-Konferenz, Montanuniversität Leoben, Österreich, 4. - 7. November 2014. Abfallverwertungstechnik & Abfallwirtschaft, Leoben.

Holm, O., Simon, F.-G., 2017. Innovative treatment trains of bottom ash (BA) from municipal solid waste incineration (MSWI) in Germany. Waste Management 59, 229–236. https://doi.org/10.1016/j.wasman.2016.09.004.

Huber, F., Blasenbauer, D., Aschenbrenner, P., Fellner, J., 2020. Complete determination of the material composition of municipal solid waste incineration bottom ash. Waste management (New York, N.Y.) 102, 677–685. https://doi.org/10.1016/j.wasman.2019.11.036.

Huber, F., 2020. Modelling of material recovery from waste incineration bottom ash. Waste management (New York, N.Y.) 105, 61–72. https://doi.org/10.1016/j.wasman.2020.01.034.

Hykš, J., Astrup, T., 2009. Influence of operational conditions, waste input and ageing on contaminant leaching from waste incinerator bottom ash: a full-scale study.

Chemosphere 76, 1178–1184. https://doi.org/10.1016/j.chemosphere.2009.06.040.
Inkaew, K., Saffarzadeh, A., Shimaoka, T., 2016. Modeling the formation of the quench product in municipal solid waste incineration (MSWI) bottom ash. Waste management (New York, N.Y.) 52, 159–168. https://doi.org/10.1016/j.wasman.2016.03.019.
ISWA, 2012. Waste-to-Energy State-of-the-Art-Report: Statistics 6th Edition. Data 2012. ISWA - the International Solid Waste Association. https://www.nswai.org/docs/ISWA6_7-000-2_WtE_State_of_the_Art_Report_2012_Revised_November_2013.pdf (accessed 15.11.22).
Joseph, A., Snellings, R., Van den Heede, P., Matthys, S., De Belie, N., 2018. The Use of Municipal Solid Waste Incineration Ash in Various Building Materials: A Belgian Point of View. Materials (Basel, Switzerland) 11 (1). https://doi.org/10.3390/ma11010141.
Jung, C., Matsuto, T., Tanaka, N., Okada, T., 2004. Metal distribution in incineration residues of municipal solid waste (MSW) in Japan. Waste Management 24, 381–391. https://doi.org/10.1016/S0956-053X(03)00137-5.
Kalbe, U., Simon, F.-G., 2020. Potential Use of Incineration Bottom Ash in Construction: Evaluation of the Environmental Impact. Waste Biomass Valor 11, 7055–7065. https://doi.org/10.1007/s12649-020-01086-2.
Keulen, A., van Zomeren, A., Harpe, P., Aarnink, W., Simons, H.A.E., Brouwers, H.J.H., 2016. High performance of treated and washed MSWI bottom ash granulates as natural aggregate replacement within earth-moist concrete. Waste management (New York, N.Y.) 49, 83–95. https://doi.org/10.1016/j.wasman.2016.01.010.
Lamers, F., 2015. Treatment of Bottom Ashes of Waste-to-Energy Installations – State of the Art –. In: Waste management. TK-Verl. Thomé-Kozmiensky, Nietwerder-Neuruppin, pp. 271–290.
Leckner, B., Lind, F., 2020. Combustion of municipal solid waste in fluidized bed or on grate - A comparison. Waste management (New York, N.Y.) 109, 94–108. https://doi.org/10.1016/j.wasman.2020.04.050.
Lederer, J., Gassner, A., Kleemann, F., Fellner, J., 2020. Potentials for a circular economy of mineral construction materials and demolition waste in urban areas: a case study from Vienna. Resources, Conservation and Recycling 161, 104942. https://doi.org/10.1016/j.resconrec.2020.104942.
Lederer, J., Bartl, A., Blasenbauer, D., Breslmayer, G., Gritsch, L., Hofer, S., Lipp, A.-M., Mühl, J., 2022. A review of recent trends to increase the share of post-consumer packaging waste to recycling in Europe. Detritus 3–17. https://doi.org/10.31025/2611-4135/2022.15198.
Luo, H., Cheng, Y., He, D., Yang, E.-H., 2019. Review of leaching behavior of municipal solid waste incineration (MSWI) ash. The Science of the total environment 668, 90–103. https://doi.org/10.1016/j.scitotenv.2019.03.004.
Makari, C., 2014. Optical Sorting for the Recovery of Glass from WIP Slags: – Pilot Plant in Bratislava –. In: Thomé-Kozmiensky, K.J., Thiel, S. (Eds.), Waste management. TK-Verl, Thomé-Kozmiensky, Neuruppin, pp. 345–354.
Maldonado-Alameda, A., Mañosa, J., Miro-Escola, J., Quintero-Payan, A.C., Chimenos, J. M., 2023. Fluidised-bed incineration bottom ash as the sole precursor of alkali-activated binders: A comparison with bottom ash from grate incinerators. Construction and Building Materials 364, 130001. https://doi.org/10.1016/j.conbuildmat.2022.130001.
Mehr, J., Haupt, M., Skutan, S., Morf, L., Raka Adrianto, L., Weibel, G., Hellweg, S., 2021. The environmental performance of enhanced metal recovery from dry municipal solid waste incineration bottom ash. Waste management (New York, N.Y.) 119, 330–341. https://doi.org/10.1016/j.wasman.2020.09.001.
Mühl, J., Feher, F., Skutan, S., Stockinger, G., Lederer, J., 2022. Rost- oder Wirbelschichtfeuerung bei Abfallverbrennungsanlagen: Was ist aus Sicht der Kreislaufwirtschaft von MVA-Aschen zu bevorzugen? In: Thiel, S., Thomé-Kozmiensky, E., Senk, D.G., Wotruba, H., Antrekowitsch, H., Pomberger, R. (Eds.), Mineralische Nebenprodukte und Abfälle 9: - Aschen, Schlacken, Stäube und Baurestmassen -. Thomé-Kozmiensky Verlag GmbH, Nietwerder, pp. 228–245.
Müller, U., Rübner, K., 2006. The microstructure of concrete made with municipal waste incinerator bottom ash as an aggregate component. Cement and Concrete Research 36, 1434–1443. https://doi.org/10.1016/j.cemconres.2006.03.023.
Nedkvitne, E.N., Borgan, Ø., Eriksen, D.Ø., Rui, H., 2021. Variation in chemical composition of MSWI fly ash and dry scrubber residues. Waste management (New York, N.Y.) 126, 623–631. https://doi.org/10.1016/j.wasman.2021.04.007.
Neuwahl, F., Cusano, G., Benavides, J.G., Holbrook, S., 2019. Best Available Techniques (BAT) Reference Document for Waste Incineration: EUR 29971 EN. Europäische Union, Luxemburg https://eippcb.jrc.ec.europa.eu/sites/default/files/2020-01/JRC118637_WI_Bref_2019_published_0.pdf (accessed 6 April 2023).
Land Niederösterreich, 2022. Wasserstandsnachrichten und Hochwasserprognosen (Information on water level and flood forecast): Gänserndorf (ZAMG) - Niederschlag. https://www.noel.gv.at/wasserstand/#/de/Messstellen/Details/11048/Niederschlag/Jahr2 (accessed 16.11.22).
Nørgaard, K.P., Hyks, J., Mulvad, J.K., Frederiksen, J.O., Hjelmar, O., 2019. Optimizing large-scale ageing of municipal solid waste incinerator bottom ash prior to the advanced metal recovery: Phase I: Monitoring of temperature, moisture content, and CO2 level. Waste management (New York N.Y.) 85, 95–105. https://doi.org/10.1016/j.wasman.2018.12.019.
Pfandl, K., Küppers, B., Scheiber, S., Stockinger, G., Holzer, J., Pomberger, R., Antrekowitsch, H., Vollprecht, D., 2020. X-ray fluorescence sorting of non-ferrous metal fractions from municipal solid waste incineration bottom ash processing depending on particle surface properties. Waste management & research : the journal of the International Solid Wastes and Public Cleansing Association, ISWA 38, 111–121. https://doi.org/10.1177/0734242X19879225.
Polettini, A., Pomi, R., 2004. The leaching behavior of incinerator bottom ash as affected by accelerated ageing. Journal of hazardous materials 113, 209–215. https://doi.org/10.1016/j.jhazmat.2004.06.009.
Purgar, A., Winter, F., Blasenbauer, D., Hartmann, S., Fellner, J., Lederer, J., Rechberger, H., 2016. Main drivers for integrating zinc recovery from fly ashes into the Viennese waste incineration cluster. Fuel Processing Technology 141, 243–248. https://doi.org/10.1016/j.fuproc.2015.10.003.
Quicker, P., Stockschläder, J., 2018. Möglichkeiten einer ressourcenschonenden Kreislaufwirtschaft durch weitergehende Gewinnung von Rohstoffen aus festen Verbrennungsrückständen aus der Behandlung von Siedlungsabfällen: Abschlussbericht [Possibilities for a resource-saving circular economy through further recovery of raw materials from solid incineration residues from the treatment of municipal waste], Dessau-Roßlau. https://www.umweltbundesamt.de/sites/default/files/medien/1410/publikationen/2018-11-27_texte_99-2018_ressourcenschonende-kreislaufwirtschaft_1.pdf (accessed 18.06.21).
Rübner, K., Haamkens, F., Linde, O., 2008. Use of municipal solid waste incinerator bottom ash as aggregate in concrete. Quarterly Journal of Engineering Geology and Hydrogeology 41, 459–464. https://doi.org/10.1144/1470-9236/07-036.
Saikia, N., Cornelis, G., Mertens, G., Elsen, J., van Balen, K., van Gerven, T., Vandecasteele, C., 2008. Assessment of Pb-slag, MSWI bottom ash and boiler and fly ash for using as a fine aggregate in cement mortar. Journal of hazardous materials 154, 766–777. https://doi.org/10.1016/j.jhazmat.2007.10.093.
Saikia, N., Mertens, G., van Balen, K., Elsen, J., van Gerven, T., Vandecasteele, C., 2015. Pre-treatment of municipal solid waste incineration (MSWI) bottom ash for utilisation in cement mortar. Construction and Building Materials 96, 76–85. https://doi.org/10.1016/j.conbuildmat.2015.07.185.
Santos, R.M., Mertens, G., Salman, M., Cizer, Ö., van Gerven, T., 2013. Comparative study of ageing, heat treatment and accelerated carbonation for stabilization of municipal solid waste incineration bottom ash in view of reducing regulated heavy metal/metalloid leaching. Journal of environmental management 128, 807–821. https://doi.org/10.1016/j.jenvman.2013.06.033.
Saqib, N., Bäckström, M., 2014. Trace element partitioning in ashes from boilers firing pure wood or mixtures of solid waste with respect to fuel composition, chlorine content and temperature. Waste management (New York, N.Y.) 34, 2505–2519. https://doi.org/10.1016/j.wasman.2014.08.025.
Saqib, N., Bäckström, M., 2015. Distribution and leaching characteristics of trace elements in ashes as a function of different waste fuels and incineration technologies. Journal of environmental sciences (China) 36, 9–21. https://doi.org/10.1016/j.jes.2015.03.006.
Scalet, B.M., Garcia Munoz, M., Sissa, A.Q., Roudier, S., Delgado Sancho, L., 2013. Best Available Techniques (BAT) Reference Document for The Manufacture of Glass: Industrial Emissions Directive 2010/75/EU Integrated Pollution Prevention and Control. EUR 25786 EN, Luxemburg. https://eippcb.jrc.ec.europa.eu/sites/default/files/2019-11/GLS_Adopted_03_2012_0.pdf (accessed 14.01.22).
Schuch, D., Lederer, J., Fellner, J., Scharff, C., 2023. Separate collection rates for plastic packaging in Austria – A regional analysis taking collection systems and urbanization into account. Waste Management 155, 211–219. https://doi.org/10.1016/j.wasman.2022.09.023.
Simon, F.-G., Vogel, C., Kalbe, U., 2021. Antimony and Vanadium in Incineration Bottom Ash - Leaching Behavior and Conclusions for Treatment Processes. Detritus 75–81. https://doi.org/10.31025/2611-4135/2021.15115.
Sorlini, S., Collivignarelli, M.C., Abbà, A., 2017. Leaching behaviour of municipal solid waste incineration bottom ash: From granular material to monolithic concrete. Waste management & research : the journal of the International Solid Wastes and Public Cleansing Association, ISWA 35, 978–990. https://doi.org/10.1177/0734242X17721340.
Stockinger, G., 2016. Nassaufbereitung von Abfallverbrennungsaschen: Betriebsergebnisse einer großtechnischen Anlage in Österreich. In: Thomé-Kozmiensky, K.J. (Ed.), Mineralische Nebenprodukte und Abfälle: Aschen, Schlacken, Stäube und Baurestmassen. TK, Neuruppin, pp. 207–222.
Šyc, M., Krausová, A., Kameníková, P., Šomplák, R., Pavlas, M., Zach, B., Pohořelý, M., Svoboda, K., Punčochář, M., 2018. Material analysis of Bottom ash from waste-to-energy plants. Waste management (New York N.Y.) 73, 360–366. https://doi.org/10.1016/j.wasman.2017.10.045.
Šyc, M., Simon, F.G., Hykš, J., Braga, R., Biganzoli, L., Costa, G., Funari, V., Grosso, M., 2020. Metal recovery from incineration bottom ash: State-of-the-art and recent developments. Journal of hazardous materials 393, 122433. https://doi.org/10.1016/j.jhazmat.2020.122433.
Todorovic, J., Ecke, H., 2006. Demobilisation of critical contaminants in four typical waste-to-energy ashes by carbonation. Waste Management 26, 430–441. https://doi.org/10.1016/j.wasman.2005.11.011.
Turner, D.A., Williams, I.D., Kemp, S., 2015. Greenhouse gas emission factors for recycling of source-segregated waste materials. Resources, Conservation and Recycling 105, 186–197. https://doi.org/10.1016/j.resconrec.2015.10.026.
van Caneghem, J., Brems, A., Lievens, P., Block, C., Billen, P., Vermeulen, I., Dewil, R., Baeyens, J., Vandecasteele, C., 2012. Fluidized bed waste incinerators: Design, operational and environmental issues. Progress in Energy and Combustion Science 38, 551–582. https://doi.org/10.1016/j.pecs.2012.03.001.
van Caneghem, J., Verbinnen, B., Cornelis, G., de Wijs, J., Mulder, R., Billen, P., Vandecasteele, C., 2016. Immobilization of antimony in waste-to-energy bottom ash by addition of calcium and iron containing additives. Waste management (New York N.Y.) 54, 162–168. https://doi.org/10.1016/j.wasman.2016.05.007.
van Caneghem, J., van Acker, K., de Greef, J., Wauters, G., Vandecasteele, C., 2019. Waste-to-energy is compatible and complementary with recycling in the circular economy. Clean Techn Environ Policy 21, 925–939. https://doi.org/10.1007/s10098-019-01686-0.

Vateva, I., Laner, D., 2020. Grain-Size Specific Characterisation and Resource Potentials of Municipal Solid Waste Incineration (MSWI) Bottom Ash: A German Case Study. Resources 9, 66. https://doi.org/10.3390/resources9060066.
Verbinnen, B., Billen, P., van Caneghem, J., Vandecasteele, C., 2017. Recycling of MSWI Bottom Ash: A Review of Chemical Barriers, Engineering Applications and Treatment Technologies. Waste Biomass Valor 8, 1453–1466. https://doi.org/10.1007/s12649-016-9704-0.
Viczek, S.A., Aldrian, A., Pomberger, R., Sarc, R., 2020. Origins and carriers of Sb, As, Cd, Cl, Cr, Co, Pb, Hg, and Ni in mixed solid waste - A literature-based evaluation. Waste management (New York, N.Y.) 103, 87–112. https://doi.org/10.1016/j.wasman.2019.12.009.
Xuan, D., Tang, P., Poon, C.S., 2018. Limitations and quality upgrading techniques for utilization of MSW incineration bottom ash in engineering applications – A review. Construction and Building Materials 190, 1091–1102. https://doi.org/10.1016/j.conbuildmat.2018.09.174.

Appendix II

Paper II:

Recovery of aluminum, magnetic ferrous metals and glass through enhanced industrial-scale treatment of different MSWI bottom ashes

Mühl, J.; Hofer, S.; Blasenbauer, D.; Lederer, J.

Waste Management 190 (2024), 557–568.
Available online: October, 28th 2024
DOI: https://doi.org/10.1016/j.wasman.2024.10.025

Waste Management 190 (2024) 557–568

Contents lists available at ScienceDirect

Waste Management

journal homepage: www.elsevier.com/locate/wasman

Research Paper

Recovery of aluminum, magnetic ferrous metals and glass through enhanced industrial-scale treatment of different MSWI bottom ashes

Julia Mühl *, Simon Hofer, Dominik Blasenbauer, Jakob Lederer

Christian Doppler Laboratory for a Recycling-based Circular Economy, Institute of Chemical, Environmental and Bioscience Engineering, TU Wien, Getreidemarkt 9/166, 1060 Vienna, Austria

ARTICLE INFO

Keywords:
Municipal solid waste incineration
Incineration bottom ash
Fluidized bed combustion
Grate incineration
Glass recycling
Metal recycling

ABSTRACT

To foster a circular economy, the EU will increase recycling targets for packaging materials, including aluminum, ferrous metals and glass. Recovery of packaging metals from incineration bottom ashes (IBA) from municipal solid waste incineration can contribute to achieving these targets. Nevertheless, recoverable metal and glass amounts from IBA, and in particular IBA from fluidized bed combustion, are rarely investigated. Therefore, this work aims to assess the recoverable amounts of aluminum, magnetic ferrous metals and glass > 4 mm from different types of IBA through enhanced treatment. In an industrial-scale treatment experiment with one batch of IBA from grate and one from fluidized bed combustion, masses and compositions of all output flows of the treatment plant were determined. Material flow analysis was used to study the distribution of the investigated materials during the treatment process. Results show that glass separation was not feasible for the grate IBA, which only contained 7 % glass > 4 mm. The fluidized bed IBA contained 42 % glass > 4 mm, of which 72 % were recovered. More aluminum and magnetic ferrous metals > 4 mm were found in the fluidized bed IBA, also exhibiting less mineral agglomeration compared to those from grate IBA. The study demonstrated that enhanced industrial IBA treatment can recover > 95 % of aluminum and magnetic ferrous metals > 4 mm, not observing significant differences between these metals. Thus, a cutting-edge IBA treatment can enable the recovery of recyclable material from IBA and therefore contribute to a circular economy. Furthermore, fluidized bed IBA shows advantages regarding its recycling options compared to grate IBA.

1. Introduction

Efficient recycling of municipal solid waste (MSW) is an important measure to establish a circular economy. Especially recycling of energy-intense materials, like metals and glass, can contribute significantly to resource conservation and reduction of greenhouse gas emissions (Dhir et al., 2018; Turner et al., 2015). In order to promote their recycling, the European Union has specified various circular economy measures, including recycling targets for packaging waste (European Parliament and Council, 2018). As of 2025, 50 % of aluminum and 70 % of ferrous metal packaging and glass is required to be recycled, rising to 60 % (aluminum), 75 % (glass) and 80 % (ferrous metal), respectively, as of 2030 (European Parliament and Council, 2018). Contrarily to packaging paper or plastics, metals and glass can be recovered from MSW incineration bottom ash (IBA) (Bruno et al., 2021).

Metal recovery from IBA, which is widely practiced, can significantly contribute to achieving the EU's material-specific recycling targets (Brunner and Morf, 2024; Lederer et al., 2022; van Caneghem et al., 2019; Warrings and Fellner, 2018). To assess and report the contribution of IBA treatment to these targets, not only the quantities, but also the aluminum and magnetic ferrous metals content in metal fractions recovered by IBA treatment have to be known (European Commission, 2019). However, for many EU countries this data is not available (Bruno et al., 2021; Fletcher and Dunk, 2023). Alternatively, the recovered amounts of metals can be calculated by material flow analysis (MFA), using specific recovery rates of metals in IBA treatment (Lederer and Schuch, 2024). Necessary data for these recovery rates are rarely provided in the literature, and, if so, primarily related to specific, mainly dry, IBA treatment technologies applied to IBA from grate incineration (GI) (Allegrini et al., 2014; Holm and Simon, 2017; Mehr et al., 2021). Hardly any data is available for wet IBA treatment with jigs as part of multi-step metal separation, or for specific IBAs like those from the less frequently used fluidized bed combustion (FBC) (Makarichi et al., 2018; Maldonado-Alameda et al., 2023), which are only included in a few

* Corresponding author.
E-mail address: julia.muehl@tuwien.ac.at (J. Mühl).

https://doi.org/10.1016/j.wasman.2024.10.025
Received 23 February 2024; Received in revised form 30 August 2024; Accepted 21 October 2024

studies (Blasenbauer et al., 2023; Leckner and Lind, 2020; Saqib and Bäckström, 2015). Additionally, the recovery of glass cullet from IBA is not investigated very often, despite its feasibility by means of sensor-based sorting, especially for IBA from FBC (FB-IBA), but also to some extent for IBA from GI (G-IBA) (Makari, 2014; Mühl et al., 2023).

The present research therefore aims to close these research gaps on material flows, contents and recovery rates of aluminum, magnetic ferrous metals, and glass in recovered material fractions from IBA by answering key questions related to the output of enhanced IBA treatment using wet multi-step metal removal technology applied to IBA from different firing technologies. Specifically, the material flows of different IBAs treated in an enhanced, wet IBA treatment plant on an industrial scale are investigated. Furthermore, it is determined which contents of aluminum, magnetic ferrous metals and glass are present in the outputs of this IBA treatment plant and what recovery rates can be achieved for these materials referring to defined particle size fractions.

To address these issues, an industrial-scale IBA treatment experiment with IBA from GI and FBC was conducted. Material flows of the treatment process were determined and its output flows were characterized, giving special focus to the packaging materials aluminum, magnetic ferrous metals and glass > 4 mm. The composition of the untreated IBAs and recovery rates of the packaging materials investigated were calculated. Overall, this study aims to assess the effects an industrial IBA treatment can have on the improvement of MSW incineration with regard to circular economy, particularly in terms of metal and glass recovery rates.

2. Materials and Methods

In the course of this study, one batch of FB-IBA and one of G-IBA were treated at an industrial IBA treatment plant. For both IBAs, MFAs after Brunner and Rechberger (2017) were performed, using the software STAN 2.6 (Cencic and Rechberger, 2008). The treatment plant was defined as the system. All of its input and output flows, consisting of different metals and minerals, were defined as goods. The materials aluminum, magnetic ferrous metals and glass > 4 mm, which are components of the goods, were defined as sub-goods. Magnetic ferrous metals in this sense include all magnetic ferrous metals, but not non-magnetic stainless steel. Only particles > 4 mm were considered for the determination of sub-goods, as previous studies by Huber et al. (2020) and Blasenbauer et al. (2023) show that the particle sizes > 4 mm clearly constitute the majority of the sub-goods (see also section 3.4).

MFAs both on the level of goods and sub-goods were modelled. The partitioning of sub-goods into the different output flows is described through transfer coefficients (Brunner and Rechberger, 2017). Based on the MFA results, potential recovery rates were calculated.

2.1. *Material flows of the IBA treatment*

Before describing the determination of the composition of the outputs from IBA treatment by sampling, the IBAs treated and the enhanced IBA treatment technology are outlined.

2.1.1. *IBAs treated*

For the industrial-scale treatment experiment, about 200 tons of one batch of G-IBA and of one FB-IBA from Austrian municipal solid waste incineration (MSWI) plants were used. According to the plant operator, the waste input to the GI plant in the month before the experiment took place was 56 % mixed MSW from households and commercial establishments, 18 % bulky waste, 16 % pretreated MSW, 4 % sludges and 6 % other waste (personal communication, 2023). Regarding the solid residues of this GI plant, G-IBA makes up 16 % of the MSW incinerated and 3 % of the MSW mass remains as fly ash (personal communication, 2022). Another 2 % of the incinerated waste is already recovered directly at the incineration plant as coarse ferrous metals via magnetic separation of the IBA. In the FBC plant, only pretreated mixed MSW from households was incinerated one month before the sampling campaign (personal communication, 2023). The pretreatment of the waste includes shredding, screening and magnetic metal separation and is outlined in detail in Blasenbauer et al. (2023). After incineration, 14 % of the incinerated MSW remain as FB-IBA and another 11 % are collected as fly ash (personal communication, 2022).

Both incineration plants were considered in a previous study by Mühl et al. (2023), where they were referred to as G-IBA Y and FB-IBA C. Furthermore, the composition of the FB-IBA was investigated by Blasenbauer et al. (2023) and the G-IBA was examined by Huber et al. (2019) and Huber et al. (2020), where it was referred to as "plant A".

2.1.2. *The industrial IBA treatment plant investigated*

For the experiment the Brantner IBA treatment plant in Austria was used. This plant can be used for the treatment of IBAs from both GI and FBC and has already been examined and described in the past, for example by Huber (2020) (referred to as 'plant B'), Pfandl et al. (2020) or Šyc et al. (2020) and is considered as state of the art (Neuwahl et al., 2019). In 2021, the treatment plant was extended according to additional treatment steps based on a pilot study by Mühl et al. (2023). Meanwhile, the plant includes an additional metal separation step and a glass separator as well as a crusher for coarse material. The scheme of the treatment plant is given in Fig. 1. Units that were added in course of the expansion are colored.

In a nutshell, the plant's aim is to recover as much metal as possible and to produce a mineral fraction with extremely low metal content, which is suitable for utilization as manufactured aggregate in concrete production. Moreover, glass can be recovered with a sensor-based glass sorter, which uses visible light to detect glass and removes it by means of compressed-air valves (Wotruba and Harbeck, 2003). Since the capacity of the glass sorter is limited and glass removal is easier for coarser particle sizes (i.e. > 8 mm), due to the distance of the compressed-air valves, glass separation is applied downstream a 9 mm sieve. Attempts to recover glass from the G-IBA at the Brantner treatment plant failed in the past due to the reasons which were also examined on a pilot scale by Mühl et al. (2023): G-IBAs contain less glass and more unburnt material, which tends to block the glass separator and thereby causes severe disturbances to the treatment plant's operation. Hence, more effort would be necessary to receive a lower glass amount compared to FB-IBAs. Therefore, glass removal is only applied to FB-IBAs at the Brantner treatment plant.

The treatment process is realized with multiple screens, magnetic and eddy current separation (ECS), a jig as key unit (pulsating water bath to separate particles based on their sinking speed), a glass separator and a specific treatment train for the fine material < 4 mm. Coarse material that is separated in the course of the treatment process is fed to a crusher with an associated magnetic separator and the crushed material is fed back to the treatment plant subsequently. The plant produces multiple output flows, all of which are listed in Table 1, together with a description and their main components. Pictures of the output flows can be found in the supplementary material (section S1). It has to be noted that all output flows also contain extraneous material due to incomplete separation (e.g. metals or mineral material remain in the *glass fraction*). Additionally, the particle sizes given for some output flows are approximate reference values. As the industrial sieving process is incomplete, especially coarser particle size fractions also contain finer particles. Particularly flat (e.g. glass cullet) or elongated (e.g. wires) particles are challenging to separate by sieving due to their proportions. Hence, glass separation is applied downstream a 9 mm sieve, but the *glass fraction* contains glass < 9 mm as well.

Categorization of output flows

In this study, the output flows were categorized into five different output categories according to their further use, which is also outlined in Table 1. This was important to identify the materials which are recovered for recycling and distinguish these from materials which are not recovered. Output flows that are directly landfilled are summarized in

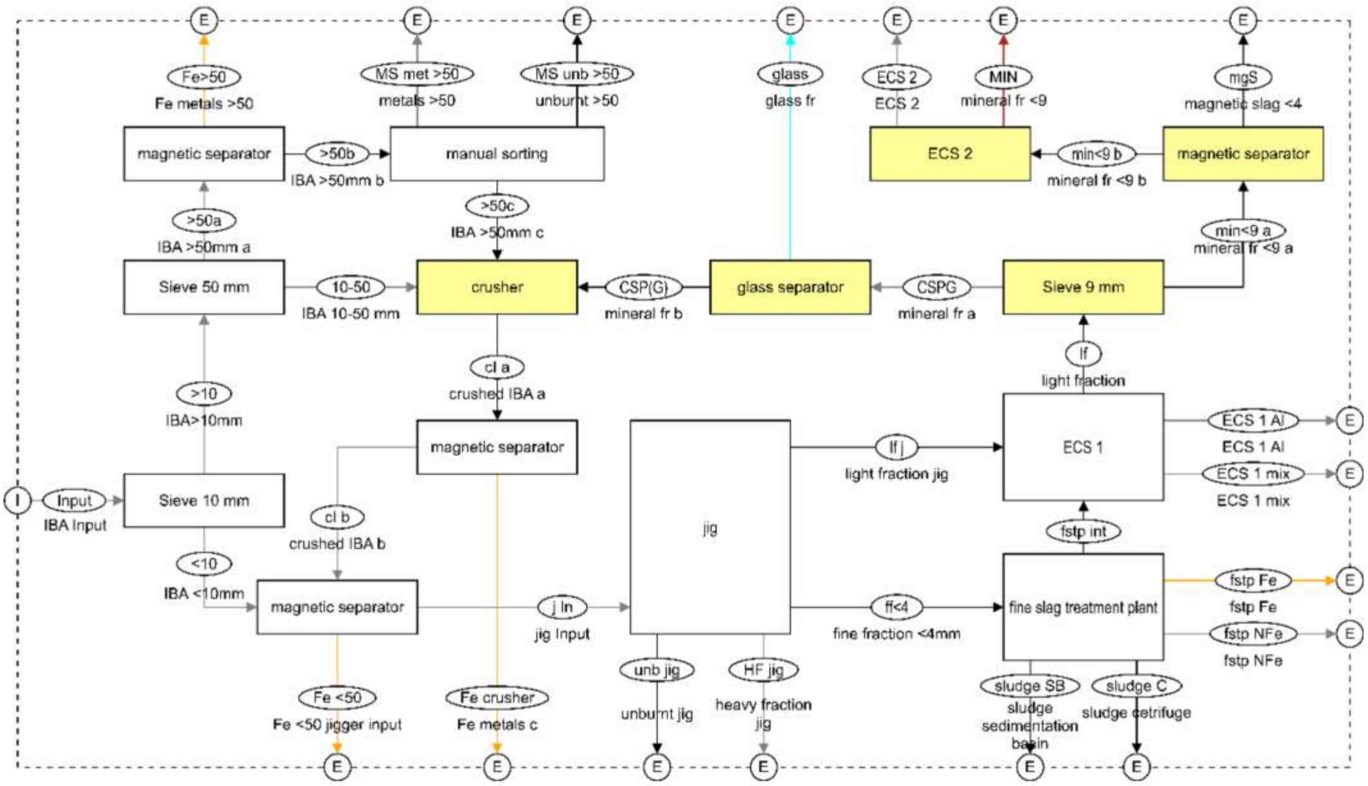

Fig. 1. Scheme of the Brantner treatment plant after its expansion in 2021. Newly added units are colored. "I" represents the input of untreated IBA to the treatment plant. Flows marked with an "E" are the output flows of the IBA treatment plant. ECS: eddy current separation.

Table 1
Overview of the output flows of the IBA treatment. ECS: eddy current separation.

Short name	Output flow	Description and major components	Output category
Fe > 50	Magnetic fraction > 50 mm	Magnetic ferrous metals > 50 mm separated by magnetic separation	*metal-rich, magnetic*
Fe crusher	Magnetic fraction after crusher	Magnetic ferrous metals separated by magnetic separation at the crusher output	*metal-rich, magnetic*
Fe < 50	Magnetic fraction separated prior to jig	Magnetic ferrous metals separated prior to the jig by magnetic separation from input material < 50 mm or from recirculated material from the crusher	*metal-rich, magnetic*
MS met > 50	Manually sorted metals > 50 mm	Metals > 50 mm from sorting cabin	*metal-rich, non-magnetic*
MS unb > 50	Manually sorted unburnt material > 50 mm	Unburnt material > 50 mm from sorting cabin	*direct disposal*
HF jig	Jig output: heavy material with high density	High-density metals (e.g. copper, zinc, brass, stainless steel) separated by the jig; but also magnetic ferrous metals, glass etc. is found in this output	*metal-rich, non-magnetic*
unb jig	Jig output: floating material	Floating material in the jig, e.g. unburnt material or lightweight aggregate	*direct disposal*
ECS 1 Al	Non-magnetic metals from first ECS, aluminum-rich fraction	Non-magnetic metals separated by ECS, mostly aluminum	*metal-rich, non-magnetic*
ECS 1 mix	Non-magnetic metals from first ECS, mixed fraction	Non-magnetic metals separated by ECS, mixed fraction (aluminum and other non-ferrous metals, minerals, glass)	*metal-rich, non-magnetic*
ECS 2	Non-magnetic metals from second ECS	Residual non-magnetic metals, removed from mineral fraction < 9 mm by ECS; high share of mineral material	*metal-rich, non-magnetic*
MIN	Mineral fraction < 9 mm	Remaining mineral fraction < 9 mm after jig and separation of metals and glass	*mineral fraction*
glass	Glass fraction	Sensor-based sorted glass fraction, mainly > 9 mm; sorted after metal separation and jig; was produced only in the case of FB-IBA	*glass fraction*
fstp Fe	Magnetic ferrous fraction < 4 mm	Magnetic fine fraction < 4 mm from fine slag treatment plant	*metal-rich, magnetic*
fstp NFe	Non-magnetic fraction < 4 mm	Heavy non-ferrous metals < 4 mm from fine slag treatment plant	*metal-rich, non-magnetic*
sludge SB	Sludge from sedimentation basin	Particle size < 1 mm	*direct disposal*
sludge C	Sludge from sludge dewatering centrifuge	Particle size < 1 mm	*direct disposal*
mgS	Magnetic slag < 4 mm	Material removed by magnetic separation prior to the second ECS; contains considerable amounts of adhesive grain from the conveyor belt; during the treatment process this flow was recirculated (G-IBA) or disposed of (FB-IBA)	*recirculation (G-IBA) / direct disposal (FB-IBA)*
CSP(G)	Ceramic, stones, porcelain, (glass) > 9 mm	Material > 9 mm that is not removed by the glass sorter in the case of the FB-IBA; in the case of the G-IBA this flow also contains glass, as the glass sorter was not in operation; during both treatment processes this flow was fed to the crusher and recirculated	*recirculation*

the output category *direct disposal*; the mineral and glass fractions both constitute their own output category, as they can possibly be utilized in the construction sector or in glass recycling, respectively (*note: the mineral fraction is not further investigated in this article since it does not contain any packaging materials*). Outputs belonging to the category *metal-rich, non-magnetic* are either directly handed on to recyclers or have to be further purified to separate metals. Either way, magnetic ferrous metals and aluminum in this category are possibly recovered and recycled. Magnetic ferrous metals can obviously also be recycled if found in the category *metal-rich, magnetic*. Aluminum is a contaminant in the category *metal-rich, magnetic* and can therefore only be recovered if transmitted to an output related to the category *metal-rich, non-magnetic*.

2.1.3. Determination of the material flows of the IBA treatment

The experiments took place in April 2022 for the G-IBA and in October 2022 for the FB-IBA during the regular operation of the plant. The plant operation and material handling were controlled by plant employees. During the sampling campaigns, the masses of most output flows were weighed by plant employees with the wheel loader when material was removed from the plant. Likewise, the amount of IBA fed to the treatment plant was weighed. For some output flows, the total mass was not weighed, as their amount was too low to be removed with the wheel loader (e.g. *fstp Fe* and *NFe*). For these flows, the total masses were extrapolated from the sample masses and the sampling durations (details see in section S1.1 in the supplementary material). The mass of *sludge SB* (m_{sSB}) was also not weighed but calculated from its density (ρ_{sSB}) and the water volume (V_{H2O}) that was refilled to the sedimentation basin after excavating the sludge, using the equation $m_{sSB} = \rho_{sSB} * V_{H2O}$. The output flow *mineral fraction*, $\dot{m}_{MIN}$, was calculated according to the following equation:

$$\dot{m}_{MIN} = \dot{m}_{IBA,IN} - \sum \dot{m}_{OUT}$$

with $\dot{m}_{IBA,IN}$ as the total input mass of the IBA and $\sum \dot{m}_{OUT}$, which is the sum of all output flows of the treatment plant as shown in Table 1, except for $\dot{m}_{MIN}$.

The fact that the experiment took place during regular plant operation led to two circumstances that had to be considered before evaluating the process. First, at the end of both sampling campaigns, different amounts of the output flows of *magnetic slag* and *CSP(G)* remained. During the treatment, these fractions were fed back regularly to the plant input and the crusher, respectively. The remaining amounts at the end of the sampling days made up 3.8 % (G-IBA) and 4.7 % (FB-IBA) of the dry input material to the treatment plant in the case of *magnetic slag* and 8.3 % (G-IBA) and 0 % (FB-IBA) in the case of *CSP(G)*. These differences distort the material flows of the output flows. Therefore, it was assumed that these residual material flows would be further processed and split into other output flows by means of modeling, which is outlined in the supplementary material (section S1.2). For example, it was assumed that 80 % of the remaining *magnetic slag* would be guided into the *mineral fraction* and 20 % into *sludge SB* after feeding it back to the plant input. All results presented in this paper imply this modeling.

The second limitation was the fact that the output flows of *magnetic slag* were not fed back to the plant input during the treatment of the FB-IBA (contrarily to the G-IBA), but were disposed of due to a change of the plant operation. This is considered in section 3.4.

2.2. Determination of the contents of aluminum, magnetic ferrous metals and glass > 4 mm in the material flows of the treatment plant

Having established the material flows of goods of the IBA treatment, the contents of relevant sub-goods had to be determined. This was done by sampling of the output flows. The input flow was not sampled since the sub-good content can be determined by MFA mass balancing (Brunner and Rechberger, 2017).

2.2.1. Sampling campaign

To assess the composition of the output flows, all of them were sampled. The internal material flows of the treatment were not quantified. Due to the heterogeneity of IBAs, special attention on representativity of the sampling is essential (Skutan et al., 2014; Vateva and Laner, 2020) and can be ensured by several measures. To compensate for variations in the IBA composition in this experiment, almost all output flows were periodically sampled every 10–15 min during the treatment of 200 tons of each type of IBA. Moreover, at least thirty increments were collected per output flow, as recommended by Gerlach and Nocerino (2003) and Gy (1992). This led to personnel-intensive sampling campaigns for at least 8 h and high primary sample masses. Different sampling devices, which were mostly purpose-built, were used for the single output flows of the treatment plant. For some output flows no periodic sampling was possible due to safety reasons (e.g. *Fe > 50*) or accessibility (e.g. *sludge SB*). In these cases, individual solutions were found. Details on the sampling of the different output flows, the number of increments and the masses sampled and manually sorted are shown in the supplementary material (section S1.1).

For further characterization of the output flows, sub-samples of the output flows were obtained primarily by fractional shoveling, as this is preferable to grab sampling (Gerlach and Nocerino, 2003).

2.2.2. Characterization of output flows

To create an MFA of the treatment plant, besides the weights, also water contents and compositions of all output flows were determined. The water content was determined in duplicate by drying sub-samples at 105 °C. The water contents of the input material to the treatment plant, i.e. the fresh IBAs, were provided by the incineration plant operator. For manual sorting, sub-samples of the output flows were sieved into the fractions < 4 mm and > 4 mm, which were also weighed. For most output flows the masses for sieving and sampling were within the range of 2–31 kg, depending on the particle size of the fraction as advised in the European Standard EN 933–11 (Austrian Standards Institute, 2011). More material was sorted in the case of coarser output flows > 50 mm (up to 600 kg). The sorted amounts of each output flow are given in the supplementary material. The constituents > 4 mm were manually sorted into magnetic metals, aluminum, other metals (e.g. stainless steel, brass, copper, coins), glass, mineral material and unburnt material. A magnet was used to identify magnetic metals. Aluminum was distinguished from other metals either by products (e.g. aluminum cans, trays or foil) or in the case of finer particles by their matt silver-grey color and softness when filed. Output flows that only contained material < 4 mm were not manually sorted (e.g. sludges). Furthermore, the output flows *Fe > 50 mm* of both IBAs and *Fe crusher* of the G-IBA were not sorted, as neither aluminum nor glass was expected in these flows. In these cases, the content of mineral material was estimated based on visual assessment and comparable output flows (i.e. *Fe < 50*). Merged agglomerates of magnetic ferrous metals and mineral material in the output flows *Fe < 50* of the G-IBA were crushed to separate metal pieces from adhesions and to determine the share of mineral material in this flow. In the case of the output flows *HF jig* and *ECS 1 mix* from the G-IBA, the visual distinction between metals and mineral material > 4 mm was not possible (Šyc et al., 2018). Therefore, components > 4 mm of these output flows were crushed with a vibratory roller (BOMAG 65S) before manual sorting. After crushing, the material was sieved with a 4 mm mesh. The share of the crushed material < 4 mm was assumed to be mineral material and glass, as most metals cannot be crushed, but are flattened (Chen et al., 2023; Šyc et al., 2020). The proportion of glass and mineral fraction > 4 mm as well as the share of material < 4 mm in the original output material before crushing were determined by sieving and manual sorting of additional sub-samples .

As a result from the hand sorting analysis, the compositions of all flows were calculated for both IBAs.

2.3. Determining material flows and recovery rates of aluminum, magnetic ferrous metals and glass > 4 mm in IBA treatment

Given the material flows of the goods and the share of the sub-goods aluminum, magnetic ferrous metals and glass > 4 mm in each output flow and therefore in the IBA input, the transfer coefficients of the sub-goods were calculated for the treatment process (Brunner and Rechberger, 2017). The transfer coefficient *TC* of a sub-good *j* to a specific output flow *i* is calculated from $TC_{j,i} = m_{j,i} / m_{IN,j}$ with $m_{j,i}$ as the mass flow of a sub-good *j* in the respective output flow *i* and $m_{IN,j}$ as the total mass of the sub-good in the input of the treatment plant (in this study only one input flow).

To assess the amounts of a sub-good in the treated IBAs that can potentially be recovered, the potential recovery rate of a sub-good was calculated. Sub-goods can only be recovered from specific output flows, which is shown by the different output categories in Table 1. Transfer coefficients *TC* of a sub-good *j* to an output category *i*, where it can potentially be recovered from, are summed up to obtain the potential recovery rate of a sub-good *j* ($pot.RR_j$), as can be seen in the following equation:

$$pot.RR_j = \sum_{i=1}^{i=n} TC_{j,i}$$

For glass, the desired output category (where it can potentially be recovered from) is the *glass fraction*. In the case of aluminum, the output category *metal-rich, non-magnetic* is the desired output category. Magnetic ferrous metals can potentially be recovered from the output category *metal-rich, magnetic*. Additionally, magnetic ferrous metals can also be obtained from the output category *metal-rich, non-magnetic* by further processing, which is usually applied to the output flows belonging to this category. For example, additional treatment (including further magnetic metal separation) of the output flows *HF jig* aims to reduce the content of mineral material and glass in this output flow and to divert magnetic ferrous metals into the category *metal-rich, magnetic*. Thereby, a cleaner flow rich in recyclable non-magnetic metals can be produced.

The potential recovery rate must not be mistaken as the recycling rate, as additional losses in the recycling process have to be considered.

3. Results and Discussion

In the following sections the major results, namely material flows of goods and sub-goods, the compositions of the material flows and potential recovery rates of the sub-goods, are presented and discussed. Additional values (e.g. water content, raw data of the treatment experiments before modeling) and numerical values related to the figures are presented in the supplementary material (section S2). All percentages given are percentages by mass.

3.1. Material flows of goods in IBA treatment

Fig. 2 shows the results of the MFAs on the level of goods standardized to 1,000 kg of dry input material. The categorization of output flows into output categories according to Table 1 is depicted as well.

By far the largest output flows are the mineral fractions (68 % of the G-IBA, 34 % of the FB-IBA) and the glass fraction > 9 mm in the case of the FB-IBA (35 %). The mineral fraction contains refractory material (e.g. glass, ceramics) and molten agglomerates, which are formed as melt products from glass, metals and mineral material during incineration or quenching (Eusden et al., 1999; Inkaew et al., 2016; Yeo et al., 2024). Recycling of glass from IBA is already practiced in Austria, but not from this plant (Lederer et al., 2023; Lipp and Lederer, 2024 (under review)). For this reason, options for the glass fraction > 9 mm need further investigation (Mühl et al., 2023).

The results in Fig. 2 also show that the output flows that have to be disposed of directly after the treatment (i.e. sludges, unburnt material) make up 11 % in the case of the G-IBA and therefore are more than twice that of those in the FB-IBA process (5 %). This mainly derives from higher amounts of sludge produced from the G-IBA treatment, due to higher amounts of fine particles compared to FB-IBA.

The output category *metal-rich, magnetic* makes up 4 % of the G-IBA and 7 % of the FB-IBA. This difference is mainly due to higher amounts of output flows containing coarse magnetic metals in the case of the FB-IBA. The amounts of output flows belonging to the category *metal-rich, non-magnetic* lie in the same range for the G-IBA (17 %) and the FB-IBA (19 %). However, there are clear differences in the amounts of output flows of this category. For example, the fraction *HF jig* makes up 4 % (G-IBA) and 2 % (FB-IBA), respectively; the output flow *ECS 1 Al*, accounts for 2 % (G-IBA) and 9 % (FB-IBA), respectively. The metal-rich categories are examined more closely in the following sections, where the composition of the output flows is considered as well.

3.2. Composition of material flows from IBA treatment

The compositions of both IBAs before the treatment were calculated from the composition and the mass shares of all output flows and are depicted in Fig. 3. Related numerical values to this calculation are given in the supplementary material (section S2.3).

From the results in Fig. 3, the total shares of the three sub-goods aluminum, magnetic ferrous metals and glass were calculated and are given in Table 2 ("Calculated share of sub-good in total IBA"). Other major constituents are material < 4 mm, which accounts for 62 % of the G-IBA and 31 % of the FB-IBA, and mineral material > 4 mm (22 % of G-IBA, 10 % of the FB-IBA). Material < 4 mm is mainly found in the mineral fraction < 9 mm or as sludge in both IBAs.

As already shown in a preceding pilot-scale experiment by Mühl et al. (2023), large differences between G-IBA and FB-IBA were observed. This primarily counts for glass. Fig. 2 shows that the *glass fraction*, which was not produced in course of the G-IBA treatment (see also section 2.1.2), accounts for 35 % of the total mass of the FB-IBA. Based on the MFA calculation, the FB-IBA input material flow to the treatment plant for the experiment contained 42 % glass > 4 mm, the one of G-IBA only 7 % (see Table 2). These values lie slightly below those reported by Huber et al. (2020) for the G-IBA and by Blasenbauer et al. (2023) for the FB-IBA, but they are within the therein stated uncertainty ranges. Generally, glass shares in IBA depend on the glass content in the incinerated MSW and therefore vary widely from 5-30 % for G-IBAs (Costa et al., 2020; Šyc et al., 2020; van de Wouw et al., 2020; Vateva and Laner, 2020). The different glass contents of the G-IBA and the FB-IBA can also be attributed to differences in the incineration process and the discharge type according to the literature (Bayuseno and Schmahl, 2010; Blasenbauer et al., 2023; Mühl et al., 2023). In GI, melting of glass and of other IBA constituents leads to lower glass contents and the production of mineral agglomerates, as already reported for example by Bayuseno and Schmahl (2010), Eusden et al. (1999), Costa et al. (2020), Blasenbauer et al. (2023) and Mühl et al. (2023). The assumption that glass in G-IBA is predominantly contained in fractions < 4 mm seems unlikely from visual inspection of the *mineral fraction < 4 mm* and can be refuted by data from Huber et al. (2020), which show that Austrian G-IBAs do not contain significant amounts of glass in the particle size fractions < 4 mm. Nevertheless, glass could be comminuted by the crusher of the treatment process, leading to higher amounts of glass < 4 mm in the G-IBA. This should be investigated in future research.

Comparing the glass separation of the FB-IBA applied in Mühl et al. (2023), the proportion of mineral to glass fraction is similar. However, the industrially produced glass fraction contained higher amounts of extraneous material (14 %) than in the pilot-scale experiment (2 %) (Mühl et al., 2023). Several factors could have caused this difference. For example, the sensor-based sorting devices were not of the same manufacturer. The most relevant difference is probably the industrial operation compared to the manual and controlled input feed that was applied at pilot scale. In any case, the extraneous material contents of the glass fraction exceeded the strict quality limits requested by the

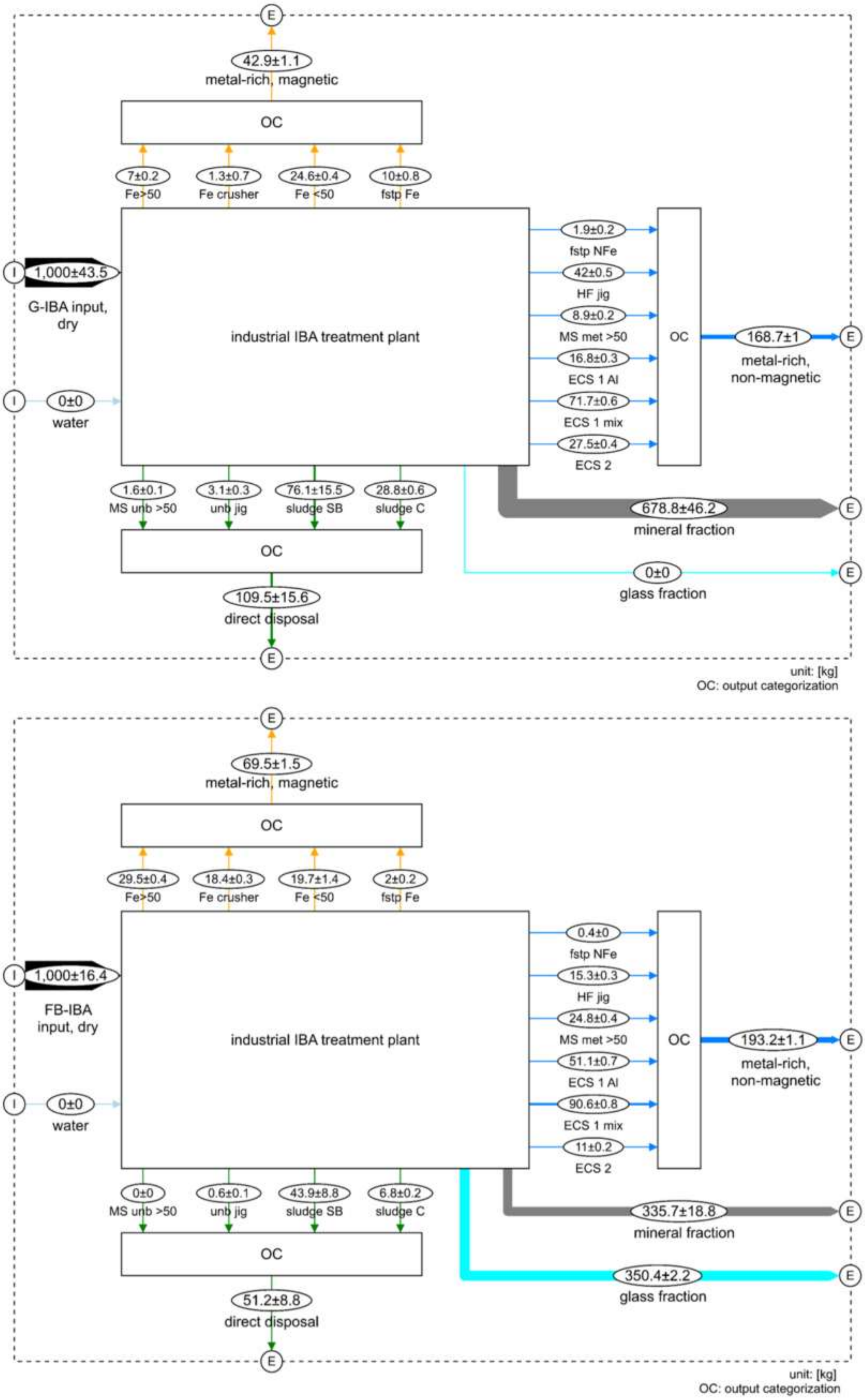

Fig. 2. Results of the material flow analysis on the level of goods per 1,000 kg of dry IBA input. Top: Grate incineration bottom ash (G-IBA), below: fluidized bed incineration bottom ash (FB-IBA).

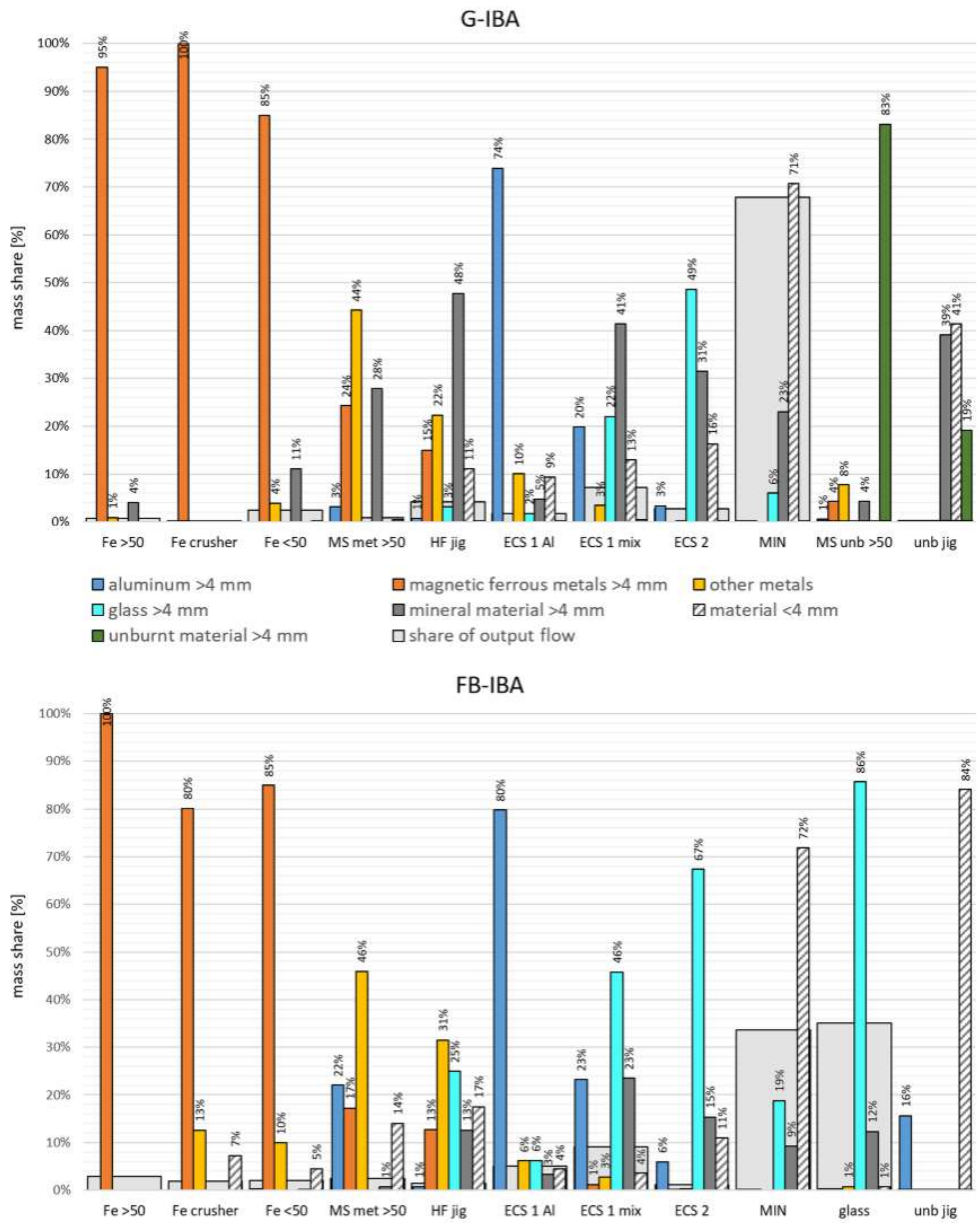

Fig. 3. Results of the composition of the output flows after the IBA treatment. Top: Grate incineration bottom ash (G-IBA), below: fluidized bed incineration bottom ash (FB-IBA). Numerical values are only given for shares > 0.5 %. Numerical values for the shares of the output flows after the IBA treatment are shown in Fig. 2 (in kg/1,000 kg). Results are based on dry mass.

packaging glass industry regarding the content of metals and ceramics, porcelain and stones (Bundesverband Glasindustrie e.V. et al., 2014). Only 20 g/t of ceramics, porcelain and stones and < 5 g/t (0.0005 %) of ferrous and non-ferrous metals are accepted by the packaging glass industry (Bundesverband Glasindustrie e.V. et al., 2014). To fulfil these requirements, further comprehensive glass treatment in form of removal of extraneous material (e.g. by means of further sensor-based sorting) is necessary and needs to be investigated.

According to the MFA calculation, the G-IBA input contained 3.8 % and the FB-IBA 6.9 % of magnetic ferrous metals > 4 mm. Magnetic ferrous metals are predominantly found in the output category *metal-rich, magnetic*, which are equally high as the magnetic ferrous metal shares (4 % of the G-IBA and 7 % of the FB-IBA, see also section 3.1). The lower amount of magnetic ferrous metals in the G-IBA can be traced back to the fact that coarse magnetic metals are removed directly after incineration at the GI plant (cf. section 2.1.1). These coarse magnetic metals account for 11 % of the solid residues of this incineration plant (Kellner et al., 2022). Therefore, the total content of magnetic ferrous metals > 4 mm in the G-IBA would sum up to nearly 16 % of the G-IBA, if these amounts were considered as well (personal communication, 2024). This share is actually quite high for G-IBAs, but can be explained by the high share of bulky waste that is incinerated in the respective grate incinerator (Huber et al., 2020). The relatively high content of magnetic ferrous metals > 4 mm in the FB-IBA, however, cannot be

Table 2
Calculated share and determined recovery rates of aluminum, magnetic ferrous metals and glass > 4 mm in the incineration bottom ashes from grate (G-IBA) and from fluidized bed (FB-IBA).

	Aluminum > 4 mm		Magnetic ferrous metals > 4 mm		Glass > 4 mm	
	G-IBA	FB-IBA	G-IBA	FB-IBA	G-IBA	FB-IBA
Calculated share of sub-good in total IBA	2.9 %	7.0 %	3.8 %	6.9 %	7.2 %	41.9 %
Potential recovery rate of sub-good	95.8 %	97.7 %	99.6 %	98.7 %	0 %	71.6 %

expected for FB-IBAs in general, since the pretreatment of the MSW prior to incineration in this FBC plant does not include magnetic metal separation of the major particle size fraction < 125 mm, which accounts for 42 % of the pretreated MSW (Blasenbauer et al., 2023). If pretreatment of the MSW would include magnetic metal separation for all particle size fractions, the share of magnetic metals in the FB-IBA would be lower (Maldonado-Alameda et al., 2023). This also shows that the input mass of magnetic ferrous metals into the MSW incineration is essential for the amounts that can be recovered from the IBA.

The MFA-modeled content of aluminum > 4 mm in the FB-IBA input (7.0 %) is more than twice as much as in the G-IBA (2.9 %). The incineration temperature is reported as the main factor for this circumstance: in GI, temperatures > 1,000 °C can be expected, which lead to significant losses of metallic aluminum due to melting and oxidation, depending on the wall thickness and particle size (Biganzoli et al., 2012; Gökelma et al., 2021; Hu et al., 2011; López et al., 2015). Thereby, metallic aluminum is transformed to droplets and alloys (Saffarzadeh et al., 2016) and not classified as aluminum > 4 mm in the manual sorting anymore (Warrings and Fellner, 2021) or discharged in particle size fractions < 4 mm or in the fly ash (Saffarzadeh et al., 2016; Vateva and Laner, 2020). On the contrary, the bed temperature of the FBC plant considered is intentionally held below the melting point of aluminum (Blasenbauer et al., 2023), leading to less oxidation and melt reactions of metallic aluminum in the FB-IBA. High turbulences in the FBC process, however, can lead to abrasion and thus discharge of aluminum to the fly ash or the fine fraction < 4 mm. Nevertheless, as neither characterization of the input MSW into the incinerators nor analyses of the solid residues < 4 mm of the GI and the FBC were within the scope of this paper, the exact behavior of aluminum during incineration was not determined. Moreover, it is likely that the aluminum contents in the waste input of the two incineration plants differed. Regarding the MSW input to the FBC it also has to be added that the MSW pretreatment prior to the FBC does not include any ECS. Adding ECS to the MSW pretreatment would decrease the amounts of aluminum > 4 mm contained in the FB-IBA (Maldonado-Alameda et al., 2023).

With respect to the total IBA composition determined in this study, the FB-IBA contains higher amounts of magnetic ferrous metals > 4 mm and of other metals > 4 mm (i.e. stainless steel, metal composites, coins, batteries etc.) (see Fig. 3). In the G-IBA, on the other hand, more mineral material was found. This is contained to a large extent in the *mineral fraction < 9 mm* but also in metal-rich output flows as adhesion or caking on metals. This lowers the quality of metal fractions from G-IBA. Also López-Delgado et al. (2003) and Tayibi et al. (2007) have reported higher quality of ferrous metal scrap from FBC compared to GI.

Higher metal contents in the FB-IBA compared to the G-IBA can also be seen from the results by Huber et al. (2020) and Blasenbauer et al. (2023). Aluminum and magnetic ferrous metals > 4 mm are a factor 1.7 and 1.4 higher in the FB-IBA assessed by Blasenbauer et al. (2023) than in the G-IBA (Huber et al., 2020). In general, reference values for metal contents in the particle size fraction > 4 mm reported by these authors are higher than those found in this experiment. Magnetic ferrous metals and aluminum > 4 mm in the G-IBA were 50 % and 13 % higher in the study by Huber et al. (2020) than in this study. Blasenbauer et al. (2023) determined 15 % more magnetic ferrous metals > 4 mm in the FB-IBA but less aluminum > 4 mm (−19 %). Especially in the case of the G-IBA, the most likely reason for this is the heterogeneity of the material, which also becomes obvious from the high standard deviations in the cited papers.

What has to be considered as well regarding recoverable amounts of metals and glass in both IBA types are the different shares of fly ash, which are produced in GI and FBC (cf. section 2.1.1). After FBC, higher shares of fly ash and lower amounts of IBA remain compared to GI (Fan et al., 2022; Mühl et al., 2023). Therefore, the same mass of a sub-good per ton of MSW incinerated leads to different shares in the G-IBA and the FB-IBA. This was also considered by Blasenbauer et al. (2023), who determined higher contents of aluminum in the FB-IBA than in the G-IBA but also showed that relative to 1 ton of MSW input similar amounts of aluminum can be recovered from both IBAs. In the case of glass, however, significantly more glass was found in the FB-IBA, which proves that glass is lost during the GI process (Blasenbauer et al., 2023).

Even though the mineral fraction is not investigated closer herein, some observations are made considering this fraction, since it constitutes a major output flow of the treatment plant: for the mineral fractions from IBA treatment, recycling in the construction sector has been the subject of many research projects for several years (Dou et al., 2017; Verbinnen et al., 2017; Xuan et al., 2018). According to the literature, the mineral fraction of G-IBAs tends to contain higher concentrations of heavy metals compared to FB-IBAs (Jung et al., 2004; Maldonado-Alameda et al., 2023; Mühl et al., 2023; Saqib and Bäckström, 2014). This may be detrimental to the utilization of the mineral fraction from G-IBA as construction material, since requirements for technical and environmental suitability have to be met (Blasenbauer et al., 2020). The lower heavy metal content of the mineral fraction from FB-IBA can be advantageous in this regard. Closer investigations on the mineral fractions produced by the treatment described herein were conducted by Mika (né Hofer) et al. (2024, under review).

3.3. Material flows and recovery rates of aluminum, magnetic ferrous metals and glass > 4 mm

Simplified MFAs for the sub-goods aluminum, magnetic ferrous metals and glass > 4 mm per ton of dry IBA input are shown in Fig. 4. The results are depicted only for the output categories. Results for all output flows are given in the supplementary material (section S2.4).

From Fig. 4 it can be seen that most sub-goods are enriched in the output categories where they can be potentially recycled from. Only in the case of glass in the G-IBA it can be seen that no recyclable fraction was produced, as outlined in section 2.1.2. In this case, glass was predominantly enriched in the *mineral fraction < 9 mm* (57 %), *ECS 1 mix* (22 %) and *ECS 2* (19 %) (see Fig. 3 and Figure A9 and A10 in the supplementary material). Glass > 4 mm from the FB-IBA was mainly found in the output flow *glass fraction* (72 %, see Fig. 4), which constitutes the major output flow of the FB-IBA, but other output flows of the FB-IBA contained remarkable glass shares as well (e.g. 67 % in *ECS 2*; 46 % in *ECS 1 mix*, see Fig. 3).

The potential recovery rates of the sub-goods are given in Table 2. Desired output categories, where a sub-good can potentially be recovered from, are relevant for the calculation of the potential recovery rates and are written in bold and italics in Fig. 4.

Table 2 shows that the potential recovery rates of aluminum and magnetic ferrous metals > 4 mm are consistently above 95 %. In this regard the IBA treatment can be seen as very successful because the vast majority of these sub-goods is enriched in the desired output flows. These potential recovery rates are also very high compared to the literature. In the case of magnetic ferrous metals, recovery rates > 80 % are reported (Allegrini et al., 2014; Boesch et al., 2014; Neuwahl et al., 2019) and sometimes also values above 90 % can be found (Bunge, 2018; Muchová and Rem, 2006). For aluminum, however, recovery

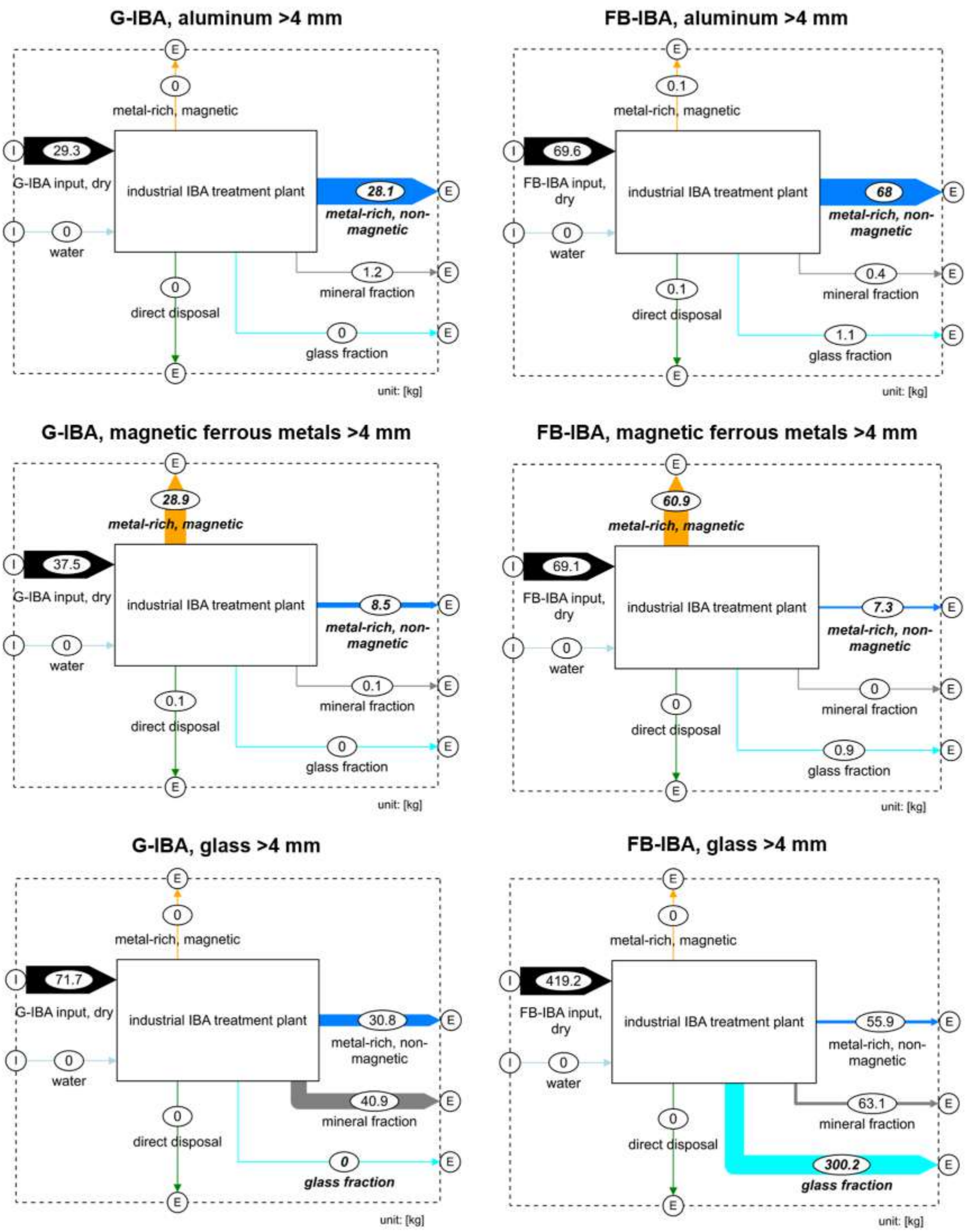

Fig. 4. Results of the material flow analysis on the level of the sub-goods aluminum, magnetic ferrous metals and glass > 4 mm (dry mass) per 1,000 kg of dry IBA input. Simplified illustration based on output categories. Left: Grate incineration bottom ash (G-IBA), right: fluidized bed incineration bottom ash (FB-IBA). Desired output categories of a sub-good (where it can potentially be recovered from) are in bold italics.

rates typically lie below 90 % in the literature (Allegrini et al., 2014; Bunge, 2018; Grosso et al., 2011; Hu and Rem, 2009). Only in the case of dry discharge of G-IBA from Swiss plants, similarly high recovery rates above 90 % are reported for non-ferrous metals (Allegrini et al., 2014). The potential recovery rates achieved in this study are only related to the particle size fractions > 4 mm, which can be a limiting factor. Nevertheless, reference data from Huber et al. (2020) and Blasenbauer et al. (2023) exhibit that magnetic ferrous metals can primarily be found in the particle size fraction > 4 mm. Only aluminum < 4 mm in the G-IBA made up 11 % of the total aluminum in the G-IBA according to Huber et al. (2020) (cf. section 3.4). However, aluminum < 4 mm can also be recovered, for example in the output flow *fstp NFe*, but this was not assessed in this study. It also has to be considered, as mentioned in section 2.3, that losses from further purification or recycling processes were not examined, but have to be expected (van Caneghem et al., 2019). These can amount to up to 35 % in the case of aluminum, as reported by Allegrini et al. (2014).

Surprisingly, no major differences between the recovery rates of aluminum and magnetic ferrous metals > 4 mm were determined, although the recovery of magnetic material is reported to be more effective than ECS for non-magnetic metals (Allegrini et al., 2014; Neuwahl et al., 2019). The occurrence of mineral material and melting effects would as well suggest that metals are more difficult to recover from the G-IBA, but this could not be observed in the present experiment.

For glass in the G-IBA, no desired output category was defined, as no glass separation was conducted. In the case of the FB-IBA 72 % of the glass was separated in the desired *glass fraction*. It has to be considered that glass separation was only conducted for material > 9 mm and about 15 % of the total glass > 4 mm in FB-IBA can be found in particle size fractions < 8 mm (Blasenbauer et al., 2023; Mühl et al., 2023). Therefore, the recovered glass amount could presumably be increased if also particles 4–8 mm were fed to the glass sorter. Nevertheless, complete separation by means of industrial-scale sieving cannot be achieved and therefore also glass 4–8 mm can be found in the glass fraction > 9 mm. To assess the amount of glass 4–8 mm in the *glass fraction* and to which extent glass removal of material 4–8 mm would increase the recovered glass amounts, additional investigations should be performed.

3.4. Limitations and uncertainty assessment

Generally, the heterogeneity of IBAs and the scientific assessment of an industrial process lead to some uncertainty factors that have to be considered for the herein presented study.

First of all, IBA composition always depends on the waste input to the incineration plant, which can vary significantly (e.g. seasonal fluctuations) (Beikmohammadi et al., 2023; Costa et al., 2020). Additionally, a relatively high amount of bulky waste is fed to the grate incinerator considered in this experiment. The composition of bulky waste in Austria, however, is not well known and therefore inhibits a direct comparison with the fluidized bed combustor.

Moreover, the regular industrial IBA treatment of the Brantner plant was followed for this study to assess practical product qualities. This led to the circumstance that the treatment of the G-IBA and the FB-IBA differed slightly, as the output flow *mgS (magnetic slag < 4 mm)* was not fed back to the plant input during the treatment of the FB-IBA (contrarily to the G-IBA), but was disposed of due to a change of the plant operation. Only remaining amounts of the *mgS* after the treatment of FB-IBA could be considered in the modeling. As the output flow *mgS* only contains material < 4 mm, this influences the particle size distribution, but not the amounts of the sub-goods considered (aluminum, magnetic ferrous metals, glass > 4 mm).

Furthermore, the handling of the huge amounts of sample material of the two IBA batches led to some limitations due to necessary reduction of the workload. As mentioned in section 2, only material > 4 mm was manually sorted. Metal pieces that were comminuted to < 4 mm during the treatment and sorting process were therefore not considered. Also, metal pieces enclosed in mineral agglomerates < 4 mm are not regarded, which is a common challenge in IBA assessment (Costa et al., 2020; Skutan, 2023; Šyc et al., 2020). As mentioned in section 2, however, aluminum and magnetic ferrous metals are predominantly contained in particle size fractions > 4 mm. More than 96 % in the cases of magnetic ferrous metals in both IBAs and aluminum in the FB-IBA are contained in particle size fractions > 4 mm (Blasenbauer et al., 2023; Huber et al., 2020). Only the G-IBA contains 11 % of aluminum < 4 mm, which was not considered. Regarding the manual sorting, it must also be added that the visual classification can cause errors. The separation of magnetic ferrous metals by a magnet is quite reliable, but the visual distinction between aluminum and other metals like lead or zinc can be tricky, particularly for smaller particles.

A factor that was also not assessed completely is the composition of output flows counting as *metal-rich, magnetic*. This could lead to a slight overestimation of magnetic ferrous metals in these fractions since extraneous material was not quantified in detail. Moreover, impurities in these fractions can cause quality losses of the scrap metals which impede their recycling. For example, a precise assessment of the copper content in magnetic metal fractions would be interesting to evaluate the scrap quality (Skutan, 2023). In the case of the output flow *unb jig* of the FB-IBA the manual sorting was only conducted for material > 16 mm, as in this floating fraction no sub-goods were expected except for crumpled aluminum foil > 16 mm. Additionally, this output flow only makes up 0.06 % of the FB-IBA, which is the second lowest amount of all output flows measured.

4. Conclusions

In the presented industrial-scale experiment it was assessed that the visible differences between G-IBA and FB-IBA also imply differences in the potential recovery of specific fractions upon treatment. By means of an IBA treatment and sampling campaign, manual sorting and material flow analysis the IBA compositions and the effect of the treatment on the distribution of recyclable material was calculated. Special focus was given to aluminum, magnetic ferrous metals and glass > 4 mm. Quantities and qualities of recovered metals from the FB-IBA were higher and glass could only be separated from the FB-IBA, which exhibits advantages regarding the recyclability of FB-IBA. Nevertheless, when comparing FBC and GI of MSW, it also has to be considered that FBC requires pretreatment of the MSW and that higher amounts of fly ash are produced than in GI (Blasenbauer et al., 2023; Leckner and Lind, 2020; Saqib and Bäckström, 2014). Therefore, coarse recyclable material is enriched in the FB-IBA, because higher amounts of the MSW incinerated are transferred to the fly ash in FBC. It has to be considered that fly ash also needs a disposal solution. This study allows for implications on the recyclability of IBAs from MSWI but it is not possible to decide whether GI or FBC is more advantageous in general. This should be assessed in the future, using a holistic approach considering the composition and pretreatment of the MSW as well as the amounts and utilization paths of fly ash.

This study also confirmed that high potential recovery rates for recyclable materials can be achieved by means of an enhanced multi-step IBA treatment. > 95 % of aluminum and magnetic ferrous metals > 4 mm in both IBAs and 72 % of glass > 4 mm in the FB-IBA were recovered on an industrial scale. Many observations that were determined at pilot scale by Mühl et al. (2023) have been verified on an industrial scale. This shows that upscaling of additional mechanical treatment steps applied to IBA flows is feasible, which is rarely investigated in the scientific literature. The additional treatment steps of the Brantner treatment plant offer a promising way to increase recovery rates of IBAs. To use these results for enhancing material recovery following the circular economy approach, it is still necessary to assess if the mineral fractions can be utilized in the building sector or elsewhere from an environmental and technical point of view. Furthermore, recycling options for glass recovered from the FB-IBA need to be examined, since high quality recycling in glass packaging requires additional upgrading steps to reduce impurities.

CRediT authorship contribution statement

Julia Mühl: Writing – review & editing, Writing – original draft, Visualization, Validation, Methodology, Investigation, Formal analysis, Data curation, Conceptualization. **Simon Hofer:** Methodology, Conceptualization, Data curation, Formal analysis, Investigation, Validation, Writing – review & editing. **Dominik Blasenbauer:** Writing – review & editing, Validation, Methodology, Investigation. **Jakob Lederer:** Writing – review & editing, Supervision, Project administration, Methodology, Funding acquisition, Conceptualization.

Declaration of competing interest

The authors declare that they have no known competing financial interests or personal relationships that could have appeared to influence the work reported in this paper.

Acknowledgements

The financial support by the Austrian Federal Ministry of Labour and Economy, the National Foundation for Research, Technology and Development and the Christian Doppler Research Association is gratefully acknowledged. Furthermore, we thankfully acknowledge the financial and non-financial support of our company partners, which are, in alphabetical order: Abfallbehandlung Ahrental GmbH, Altstoff Recycling Austria AG, Brantner Österreich GmbH, Holding Graz Kommunale Dienstleistungen GmbH, Lenzing Aktiengesellschaft, Linz Service GmbH, MM Board & Paper, Wien Energie GmbH, and Wopfinger Transportbeton Ges.m.b.H. In addition, we thank Magistratsabteilung MA 48, the public Waste Management provider of Vienna, for its non-financial support and all student assistants involved for their hard work and persevering hand sorting. The TU Wien Bibliothek is thanked for financial support through its Open Access Funding Program.

Appendix A. Supplementary material

Supplementary data to this article can be found online at https://doi.org/10.1016/j.wasman.2024.10.025.

Data availability

Data will be made available on request.

References

Allegrini, E., Maresca, A., Olsson, M.E., Holtze, M.S., Boldrin, A., Astrup, T.F., 2014. Quantification of the resource recovery potential of municipal solid waste incineration bottom ashes. Waste Management (New York N.Y.) 34, 1627–1636. https://doi.org/10.1016/j.wasman.2014.05.003.

Bayuseno, A.P., Schmahl, W.W., 2010. Understanding the chemical and mineralogical properties of the inorganic portion of MSWI bottom ash. Waste Management (New York N.Y.) 30, 1509–1520. https://doi.org/10.1016/j.wasman.2010.03.010.

Beikmohammadi, M., Yaghmaeian, K., Nabizadeh, R., Mahvi, A.H., 2023. Analysis of heavy metal, rare, precious, and metallic element content in bottom ash from municipal solid waste incineration in Tehran based on particle size. Sci. Rep. 13, 16044. https://doi.org/10.1038/s41598-023-43139-1.

Biganzoli, L., Gorla, L., Nessi, S., Grosso, M., 2012. Volatilisation and oxidation of aluminium scraps fed into incineration furnaces. Waste Management (new York N. Y.) 32, 2266–2272. https://doi.org/10.1016/j.wasman.2012.06.003.

Blasenbauer, D., Huber, F., Lederer, J., Quina, M.J., Blanc-Biscarat, D., Bogush, A., Bontempi, E., Blondeau, J., Chimenos, J.M., Dahlbo, H., Fagerqvist, J., Giro-Paloma, J., Hjelmar, O., Hyks, J., Keaney, J., Lupsea-Toader, M., O'Caollai, C.J., Orupõld, K., Pająk, T., Simon, F.-G., Svecova, L., Šyc, M., Ulvang, R., Vaajasaari, K., van Caneghem, J., van Zomeren, A., Vasarevičius, S., Wégner, K., Fellner, J., 2020. Legal situation and current practice of waste incineration bottom ash utilisation in Europe. Waste Management (New York N.Y.) 102, 868–883. https://doi.org/10.1016/j.wasman.2019.11.031.

Blasenbauer, D., Huber, F., Mühl, J., Fellner, J., Lederer, J., 2023. Comparing the quantity and quality of glass, metals, and minerals present in waste incineration bottom ashes from a fluidized bed and a grate incinerator. Waste Management (new York N.Y.) 161, 142–155. https://doi.org/10.1016/j.wasman.2023.02.021.

Boesch, M.E., Vadenbo, C., Saner, D., Huter, C., Hellweg, S., 2014. An LCA model for waste incineration enhanced with new technologies for metal recovery and application to the case of Switzerland. Waste management (New York. N.Y.) 34, 378–389. https://doi.org/10.1016/j.wasman.2013.10.019.

Brunner, P.H., Morf, L.S., 2024. Waste to energy, indispensable cornerstone for circular economy: A mini-review. Waste management & research : the journal of the International Solid Wastes and Public Cleansing Association, ISWA, 734242X241227376. Doi: 10.1177/0734242X241227376.

Brunner, P.H., Rechberger, H., 2017. Handbook of material flow analysis: For environmental, resource, and waste engineers. CRC Press Taylor & Francis Group, Boca Raton, London, New York, 435 pp.

Bruno, M., Abis, M., Kuchta, K., Simon, F.-G., Grönholm, R., Hoppe, M., Fiore, S., 2021. Material flow, economic and environmental assessment of municipal solid waste incineration bottom ash recycling potential in Europe. J. Clean. Prod. 317, 128511. https://doi.org/10.1016/j.jclepro.2021.128511.

Bunge, R., 2018. Recovery of Metals from Waste Incineration Bottom Ash. In: Holm, O., Thomé-Kozmiensky, E. (Eds.), Removal, Treatment and Utilisation of Waste Incineration Bottom Ash. Thomé-Kozmiensky Verlag GmbH, Nietwerder, pp. 63–143.

Cencic, O., Rechberger, H., 2008. Material flow analysis with software STAN. J. Environ. Eng. Manage. 2008, 3–7.

Chen, B., Perumal, P., Illikainen, M., Ye, G., 2023. A review on the utilization of municipal solid waste incineration (MSWI) bottom ash as a mineral resource for construction materials. Journal of Building Engineering 71, 106386. https://doi.org/10.1016/j.jobe.2023.106386.

Costa, G., Polettini, A., Pomi, R., Spagnuolo, R., 2020. Enhanced Separation of Incinerator Bottom Ash: Composition and Environmental Behaviour of Separated Mineral and Weakly Magnetic Fractions. Waste Biomass Valor 11, 7079–7095. https://doi.org/10.1007/s12649-020-01106-1.

Dhir, R.K., de Brito, J., Ghataora, G.S., Lye, C.Q., 2018. Sustainable construction materials: Glass cullet. Woodhead Publishing, Duxford, p. 462.

Dou, X., Ren, F., Nguyen, M.Q., Ahamed, A., Yin, K., Chan, W.P., Chang, V.-W.-C., 2017. Review of MSWI bottom ash utilization from perspectives of collective characterization, treatment and existing application. Renew. Sustain. Energy Rev. 79, 24–38. https://doi.org/10.1016/j.rser.2017.05.044.

European Parliament and Council, 2018. Directive (EU) 2018/ of the European Parliament and of the Council of 30 May 2018 amending Directive 94/62/EC on packaging and packaging waste.

European Commission, 2019. COMMISSION IMPLEMENTING DECISION (EU) 2019/ 665 - of 17 April 2019 - amending Decision 2005/ 270/ EC establishing the formats relating to the database system pursuant to European Parliament and Council Directive 94/ 62/ EC on packaging and packaging waste - (notified under document C(2019) 2805), in: Official Journal of the European Union.

Eusden, J., Eighmy, T., Hockert, K., Holland, E., Marsella, K., 1999. Petrogenesis of municipal solid waste combustion bottom ash. Appl. Geochem. 14, 1073–1091.

Fan, C., Wang, B., Ai, H., Liu, Z., 2022. A comparative study on characteristics and leaching toxicity of fluidized bed and grate furnace MSWI fly ash. J. Environ. Manage. 305, 114345. https://doi.org/10.1016/j.jenvman.2021.114345.

Fletcher, C.A., Dunk, R., 2023. Recovery and utilisation of municipal solid waste incineration bottom ash: implications for European waste management strategy. Detritus 43–57. https://doi.org/10.31025/2611-4135/2023.17274.

Gerlach, R.W., Nocerino, J.M., 2003. Guidance for Obtaining Representative Laboratory Analytical Subsamples from Particulate Laboratory Samples. U.S. Environmental Protection Agency. https://clu-in.org/download/char/epa_subsampling_guidance.pdf (accessed 14.12.22).

Bundesverband Glasindustrie e.V; BDE Bundesverband der Deutschen Entsorgungs-, Wasser- und Rohstoffwirtschaft e. V; bvse-Bundesverband Sekundärrohstoffe und Entsorgung e.V., 2014. Leitlinie „Qualitätsanforderungen an Glasscherben zum Einsatz in der Behälterglasindustrie": Standardblatt T 120 [Guideline "Quality requirements for glass cullet for the use in the packaging glass industry"].

Gökelma, M., Vallejo-Olivares, A., Tranell, G., 2021. Characteristic properties and recyclability of the aluminium fraction of MSWI bottom ash. Waste Management (new York N.Y.) 130, 65–73. https://doi.org/10.1016/j.wasman.2021.05.012.

Grosso, M., Biganzoli, L., Rigamonti, L., 2011. A quantitative estimate of potential aluminium recovery from incineration bottom ashes. Resour. Conserv. Recycl. 55, 1178–1184. https://doi.org/10.1016/j.resconrec.2011.08.001.

Gy, P., 1992. Sampling of heterogeneous and dynamic material systems: Theories of heterogeneity, sampling, and homogenizing. Elsevier, Amsterdam, New York, p. 653.

Holm, O., Simon, F.-G., 2017. Innovative treatment trains of bottom ash (BA) from municipal solid waste incineration (MSWI) in Germany. Waste Manag. 59, 229–236. https://doi.org/10.1016/j.wasman.2016.09.004.

Hu, Y., Rem, P., 2009. Aluminium alloys in municipal solid waste incineration bottom ash. Waste Management & Research : the Journal of the International Solid Wastes and Public Cleansing Association, ISWA 27, 251–257. https://doi.org/10.1177/0734242X08095564.

Hu, Y., Bakker, M.C.M., de Heij, P.G., 2011. Recovery and distribution of incinerated aluminum packaging waste. Waste Management (new York N.Y.) 31, 2422–2430. https://doi.org/10.1016/j.wasman.2011.07.021.

Huber, F., 2020. Modelling of material recovery from waste incineration bottom ash. Waste management (New York N.Y.) 105, 61–72. https://doi.org/10.1016/j.wasman.2020.01.034.

Huber, F., Blasenbauer, D., Aschenbrenner, P., Fellner, J., 2019. Chemical composition and leachability of differently sized material fractions of municipal solid waste incineration bottom ash. Waste Management (new York N.Y.) 95, 593–603. https://doi.org/10.1016/j.wasman.2019.06.047.

Huber, F., Blasenbauer, D., Aschenbrenner, P., Fellner, J., 2020. Complete determination of the material composition of municipal solid waste incineration bottom ash. Waste Management (new York N.Y.) 102, 677–685. https://doi.org/10.1016/j.wasman.2019.11.036.

Inkaew, K., Saffarzadeh, A., Shimaoka, T., 2016. Modeling the formation of the quench product in municipal solid waste incineration (MSWI) bottom ash. Waste Management (new York N.Y.) 52, 159–168. https://doi.org/10.1016/j.wasman.2016.03.019.

Austrian Standards Institute, 2011. ÖNORM EN 933-11: Prüfverfahren für geometrische Eigenschaften von Gesteinskörnungen: Teil 11: Einteilung der Bestandteile in grober recyclierter Gesteinskörnung [Tests for geometrical properties of aggregates – Part 11: Classification test for the constituents of coarse recycled aggregate] ICS 91.100.15.

Jung, C., Matsuto, T., Tanaka, N., Okada, T., 2004. Metal distribution in incineration residues of municipal solid waste (MSW) in Japan. Waste Manag. 24, 381–391. https://doi.org/10.1016/S0956-053X(03)00137-5.

Kellner, M., Schindler, I., Jany, A., 2022. Status report waste incineration: Reporting year 2020. Umweltbundesamt, Wien.

Leckner, B., Lind, F., 2020. Combustion of municipal solid waste in fluidized bed or on grate - A comparison. Waste Management (new York N.Y.) 109, 94–108. https://doi.org/10.1016/j.wasman.2020.04.050.

Lederer, J., Bartl, A., Blasenbauer, D., Breslmayer, G., Gritsch, L., Hofer, S., Lipp, A.-M., Mühl, J., 2022. A review of recent trends to increase the share of post-consumer packaging waste to recycling in Europe. Detritus 3–17. https://doi.org/10.31025/2611-4135/2022.15198.

Lederer, J., Feher, F., Skutan, S., 2023. Sensorgestützte VIS-Sortierung zur Charakterisierung und Glasentfernung von Müllverbrennungs-Bettaschen [Sensor-based VIS sorting for characterization and glass removal from MSWI bottom ashes from fluidized bed combustion]. Österr Wasser- Und Abfallw. https://doi.org/10.1007/s00506-023-01001-8.

Lederer, J., Schuch, D., 2024. The contribution of waste and bottom ash treatment to the circular economy of metal packaging: A case study from Austria. Resour. Conserv. Recycl. 203, 107461. https://doi.org/10.1016/j.resconrec.2024.107461.

Lipp, A.-M., Lederer, J., 2024 (under review). The Circular Economy of Packaging Waste in Austria: An Evaluation Based on Statistical Entropy and Material Flow Analysis. Resources, Conservation and Recycling.

López, F.A., Román, C.P., García-Díaz, I., Alguacil, F.J., 2015. Oxidation and waste-to-energy output of aluminium waste packaging during incineration: A laboratory study. Waste Management (new York N.Y.) 43, 162–167. https://doi.org/10.1016/j.wasman.2015.06.025.

López-Delgado, A., Peña, C., López, V., López, F.A., 2003. Quality of ferrous scrap from MSW incinerators: a case study of Spain. Resour. Conserv. Recycl. 40, 39–51. https://doi.org/10.1016/S0921-3449(03)00024-7.

Makari, C., 2014. Optical Sorting for the Recovery of Glass from WIP Slags: – Pilot Plant in Bratislava –. In: Thomé-Kozmiensky, K.J., Thiel, S. (Eds.), Waste Management. TK-Verl, Thomé-Kozmiensky, Neuruppin, pp. 345–354.

Makarichi, L., Jutidamrongphan, W., Techato, K., 2018. The evolution of waste-to-energy incineration: A review. Renew. Sustain. Energy Rev. 91, 812–821. https://doi.org/10.1016/j.rser.2018.04.088.

Maldonado-Alameda, A., Mañosa, J., Miro-Escola, J., Quintero-Payan, A.C., Chimenos, J. M., 2023. Fluidised-bed incineration bottom ash as the sole precursor of alkali-activated binders: A comparison with bottom ash from grate incinerators. Constr. Build. Mater. 364, 130001. https://doi.org/10.1016/j.conbuildmat.2022.130001.

Mehr, J., Haupt, M., Skutan, S., Morf, L., Raka Adrianto, L., Weibel, G., Hellweg, S., 2021. The Environmental Performance of Enhanced Metal Recovery from Dry Municipal Solid Waste Incineration Bottom Ash. Waste Management (new York N. Y.) 119, 330–341. https://doi.org/10.1016/j.wasman.2020.09.001.

Mika (né Hofer), S., Mühl, J., Skutan, S., Aschenbrenner, P., Limbeck, A., Lederer, J., 2024, under review. Substance flows of heavy metals in industrial-scale municipal solid waste incineration bottom ash treatment: a case study from Austria. Waste Management.

Muchová, L., Rem, P.C., 2006. Metal content and recovery of MSWI bottom ash in Amsterdam. In: Waste Management and the Environment III. WASTE. WIT Press, Southampton, pp. 211–216.

Mühl, J., Skutan, S., Stockinger, G., Blasenbauer, D., Lederer, J., 2023. Glass recovery and production of manufactured aggregate from MSWI bottom ashes from fluidized bed and grate incineration by means of enhanced treatment. Waste Manag. 168, 321–333. https://doi.org/10.1016/j.wasman.2023.05.048.

Neuwahl, F., Cusano, G., Benavides, J.G., Holbrook, S., 2019. Best Available Techniques (BAT) Reference Document for Waste Incineration: EUR 29971 EN. Europäische Union, Luxemburg. https://eippcb.jrc.ec.europa.eu/sites/default/files/2020-01/JRC118637_WI_Bref_2019_published_0.pdf (accessed 6 April 2023).

Pfandl, K., Küppers, B., Scheiber, S., Stockinger, G., Holzer, J., Pomberger, R., Antrekowitsch, H., Vollprecht, D., 2020. X-ray fluorescence sorting of non-ferrous metal fractions from municipal solid waste incineration bottom ash processing depending on particle surface properties. Waste Management & Research : the Journal of the International Solid Wastes and Public Cleansing Association, ISWA 38, 111–121. https://doi.org/10.1177/0734242X19879225.

Saffarzadeh, A., Arumugam, N., Shimaoka, T., 2016. Aluminum and aluminum alloys in municipal solid waste incineration (MSWI) bottom ash: A potential source for the production of hydrogen gas. Int. J. Hydrogen Energy 41, 820–831. https://doi.org/10.1016/j.ijhydene.2015.11.059.

Saqib, N., Bäckström, M., 2014. Trace element partitioning in ashes from boilers firing pure wood or mixtures of solid waste with respect to fuel composition, chlorine content and temperature. Waste management (New York, N.Y.) 34, 2505–2519. Doi: 10.1016/j.wasman.2014.08.025.

Saqib, N., Bäckström, M., 2015. Distribution and leaching characteristics of trace elements in ashes as a function of different waste fuels and incineration technologies. J. Environ. Sci. (China) 36, 9–21. https://doi.org/10.1016/j.jes.2015.03.006.

Skutan, S., Gloor, R., Morf, L., 2014. Methodenband: Probenahme, Probenaufbereitung und Analyse fester Rückstände der thermischen Abfallbehandlung und deren Aufbereitungsprodukten. ZAR Stiftung Zentrum für nachhaltige Abfall- und Ressourcennutzung, 60 pp.

Skutan, S., 2023. Bestimmung der NE-Metallgehalte von KVA-Schlacken im Kanton Zürich: Methodenentwicklung und Messkampagnen im November 2021 und September 2022 [Determination of Non-Ferrous Metal Contents of IBA in the Canton of Zurich]. Endbericht. Ingenieurbüro Stefan Skutan e.U., St. Andrä-Wördern. https://www.zh.ch/content/dam/zhweb/bilder-dokumente/themen/umwelt-tiere/abfall-rohstoffe/abfallwirtschaft/publikationen/kehrichtverwertung-kva/schlackenprojekt_zh_kva_schlussbericht_2023.pdf (accessed 23.08.23).

Šyc, M., Krausová, A., Kameníková, P., Šomplák, R., Pavlas, M., Zach, B., Pohořelý, M., Svoboda, K., Punčochář, M., 2018. Material analysis of Bottom ash from waste-to-energy plants. Waste Management (new York N.Y.) 73, 360–366. https://doi.org/10.1016/j.wasman.2017.10.045.

Šyc, M., Simon, F.G., Hykš, J., Braga, R., Biganzoli, L., Costa, G., Funari, V., Grosso, M., 2020. Metal recovery from incineration bottom ash: State-of-the-art and recent developments. J. Hazard. Mater. 393, 122433. https://doi.org/10.1016/j.jhazmat.2020.122433.

Tayibi, H., Peña, C., López, F.A., López-Delgado, A., 2007. Management of MSW in Spain and recovery of packaging steel scrap. Waste Manag. 27, 1655–1665. https://doi.org/10.1016/j.wasman.2006.09.012.

Turner, D.A., Williams, I.D., Kemp, S., 2015. Greenhouse gas emission factors for recycling of source-segregated waste materials. Resour. Conserv. Recycl. 105, 186–197. https://doi.org/10.1016/j.resconrec.2015.10.026.

van Caneghem, J., de Coster, E., Vandenbergh, K., de Broyer, S., Lambrix, N., Weemaels, L., 2019. Closing the household metal packaging cycle through recovery of scrap from waste-to-energy bottom ash: The case study of Flanders. Resour. Conserv. Recycl. 144, 115–122. https://doi.org/10.1016/j.resconrec.2019.01.028.

van de Wouw, P.M.F., Loginova, E., Florea, M.V.A., Brouwers, H.J.H., 2020. Compositional modelling and crushing behaviour of MSWI bottom ash material classes. Waste Management (new York N.Y.) 101, 268–282. https://doi.org/10.1016/j.wasman.2019.10.013.

Vateva, I., Laner, D., 2020. Grain-Size Specific Characterisation and Resource Potentials of Municipal Solid Waste Incineration (MSWI) Bottom Ash: A German Case Study. Resources 9, 66. https://doi.org/10.3390/resources9060066.

Verbinnen, B., Billen, P., van Caneghem, J., Vandecasteele, C., 2017. Recycling of MSWI Bottom Ash: A Review of Chemical Barriers, Engineering Applications and Treatment Technologies. Waste Biomass Valor 8, 1453–1466. https://doi.org/10.1007/s12649-016-9704-0.

Warrings, R., Fellner, J., 2018. Current status of circularity for aluminum from household waste in Austria. Waste management (New York N.Y.) 76, 217–224. https://doi.org/10.1016/j.wasman.2018.02.034.

Warrings, R., Fellner, J., 2021. How to increase recycling rates. The case of aluminium packaging in Austria. Waste Management & Research : the Journal of the International Solid Wastes and Public Cleansing Association, ISWA 39, 53–62. https://doi.org/10.1177/0734242X20947161.

Wotruba, H., Harbeck, H., 2003. Sensor-Based Sorting, in: Ullmann's Encyclopedia of Industrial Chemistry. Wiley.

Xuan, D., Tang, P., Poon, C.S., 2018. Limitations and quality upgrading techniques for utilization of MSW incineration bottom ash in engineering applications – A review. Constr. Build. Mater. 190, 1091–1102. https://doi.org/10.1016/j.conbuildmat.2018.09.174.

Yeo, R.J., Sng, A., Wang, C., Tao, L., Zhu, Q., Bu, J., 2024. Strategies for heavy metals immobilization in municipal solid waste incineration bottom ash: a critical review. Rev. Environ. Sci. Biotechnol. https://doi.org/10.1007/s11157-024-09694-3.

Appendix III

Paper III:

Upgrading and Characterization of Glass recovered from MSWI Bottom Ashes from Fluidized Bed Combustion

Mühl, J.; Mika, S.; Tischberger-Aldrian, A.; Lederer, J.

Recycling 10,63 (2025).
Available online: April, 07th 2025
DOI: https://doi.org/10.3390/recycling10020063

recycling

MDPI

Article

Upgrading and Characterization of Glass Recovered from MSWI Bottom Ashes from Fluidized Bed Combustion

Julia Mühl [1,*], Simon Mika [1], Alexia Tischberger-Aldrian [2] and Jakob Lederer [1]

[1] Christian Doppler Laboratory for a Recycling-Based Circular Economy, Institute of Chemical, Environmental and Bioscience Engineering, TU Wien, Getreidemarkt 9/166, 1060 Vienna, Austria; simon.mika@tuwien.ac.at (S.M.); jakob.lederer@tuwien.ac.at (J.L.)

[2] Chair of Waste Processing Technology and Waste Management, Montanuniversität Leoben, Franz Josef-Straße 18, 8700 Leoben, Austria; alexia.tischberger-aldrian@unileoben.ac.at

* Correspondence: julia.muehl@tuwien.ac.at

Abstract: Glass in mixed municipal solid waste (MSW) is often lost for recycling. Glass recovery from incineration bottom ash (IBA) after MSW incineration (MSWI) is technically feasible by sensor-based sorting, but rarely applied. Especially IBAs from fluidized bed combustion contain high recoverable glass amounts, but upgrading this glass is required for recycling in the packaging glass industry. This study examines different upgrading setups based on sensor-based sorting to improve the glass quality from two Austrian fluidized bed IBAs. Sensor-based sorting removed extraneous material like ceramic, stones, porcelain, metals, and lead glass. The fractions produced were characterized by manual sorting and X-ray fluorescence analysis. The glass fractions before upgrading contained 85–89% glass, of which 67% and 83% could be recovered after four sorting steps. Previous sieving caused high glass losses and is therefore not recommended. By sensor-based sorting, the extraneous material contents were lowered from 13% and 9% in the two IBAs to below 2.2%. Four-step upgrading could even ensure extraneous material contents <0.11% and Pb contents <200 mg/kg. Although limit values for packaging glass recycling were still exceeded, this study shows that upgrading of glass recovered from fluidized bed IBAs suggests a novel opportunity to enhance closed-loop glass recycling, thereby reducing the amount of landfilled glass.

Keywords: circular economy; waste glass; glass recycling; municipal solid waste incineration; incineration bottom ash; fluidized bed combustion; mechanical treatment; sensor-based sorting

Academic Editor: Giovanni De Feo

Received: 25 February 2025
Revised: 19 March 2025
Accepted: 1 April 2025
Published: 7 April 2025

Citation: Mühl, J.; Mika, S.; Tischberger-Aldrian, A.; Lederer, J. Upgrading and Characterization of Glass Recovered from MSWI Bottom Ashes from Fluidized Bed Combustion. *Recycling* **2025**, *10*, 63. https://doi.org/10.3390/recycling10020063

1. Introduction

Glass is a versatile and durable material, widely used in applications ranging from packaging to construction [1]. Although primary glass production is very material- and energy-intense, the ecological advantage of glass lies in its infinite recyclability without quality loss [2,3]. Several recycling options for waste glass, including both closed- and open-loop processes, are available and investigated in the literature [4,5]. For example, glass cullet can be used in foam glass production [6–8] or in other fields of the construction sector [9–13]. Yet, closed-loop recycling in the packaging glass industry is seen as the most desirable recycling path, since this saves raw materials and energy, and the material can be utilized as such [14]. Using 10% crushed glass (cullet) in packaging glass recycling allows for 2.0–3.0% energy savings in the process [15–17]. To ensure high quality and avoid process disturbances, recycling in the packaging glass industry requires strict quality standards regarding the content of extraneous material, like ceramic, stones, porcelain, and other non-glass mineral-based material (CSP) or metal pieces and heavy metals [1,18]. Therefore, waste glass cullet has to be processed in multi-stage treatment, including color sorting, sieving, and removal of extraneous material [19]. Whereas sensor-based sorting using the visible light spectrum (VIS) is applied for the distinction between different colors and extraneous material, lead glass can be removed by utilization of ultraviolet (UV) light or X-ray fluorescence (XRF) [20–22].

The foundation for high-grade recycling is the separate collection of waste glass, which is well-developed in the European Union (EU) [14,23]. This already secured the required recycling rate for packaging glass above 75% in 2022 in the EU, which is the value set as a recycling target as of 2030 [24,25]. Yet, 20% of the glass was not collected separately in the EU in 2022 [26]. In single EU countries like Hungary, Greece, or Portugal, the packaging glass collection rates were significantly lower, accounting for 22–51% [26]. Globally, high landfill rates and clearly lower recycling rates, around 35%, are reported for container glass [27,28]. This also counts for highly industrialized countries like the United States or Japan [28,29].

Glass that is not collected separately is primarily disposed of in mixed municipal solid waste (MSW). Besides the improvement of separate collection, glass recovery from mixed MSW is a measure to make glass still available for recycling [2,30]. This can be realized by mechanical biological treatment plants, but this process is only applied to portions of the mixed MSW in single countries [31–33]. Usually, mixed MSW is predominantly either landfilled or incinerated in the EU [34]. After MSW incineration (MSWI), glass remains as a solid residue in the mineral fraction of the incineration bottom ash (IBA) [35–37]. Depending on factors like the state of separate collection in a country, varying glass shares of 5–30% contained in IBA from grate incineration, which is the predominant MSWI technology, are reported [38–41]. Even higher glass amounts (up to 47%) were determined in IBA from fluidized bed combustion, which is a subordinate MSWI technology but highly used in single countries, such as Austria [37]. In contrast to metals, which are recovered from IBA to a substantial amount, thereby contributing to higher metal recycling rates, glass in mixed MSW is usually not recovered from IBAs [42,43]. The glass in IBAs is landfilled to a large extent or, in the case of recycling of the mineral fraction of IBAs, utilized as mineral material, for example in the construction sector [44,45]. In both cases, the glass is lost for closed-loop recycling.

Nevertheless, glass recovery from IBA is technically possible by sensor-based sorting, as shown in studies by Makari [46] and Mühl et al. [47]. Whereas Makari [46] only examined glass from grate IBA and did not delve into detail regarding recoverable amounts, glass quality, or utilization paths, Mühl et al. [47] investigated pilot-scale glass recovery from three different IBAs from grate incineration and from three others from fluidized bed incineration. The latter study found that comparatively low amounts of glass not suitable for glass recycling can be recovered from grate IBA. Significantly higher glass amounts in better quality could be recovered on a pilot scale from the fluidized bed IBAs (FB-IBAs) investigated. Based on these findings, an industrial Austrian IBA treatment plant was expanded and equipped with a sensor-based glass sorter. Additional work by Mühl et al. [48] showed that this glass sorter is capable of industrially recovering high glass amounts from FB-IBA, amounting to 300 kg of pure glass per ton of IBA input, but no glass from grate IBA could be recovered industrially. However, the requirements of the packaging glass industry were not met by the glass recovered from FB-IBA in both studies, and further upgrading of the glass fraction was suggested but not investigated by the authors. Additionally, the detailed composition of glass fractions from FB-IBAs has not been thoroughly investigated yet, and no data is available on the chemical composition of glass cullet derived from IBA. Hence, it remains unclear which glass quality can be achieved after upgrading and whether upgraded glass from FB-IBA is suitable for closed-loop recycling.

To close this research gap, glass fractions industrially recovered from FB-IBAs were upgraded by additional sensor-based sorting in different upgrading setups. The performance of the upgrading processes was evaluated and it was examined whether the produced glass fractions could meet the requirements of the packaging glass industry. Therefore, material fractions produced from the upgrading processes were characterized by determining their macroscopic composition and heavy metal content, focusing especially on the Pb content. Thereby, this work strives to answer the following research questions:

- Which quality can be achieved by different upgrading setups of glass fractions recovered from FB-IBA?
- Do the glass fractions after upgrading meet the requirements for recycling in the packaging glass industry?
- Can lead glass be successfully removed by upgrading?

By answering these questions, this study aims to identify new opportunities for closed-loop glass recycling, simultaneously reducing the amount of landfilled glass. Most of these examinations are assessed and published for the first time since hardly any data about glass from MSWI, particularly from fluidized bed combustion, is available.

2. Materials and Methods

2.1. Glass Fractions Used for Upgrading

Two glass fractions from FB-IBAs from two different fluidized bed MSWI plants in Austria were used to address the research issues. The glass fractions were generated by industrial IBA treatment at the Austrian treatment plant of the Brantner Österreich GmbH (Austria) company. This plant has already been investigated several times and includes wet treatment in a jig and multiple metal separation steps [40,49]. After examinations by Mühl et al. [47], the Brantner treatment plant was expanded in 2021, as described and illustrated with a treatment scheme in Mühl et al. [48]. By now, glass fractions can also be recovered from FB-IBAs on an industrial scale. The plant extension includes additional metal separation and glass removal. The glass separator in operation is a *Mogensen MSort AX* type for sensor-based glass sorting of wet cullet using optical light. The two glass fractions investigated are referred to as FB-IBA B and C, according to the FB-IBAs, which they are recovered from in analogy to Mühl et al. [47], where these FB-IBAs were already examined. Information on the MSWI plants, where these IBAs stem from, is given by Mühl et al. [47]. These two FB-IBAs were chosen for the experiment to determine possible differences in the glass fractions, for instance, caused by varying MSWI input and incineration temperature. Whereas FB-IBA C derives from an MSWI plant where pretreated MSW is incinerated almost solely, in the plant producing FB-IBA B also mixed MSW, industrial, commercial, and bulky waste is used as a fuel [47]. Furthermore, the MSWI plant of FB-IBA C works with a comparatively low incineration temperature, which will be discussed further below in Section 3.4 [1] (personal communication , 2024). Pictures of the two glass fractions before upgrading are given in the Supplementary Material (Figure S1).

Sampling of the glass fraction FB-IBA C was conducted in the course of the industrial-scale treatment experiment described by Mühl et al. [48]. In this work, one IBA from fluidized bed combustion was industrially treated, thereby also producing a glass fraction, accounting for 35% of the total IBA amount treated. 47 samples of this glass fraction were collected during a treatment time of more than eight hours. For sampling, a large tarp

(1 m × 1.5 m) was held under the falling material stream in accordance with Gerlach and Nocerino [50]. Thereby, 440 kg of sample mass was collected for this study.

The second glass fraction from FB-IBA B was generated analogously to FB-IBA C in a separate industrial treatment and sampling run. Since this treatment run was not investigated in such detail, the share of glass fraction produced relative to the IBA treated is not known in this case. The same procedure as for FB-IBA C was used to obtain samples of the glass fraction, but sampling was carried out within 100 min. 33 samples, accounting for 330 kg, were taken during this time.

2.2. Upgrading of the Glass Fractions

The glass fractions FB-IBA B and C from the industrial treatment, which are primarily of particle size >9 mm [48], were further upgraded to determine if the requirements of the packaging glass industry could be met thereafter. For the upgrading, sensor-based glass sorting was applied using the VIS- and UV-based sorter *CLARITY* by Binder + Co AG (Gleisdorf, Austria), which is shown in the Supplementary Material (Figure S2). This sorting machine can simultaneously remove various types of extraneous material from the glass cullet. In only one sorting step metals, CSP, lead glass and heat-resistant glass can be detected based on sensor-fusion and ejected from the glass cullet by compressed air [46,51]. Thereby, each sorting step produces a fraction enriched in glass, referred to as *GL* fractions, and one fraction containing extraneous material, referred to as *EM* fractions. Two different upgrading setups were used and compared. For these setups, the glass fractions from industrial treatment were split into halves, and one half was used for each of them. In the first upgrading setup, referred to as *US_I–IV*, glass separation was applied consecutively in multiple upgrading steps to the unsieved glass fractions. In the second upgrading setup, *US_8–16*, the aim was to examine the effect of previous sieving of the glass fraction before applying a single glass separation step. The upgrading setups are described in the following section and are shown in Figure 1.

2.2.1. Upgrading Setup *US_I–IV*: Multi-Step Upgrading of Unsieved Glass Fractions

In experiment *US_I–IV* the glass fractions from industrial IBA treatment were consecutively fed four times into sensor-based sorting to eject extraneous material. The extraneous material removed from the glass fraction by negative sorting was collected and weighed. The glass fraction was weighed and fed into the glass sorter again.

As it was the aim of this experimental setup to produce a glass fraction complying with the requirements of the packaging glass industry, the expected number of upgrading runs necessary was determined in advance. From reference data by Mühl et al. [47], who reported up to 13% CSP and 1% metals in the glass fractions generated by pilot-scale treatment, it was assumed that the strict regulations for packaging glass require more than one additional sorting step. To estimate the number n of upgrading steps necessary for meeting the limit values, the following Equation (1) was used:

$$log_{RC}\left(\frac{LV}{EM}\right) = n \quad (1)$$

In this equation, *RC* is the residual content of extraneous material after each sorting step. In this case, it was assumed that each upgrading run reduces the content of extraneous material by 90%, thereby resulting in *RC* being 0.1 (10%). *LV* stands for the limit value given in Bundesverband Glasindustrie e.V. et al. [18] for CSP and metals (0.002% for CSP, 0.0003% for non-ferrous metals, and 0.0002% for ferrous metals). *EM* is the content of extraneous material reported by Mühl et al. [47]. The highest value determined for n was 3.6, which was calculated for FB-IBA B with 8.8% of CSP (*EM*), compared to the limit value of 0.002% (*LV*). Therefore, four additional upgrading runs were applied to the glass in the present study.

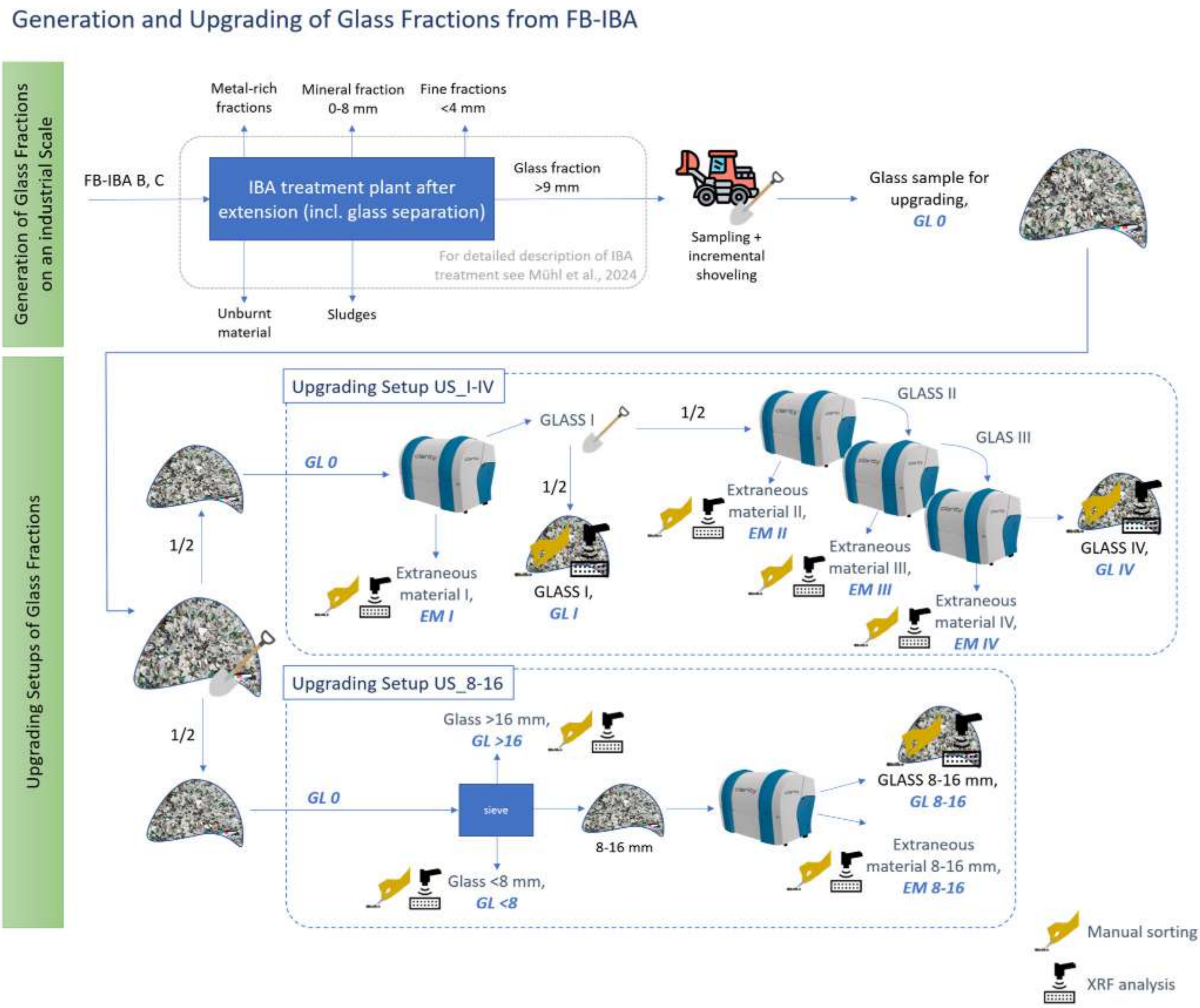

Figure 1. Representation of the experimental setup. A detailed description of the IBA treatment can be found in Mühl et al. [48]. FB-IBA: Fluidized bed incineration bottom ash.

After the first glass removal step, the glass fraction was split to obtain a reference sample to characterize the glass composition. Glass fractions produced in this upgrading setup are referred to as *GL I–IV*, according to the number of upgrading runs and extraneous material fractions are denoted as *EM I–IV* accordingly. The extraneous material from every sorting step as well as the glass fractions from the fourth and the first sorting step after splitting were used for characterization.

2.2.2. Upgrading Setup *US_8–16*: Single-Step Upgrading of Sieved Glass Fractions 8–16 mm

As reported by Šyc et al. [40], processing of narrower particle size fractions of IBA is more efficient and, therefore, shows better results. According to Peukert et al. [51] and Wotruba and Harbeck [52], the largest particles should not exceed three times the size of the smallest particles. Since the glass fractions from industrial IBA treatment mainly contain particles of 8–35 mm, this requirement is not fulfilled. To evaluate the benefits of sensor-based glass sorting from a narrower particle size fraction, upgrading of sieved glass fractions was also examined. Therefore, the industrially produced glass fractions from FB-IBA B and C were sieved with a vibrating screen (*FleXiever mini screener*, *SMO LLC*). First, a 16 mm sieve deck was used. Subsequently, the material <16 mm was sieved with an 8 mm sieve deck. All particle size fractions produced, i.e., <8 mm, >16 mm, and 8–16 mm, were collected and weighed. The particle size fraction 8–16 mm was used for comparative single-step upgrading with the sensor-based glass sorter since this fraction contains the highest glass shares [37]. The outputs of the sorter, *GL 8–16* and *EM 8–16*, were weighed and used for characterization.

2.3. Fractions' Compositions and Material Flows

The compositions of the fractions of both upgrading setups were either determined by manual sorting of the material >4 mm or calculated using material flow analysis based on Brunner and Rechberger [53].

2.3.1. Manual Sorting

For the manual sorting of the glass fractions, the standard EN 933-11 [54] recommends manually sorting of at least 1000 particles of each fraction. Depending on the particle size fractions, this corresponds to 0.5 kg (fraction < 8 mm), 2 kg (8–16 mm), and 10 kg (16–32 mm) of sample mass. These masses were obtained by sieving with a *HAVER EML 450 digital plus N* test sieve shaker, using 4, 8, and 16 mm meshes, followed by fractional shoveling to reduce sample masses. If the masses available for sorting were below the masses required by the standard, the total sample mass available was used for sorting. Fractions from upgrading setup *US_8–16* were only sieved with a 4 mm mesh to remove fine material and dust before sorting, as they were already sieved before glass removal. According to their visual appearance, the particles > 4 mm were sorted into glass of different colors (clear, green, amber); other glass, including glass of other colors, molten glass agglomerates or highly tarnished glass; metals; and non-glass mineral-based material (CSP), which contains ceramic, stones, porcelain, building material (e.g., concrete, brick), and molten agglomerates. Throughout this work, non-glass mineral-based extraneous material is summarized as CSP.

2.3.2. Material Flow Analysis

During the course of the upgrading setups, all fractions were weighed to create material flow analyses, which allowed for an evaluation of the upgrading processes. Additionally, the compositions of fractions that were not sorted manually could be calculated, using the software STAN, version 2.6.801. This was applied to the input glass fractions before upgrading and to the fractions *GL II* and *GL III* of *US_I–IV*. Through material flow analysis, the Pb content in the glass input (*GL 0*) could also be calculated after XRF analysis.

2.4. Chemical Analysis of the Fractions

2.4.1. XRF and Cr(VI) Analysis

To determine the elemental composition of the fractions produced, XRF analysis was used. This is important to detect heavy metals like Pb, Cd and Hg, which are restricted in glass cullet in the packaging glass industry [18]. For the XRF analysis, subsamples were comminuted to <500 µm by crushing and milling, which is detailed in the Supplementary Material (Section S1.3.1). The powder < 500 µm was pressed into pellets and analyzed with a hand-held XRF analyzer, type *ThermoScientific Niton XL3t GOLDD+* with Portable Test Stand (testing mode "*TestAll Geo*"). Each sample was measured four times, and the results were averaged. The share of the tableting aid, which dilutes the analytes, was considered by dividing the results by 0.8. For results below the detection limit, the measurement value was assumed to be the standard deviation.

The three milled glass fractions of each FB-IBA (*GL I*, *GL IV*, and *GL 8–16*) were also analyzed for their content of Cr(VI) by total digestion in accordance with the standards EN 13656:2002-12 [54] and DIN 38405-52 [55], as this parameter is requested by the packaging glass industry.

2.4.2. Determination of Lead Glass by UV-C Light

To estimate if lead glass contributes substantially to the Pb content in the glass fractions, the share of lead glass shards in the glass fractions was determined. Thereby, it could be approximated which Pb concentration results from the lead glass. This concentration was compared to the results of the XRF analysis. Detection of lead glass shards was done using a UV-C lamp with a wavelength of 254 nm (type *analytikjena UVS-26P*), as lead glass shines purple when exposed to this light [56,57]. A picture of this effect is shown in the Supplementary Material (Figure S5). Only the clear glass fractions after manual sorting were investigated since lead glass is typically clear. The mass of lead glass detected in each fraction i ($m_{LG,i}$) was weighed. It was estimated that lead glass contains 15–25% of *Pb* [4,58]. Thereby, an expectated range of the *Pb* concentration $c_{Pb,i}$ in each glass fraction i could be calculated using the masses of the total glass fractions ($m_{GF,i}$) and Equation (2), where x is the share of *Pb* in lead glass (estimation range 0.15–0.25):

$$c_{Pb,i} = x * \frac{m_{LG,i}}{m_{GF,i}} \quad (2)$$

The concentration range calculated was further compared to the *Pb* results determined by XRF analysis.

3. Results and Discussion

The following sections present and discuss the major results regarding material flows, fractions' compositions, and chemical analysis. Additional and related values can be found in the Supplementary Material (Section S2).

3.1. Material Flows of the Upgrading Setups

In the following, the material flows of the upgrading setups *US_I–IV* and *US_8–16* are shown as Sankey diagrams. Figure 2 presents the material flows of the four-step upgrading of glass conducted in setup *US_I–IV*. The results are normalized to 1 ton of input material.

Figure 2 shows that 85% (FB-IBA B) and 89% (FB-IBA C) per ton of glass fraction fed into the upgrading are glass. After four consecutive glass removal steps, very clean glass fractions could be produced, containing almost no extraneous material or metals. However, per ton of input, 0.29 t (FB-IBA B) and 0.15 t (FB-IBA C), which account for 34% and 17% of the glass contained in the glass fractions, are lost in the extraneous material fractions after the four-step upgrading. In total, 57% (FB-IBA B) and 74% (FB-IBA C) of the total material input fed into the upgrading could be obtained as pure glass. More than 99% of CSP and metals were separated into extraneous material fractions.

The material flows of the single-step upgrading with previous sieving of the glass fractions (*US_8–16*) are given in Figure 3.

In setup *US_8–16*, similar glass shares were determined in the input material as in *US_I–IV* (86% and 88%). Per ton of input, 0.440 t (44% of the input) and 0.56 t (56% of the input) of glass could be enriched in the upgraded glass fraction 8–16 mm (*GL 8–16*) in the case of the FB-IBA B and C, respectively. Since FB-IBA B contains 86% and FB-IBA C 88% of glass, this accounts for 51% (FB-IBA B) and 64% (FB-IBA C) of the total glass fed into the sieving and glass removal. Through sieving of 1 t of glass fraction, 276 kg of glass in FB-IBA B were lost in the fractions >16 mm and <8 mm, as these particle size fractions also contain glass. Additionally, 141 kg of glass were missorted into the extraneous material 8–16 mm (*EM 8–16*). In total, 417 kg, which account for 49% of the glass, were lost during the upgrading of FB-IBA B. Regarding the upgrading of one ton of glass fraction from FB-IBA C, 294 kg of glass were lost in the sieved fractions. Together with 21 kg removed with the extraneous fraction 8–16 mm, 315 kg of glass, which corresponds to 36% of the glass input, are no longer available in the produced glass fraction 8–16 mm of FB-IBA C.

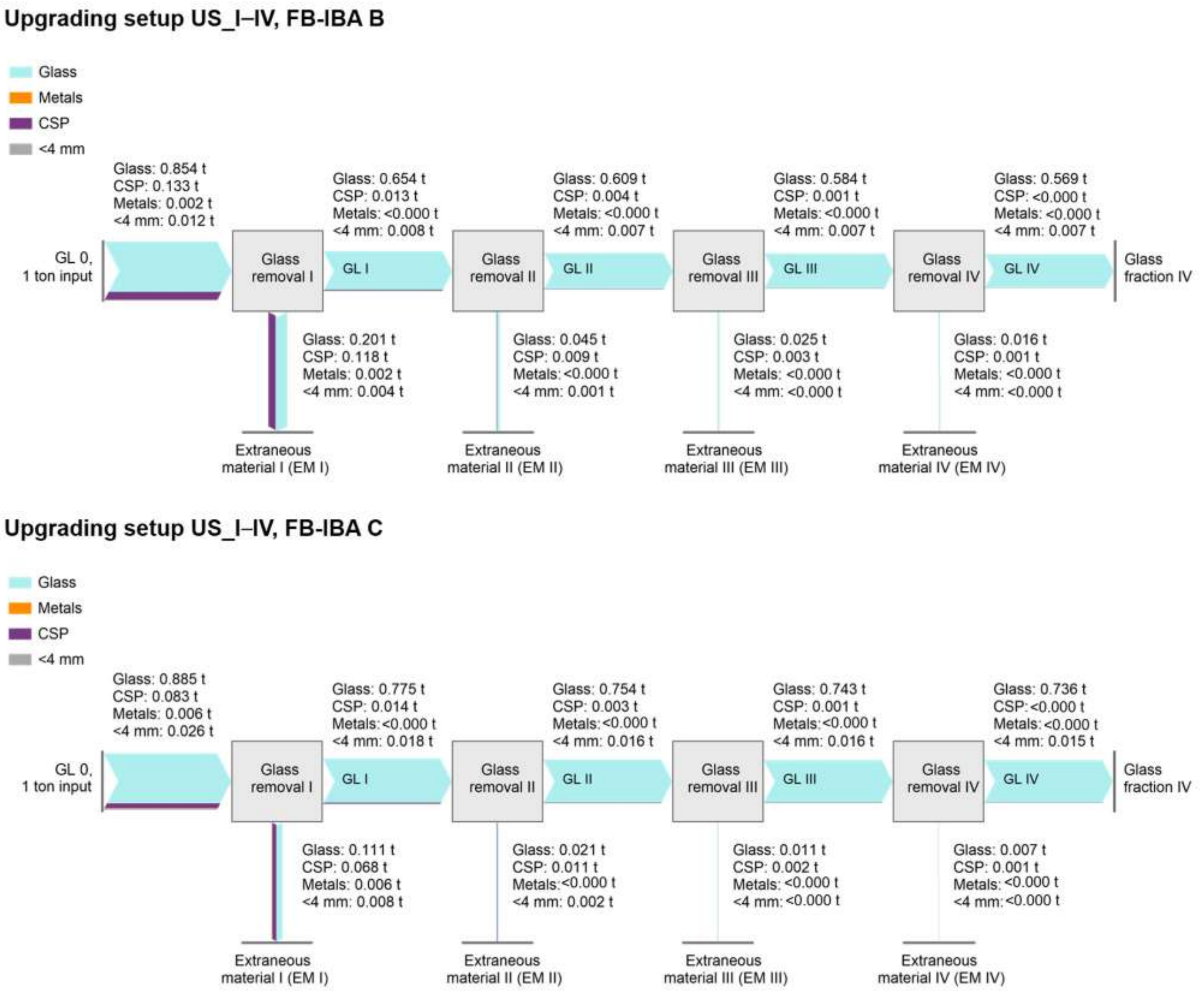

Figure 2. Results of upgrading setup *US_I–IV*: Material flows of FB-IBA B (**above**) and FB-IBA C (**below**) per 1 ton of glass fraction as input material.

Regarding sieving of the input material before glass removal, approximately a third of the glass (32% of FB-IBA B and 33% of FB-IBA C) was separated into the sieved fractions >16 mm and <8 mm in both cases. Hence, sieving causes a substantial loss of glass if glass is not removed from the other particle size fractions as well. Concerning extraneous material in *US_8–16*, only 10 kg and 7 kg of CSP were found in the glass fractions 8–16 mm (*GL 8–16*) of FB-IBA B and C, respectively. In both cases, 92% of the extraneous material were removed from the glass fraction 8–16 mm by sieving and glass separation.

3.2. *Compositions of the Glass Fractions*

Figure 4 presents the compositions of the glass fractions produced in the two upgrading setups. Further data on the composition of particle size fractions or extraneous material fractions, respective numerical values and pictures of the manually sorted material are given in the Supplementary Material (Section S2).

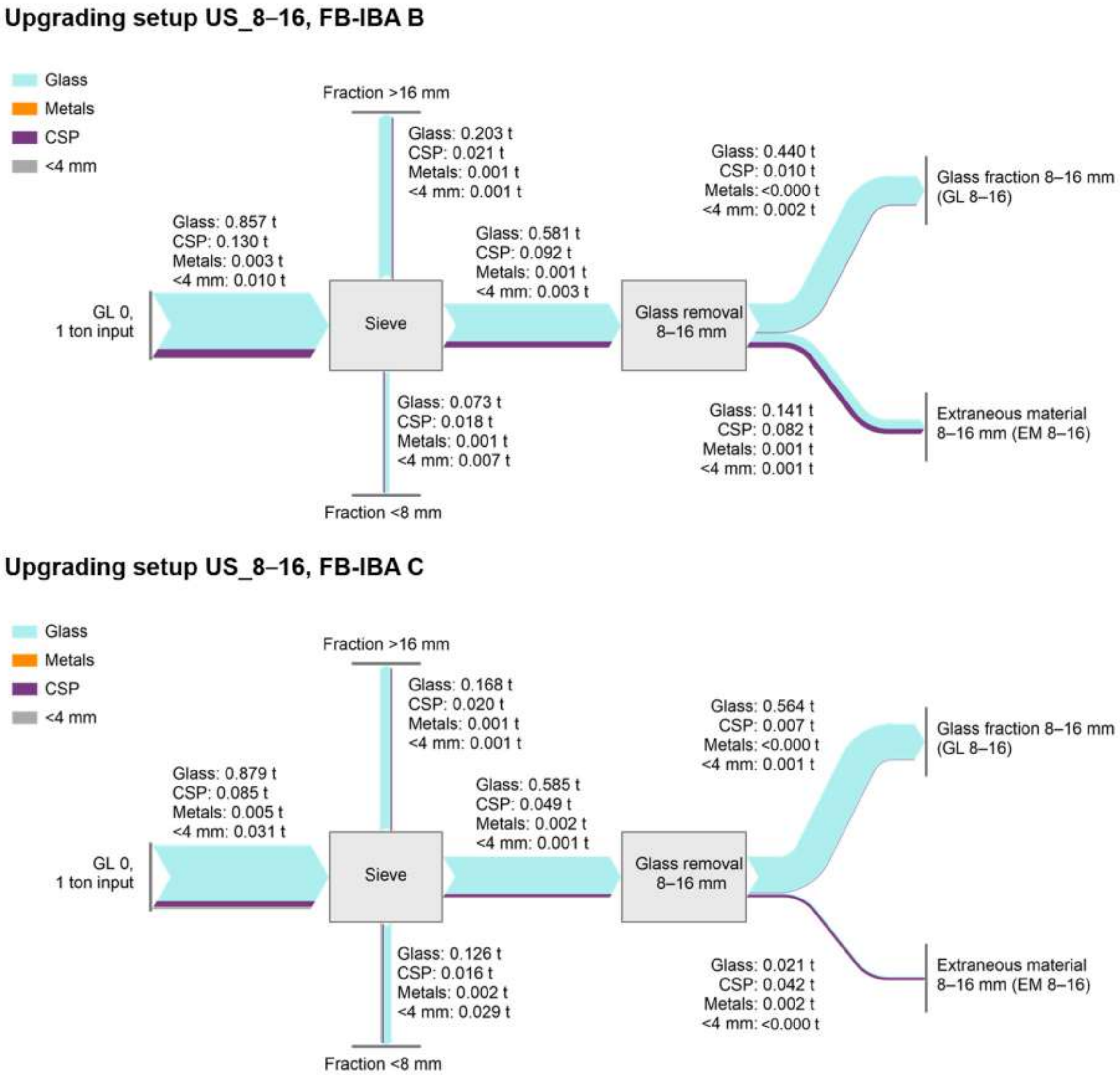

Figure 3. Results of upgrading setup *US_8–16*: Material flows of FB-IBA B (**above**) and FB-IBA C (**below**) per 1 ton of glass fraction as input material.

On the left side in Figure 4 the compositions of the glass fractions before upgrading are depicted, which are referred to as "*GL 0*" therein. These values are the mean value of the compositions calculated from both upgrading setups. The input fractions *GL 0* contain mostly clear glass (56–58%), followed by green glass (21–26%). The content of amber glass does not exceed 3%, which can be traced back to the fact that amber glass in Austria is primarily used for beer bottles, which are predominantly part of a deposit refund system and therefore not disposed of in MSW. A total of 3–5% of "other glass" was found in the glass fractions. FB-IBA B contains more "other glass" and CSP than FB-IBA C. Extraneous material (CSP and metals) made up 13% (FB-IBA B) and 9% (FB-IBA C) in total before upgrading. After upgrading, the lowest CSP content determined was 0.1% for both IBAs after four-step upgrading. The metal contents were in the range of 0.004–0.04% after upgrading with the lowest content achieved in single-step upgrading of *US_8–16*.

The *fraction* residues < 4 mm is given in all results but is not further examined, as it can be expected that this fraction can be easily removed by sieving or appropriate dust extraction during an industrial upgrading process.

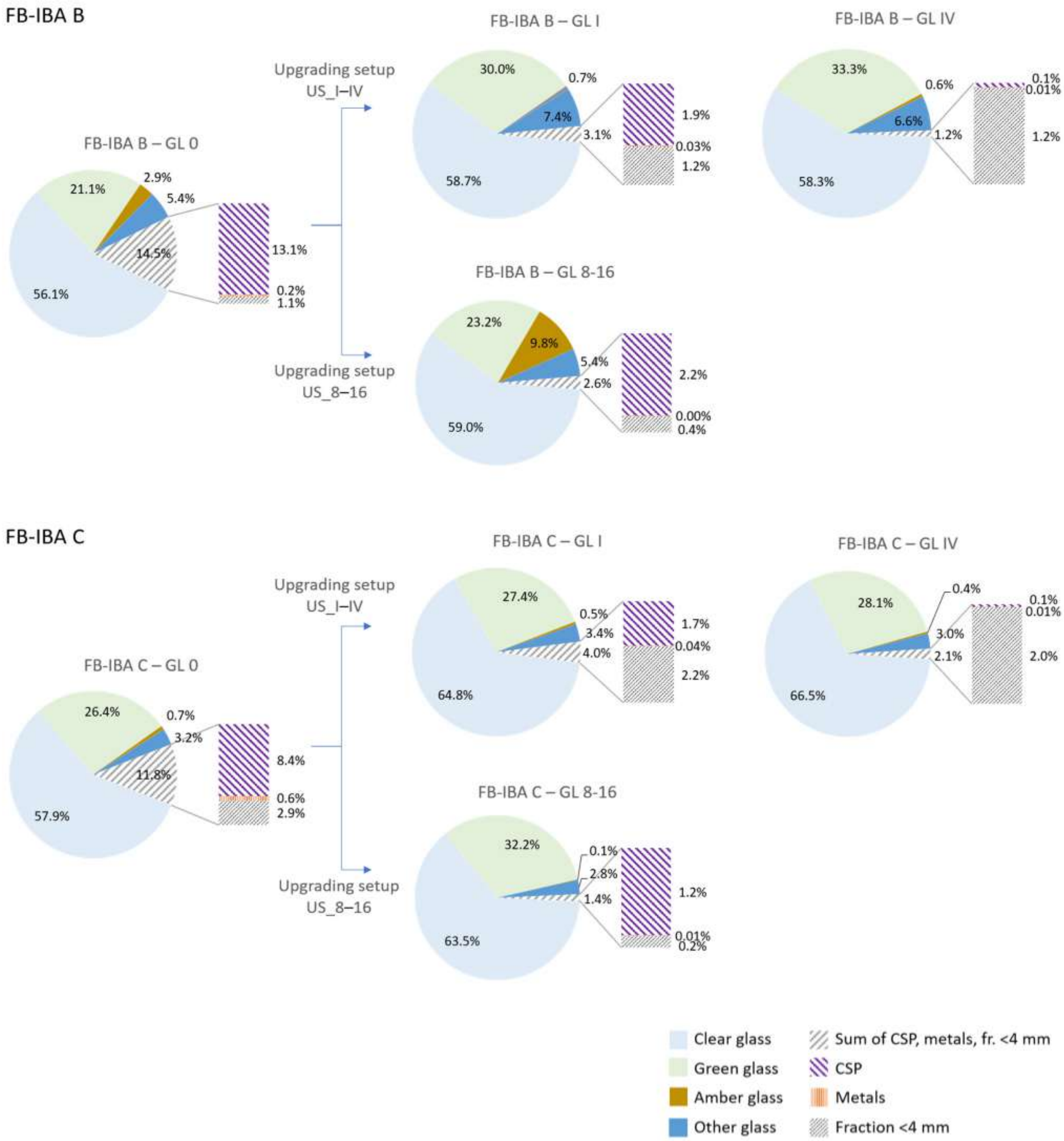

Figure 4. Compositions of glass fractions. Glass from fluidized bed incineration bottom ash (FB-IBA) B (**above**), from FB-IBA C (**below**). Other glass includes glass of other colors, molten agglomerates, or highly tarnished glass. CSP: non-glass mineral-based extraneous material (e.g., ceramic, stones, porcelain, building material).

3.3. *Results of Chemical Analysis of the Fractions*

3.3.1. Results of XRF and Cr(VI) Analysis

Pb, Cd, Hg, and Cr(VI) are limited to 200 mg/kg in the packaging glass industry and were therefore analyzed [18]. The results can be found in the Supplementary Material

(Table S6). For Cd, Hg and Cr(VI) all measurements were determined to be below the detection limits, which correspond to 15 mg/kg (Cd), 13 mg/kg (Hg), and 2 mg/kg (Cr(VI)), respectively. For Cd and Hg the detection limit was calculated by three times the standard deviation [59]. Only in the case of Pb were relevant concentrations measured, which are depicted in Figure 5. Therefore, Pb is the only critical parameter to meet the limit value of the packaging glass industry. In the glass fractions after upgrading, Pb concentrations are in the range of 110–272 mg/kg.

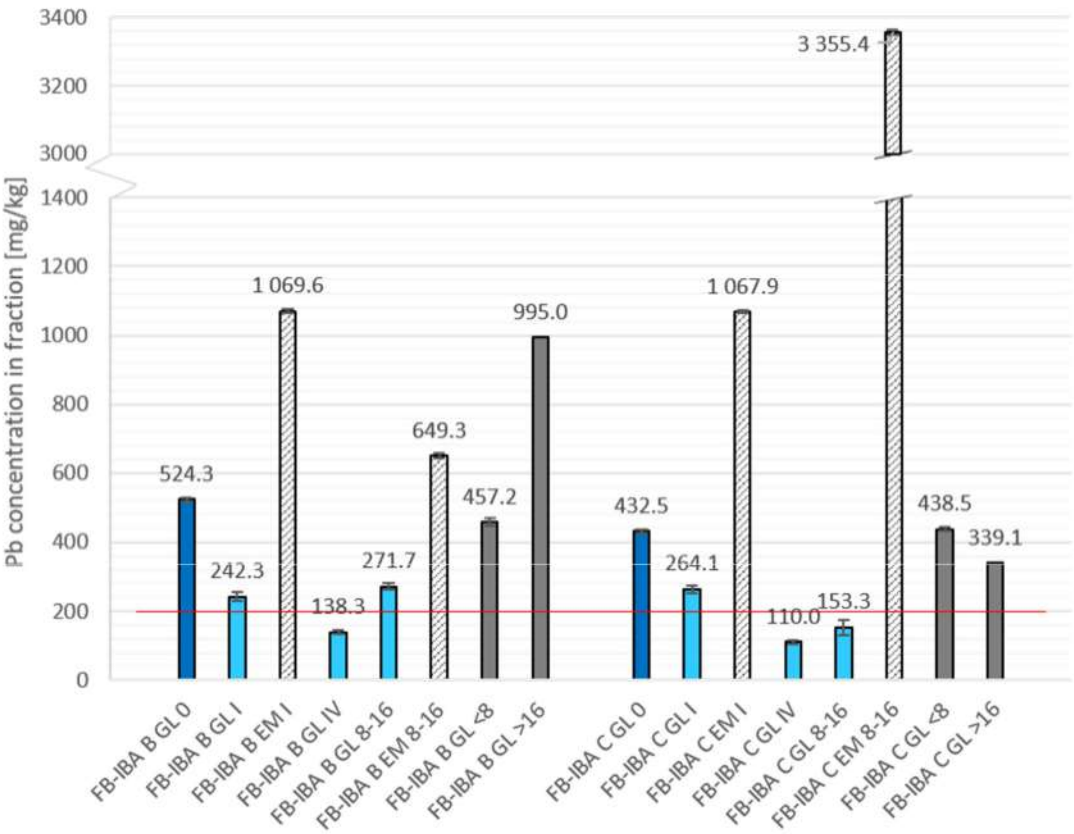

Figure 5. Pb concentrations in different fractions.

The content of Pb in the input glass fractions (*GL 0*) could be calculated by a material flow analysis on the basis of Pb, which is shown in the Supplementary Material (Tables S7 and S8). Consistent results were determined in both upgrading setups. The Pb content of FB-IBA B was calculated as 511 mg/kg (*US_I–IV*) and 538 mg/kg (*US_8–16*) and those of FB-IBA C to 419 mg/kg (*US_I–IV*) and 446 mg/kg (*US_8–16*), resulting in the mean values given in Figure 5.

A comparison of the glass and extraneous material fractions demonstrates that Pb can be enriched in the latter by upgrading. The glass sorter is able to detect and remove ceramics and lead glass, which both contain higher amounts of Pb than waste glass, according to the literature: Götze et al. [60] reported Pb concentrations around 200 mg/kg in waste glass [60]. Investigations by Turner [61] presented color-dependent Pb concentrations in glass in the range of 46–202 mg/kg. Significantly higher Pb concentrations of 900–2000 mg/kg were reported in ceramics [58] and particularly in lead glass with 180,000–270,000 mg/kg PbO [4]. Mika et al. [62] and Blasenbauer et al. [37] provide reference data for the glass fraction of FB-IBA C. Mika et al. [62] determined 370 mg/kg of Pb by total digestion and inductively coupled plasma optical emission spectrometry (ICP-OES) of the glass fraction industrially recovered. This is slightly below the value determined in this study (433 mg/kg) but lies within a plausible range. Blasenbauer et al. [37] detected higher Pb contents of 630 mg/kg in glass manually sorted from untreated IBA. A possible reason for the lower value in the present study is that lead glass might also be depleted in the glass fraction by IBA treatment. For example, the heavy material fraction separated by their sinking speed in the jig also contains high glass amounts [48]. Regarding Cd contents, which were below the detection limit in the present work, Mika et al. [62] reported 8.6 mg/kg. Cd concentrations in various glass fractions analyzed by Turner [61] and in glass from IBA analyzed by Blasenbauer et al. [37] did not surpass 22 mg/kg. Hence, this parameter is clearly less decisive for compliance with the limit value of the packaging glass industry compared to Pb.

Results of the XRF analysis of further parameters are given in the Supplementary Material (Table S9). Therein, also the mass share of manually sorted metals during sample preparation before XRF analysis is shown, which lay between 0.01% and 3.88%.

3.3.2. Results of Determination of Lead Glass by UV-C Light

The results from manual lead glass sorting using a UV-C lamp are given in the Supplementary Material (Table S10). The mass share of lead glass shards in each glass fraction did not exceed 1.5%. Only extraneous material fractions produced from further processing showed higher lead glass shares of up to 3.2%, which confirms the success of the lead glass removal by sensor-based sorting. The calculation of the Pb content in each fraction, based on the mass share of lead glass, is shown in Figure 6. These values are compared to the Pb concentrations measured by XRF.

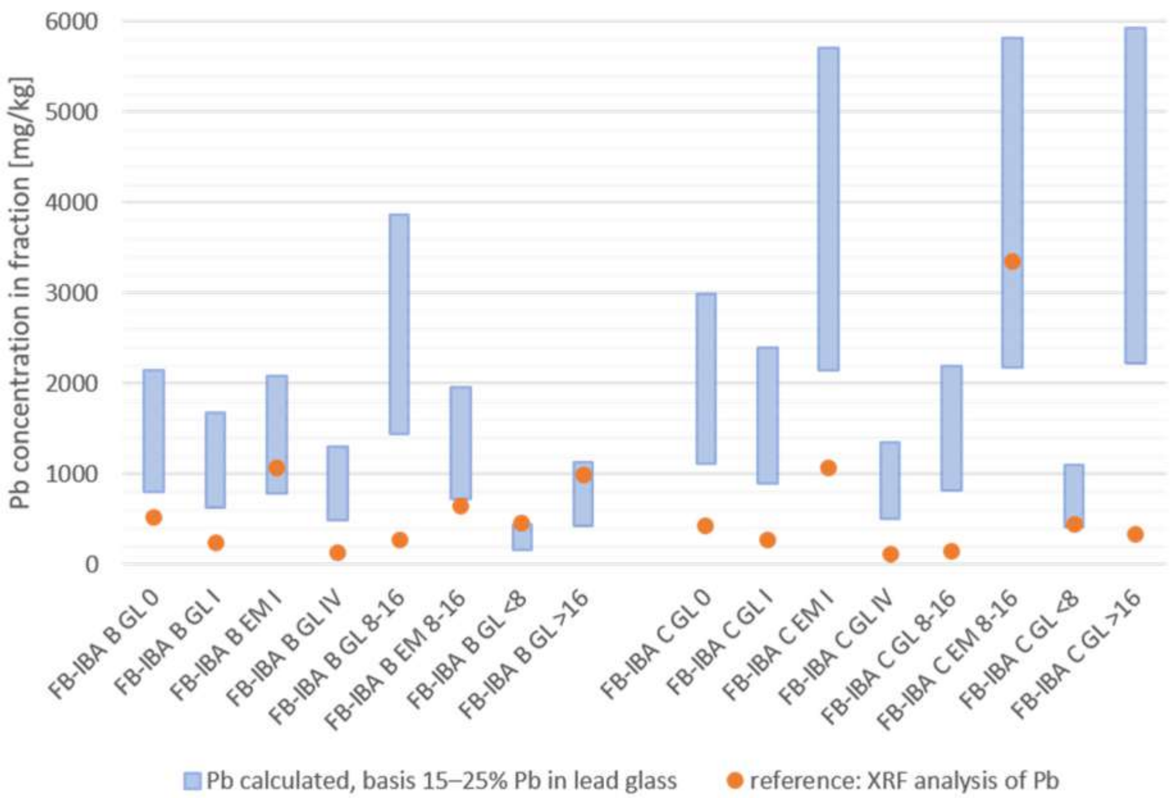

Figure 6. Pb concentrations in fractions determined by XRF analysis and calculation from manually sorted lead glass using a UV-C lamp.

From these results, it can be seen that the UV-C lamp can only be used for a tentative estimation of lead glass and is not suitable for an exact determination of Pb. Pb concentrations calculated from the mass of lead glass were considerably higher than the XRF values. However, this suggests that lead glass shards are a predominant Pb carrier in the FB-IBA glass fractions. Accordingly, the Pb concentration in waste glass can be reduced by the removal of lead glass.

3.4. Evaluation of the Upgrading Setups

A comparison of the recoverable glass from the upgrading setups is shown in Figure 7. Respective numerical values can be found in the Supplementary Material (Tables S11 and S12). This is important, as not only the quality but also the quantity of the glass is decisive for the feasibility of the glass recovery.

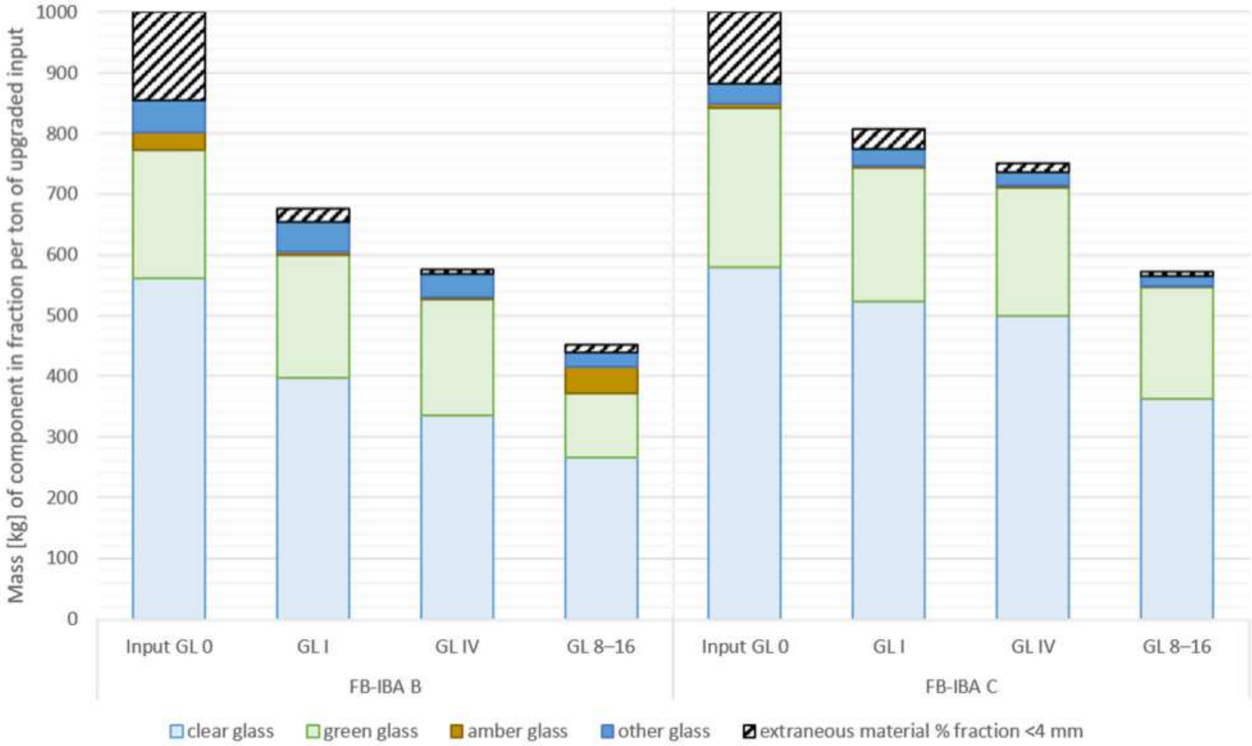

Figure 7. Masses of the components in 1 ton of input glass fraction (*GL 0*) and in the upgrading of 1 ton of material. Left side: glass from fluidized bed incineration bottom ash (FB-IBA) B, right side: from FB-IBA C. Other glass includes glass of other colors, molten agglomerates, or highly tarnished glass. CSP: non-glass mineral-based extraneous material (e.g., ceramic, stones, porcelain, building material).

From Figure 7 it becomes clear that upgrading of the glass fractions causes material losses. In particular, sieving of the glass fractions in *US_8–16* resulted in high glass losses of about a third of the glass if only the glass fraction 8–16 mm is further upgraded, as described in Section 3.1. Comparison of the first sensor-based sorting step of both upgrading setups shows that in *US_I–IV* 76% (FB-IBA B) and 88% (FB-IBA C) of the glass in the input fraction (*GL 0*) were still available in the fraction *GL I*, accounting for 654 kg and 774 kg. On the other hand, in *GL 8–16* of *US_8–16* only 51% or 440 kg (FB-IBA B) and 64% or 564 kg (FB-IBA C), respectively, of the glass in *GL 0* were present, which amounts to 440 kg (FB-IBA B) and 564 kg (FB-IBA C). Since the glass fractions produced by this first sorting step show similar shares of contaminants after sieving (*GL 8–16*) compared to the single-step upgrading of unsieved glass fractions (*GL I*), the upgrading of unsieved glass fractions in upgrading setup *US_I–IV* turns out to be more advantageous. Only the metal removal from the narrower particle size in *US_8–16* showed notably better results. The necessary effort for sieving is not considered to be reasonable. This might be even more relevant for IBAs where glass is not predominantly concentrated in one particle size fraction, which is the case in the study by Del Valle-Zermeño et al. [41], since more glass would be lost in the other particle size fractions through sieving.

Yet, an adapted upgrading setup, where glass is also recovered from the sieved fractions could make a difference and reduce glass losses. In upgrading setup *US_8–16*, the sieved fractions contain a third of the glass, thereof 24% (FB-IBA B) and 19% (FB-IBA C), respectively, in the particle size fraction >16 mm. If the glass is additionally recovered from this coarser fraction, the glass potential could be clearly increased. Also glass recovery from the fraction <8 mm should be examined, but the fine fraction 0–4 mm needs to be sieved beforehand, as it possibly impedes the process [63].

In addition to sieve losses, imperfection of sensor-based sorting can always cause falsely ejected glass into extraneous material fractions. This can, for example, be caused by overlapping particles, large particle size differences, or fine particles in the material [63]. Tarnished glass, which has a less translucent surface, can also impede glass detection, since the glass might falsely be detected as mineral material. Therefore, more glass is missorted into extraneous material fractions. In this study, higher contents of tarnished glass occurred in FB-IBA B, as can be seen in the pictures of the glass fractions in the Supplementary Material (Section S2.2). This presumably leads to the notable difference between FB-IBA B and C regarding the recovered glass amounts in both upgrading setups. Although both FB-IBAs contain similar amounts of glass in the input, clearly higher amounts of all glass fractions could be produced from FB-IBA C. The higher content of tarnished glass is presumably caused by the higher incineration temperature in the MSWI plant where FB-IBA B originates from [1]. At higher temperatures, melt reactions occur on the surface of the glass shards, while the sand in the fluidized bed causes abrasion on the softened glass. This indicates that glass upgrading is highly dependent on the actual material and cannot be generalized for all FB-IBAs.

Evaluating the multi-step upgrading setup *US_I–IV*, Figure 4 shows that the purest glass fractions are produced after the four-step glass removal. *GL IV* consists of 99.9% of glass in the case of both FB-IBAs. Furthermore, Pb can be successfully depleted by multi-step upgrading, as shown in Figure 5. Nevertheless, glass is lost in each sorting step of the upgrading by wrong ejection into extraneous material fractions. As determined in Section 3.1, 67% (FB-IBA B) and 83% (FB-IBA C) of the total glass in the input were recovered after four treatment runs. *GL I* of *US_I–IV* contained 76% (FB-IBA B) and 88% (FB-IBA C) of the total glass but contained nearly 2% of extraneous material in both cases.

It could be seen from this study that the success of the glass recovery is highly dependent on the configuration of the upgrading. Therefore, a more suitable upgrading constellation can possibly be found, especially if the compositions of the glass fractions are considered. According to the authors' experiences, the order of negative or positive sorting and the content of extraneous material in the original glass fraction strongly influence the recovery outcome. Chen et al. [63] also report that depending on the target of the sorting step (i.e., high yields or high purity) different sorting settings have to be applied.

3.5. Suitability of the Glass Fractions in the Packaging Glass Industry

To utilize glass cullet in a glass melting furnace, specific requirements must be met. Besides humidity and the content of organic material, which can be easily met by glass from incineration residues, the contents of CSP and metals are also limited. The CSP content in the glass cullet must not exceed 20 mg/kg (0.002%); for ferrous and non-ferrous metal pieces, the threshold is 2 mg/kg and 3 mg/kg, respectively, which equals 0.0002% and 0.0003% [18]. Also, the sum of the heavy metals Pb, Cd, Cr(VI) and Hg has to be below 200 mg/kg. Despite very low shares of extraneous material, especially after the four-step upgrading, the study's outcome suggests that multi-step upgrading is insufficient for meeting the requirements of the packaging glass industry, since minimum CSP contents of 0.1% were determined. In general, these highly stringent thresholds for CSP and metals are challenging to verify. For example, a small metal piece in several hundred kilograms of glass can lead to rejection of the material. Aldrian et al. [64] reported, though, that these limit values are exceeded even by one of the largest Austrian waste glass treatment plants, where ferrous and non-ferrous metal contents up to 0.3% and 0.7%, respectively, were assessed. Additionally, studies from other countries report lower quality requirements for glass, e.g., 98% purity in Portugal [31] or 96% purity in the UK [30]. Therefore, dialogues with local glass producers can also be suggested to inquire the respective specifications.

Regarding the heavy metal content examined in Section 3.3.1, the present study found that Pb is primarily relevant to the corresponding threshold. Only the glass fractions after four-step upgrading and one glass fraction 8–16 mm met the 200 mg/kg limit, which implies that multiple lead glass separation steps are necessary to comply with the requirements safely. To evaluate whether limit values can, in principle, be achieved through optimized treatment, investigations into further upgrading and adapted treatment configurations are necessary.

An issue that must be addressed concerning the recycling of glass from mixed MSW in FB-IBAs is that, by definition, only specific glass types should be disposed of in mixed MSW in Austria. This means that special glasses, e.g., lead glass or heat-resistant glass, are supposed to be enriched in mixed MSW and, therefore, in the FB-IBAs. Consequently, undesirable glass types for the packaging glass industry are concentrated in MSW. Yet, data from Austria indicate that the abundant amount of glass in mixed MSW is packaging glass that is not disposed of correctly in the separate glass waste collection [65]. Moreover, almost 20% of the packaging glass in Austria is not collected separately and is therefore lost for recycling if not recovered from FB-IBAs [33]. Nevertheless, since the glass recycling target of the EU, which is set to 75% as of 2030, has already been attained in Austria, there is no regulative incentive to improve the amount of glass recycled [24]. Furthermore, it has to be considered that the ecological benefit of glass recycling is highly dependent on the transport distance and the processing effort [66,67]. These factors are also critical for the economic feasibility of the upgrading scenarios. Each processing step consumes energy, with the utilization of compressed air being one of the most relevant cost factors in the case of sensor-based sorting [20]. Therefore, the environmental footprint and financial aspects of glass recovery from FB-IBAs should also be determined when developing a specific upgrading scenario in the future. Additionally, further recycling options, including open-loop recycling, should be assessed for glass from IBA as this might reduce the necessary upgrading effort [68–70]. It must also be mentioned that the practical feasibility of glass upgrading from FB-IBA is strongly dependent on the respective local market where it is applied. Factors like the disposal costs for landfilling or transport distances between the MSWI plant, the IBA treatment plant and the packaging glass industry strongly influence environmental and financial practicability. Furthermore, local collection rates and available amounts of glass cullet from separate MSW collection affect the demand for recovered glass from IBA and consequentially the market price.

3.6. Limitations

Regarding the upgrading setups conducted, some uncertainties must be considered when evaluating the results. As is the case for waste characterization in general, heterogeneity of the material is a crucial issue. This also counts for IBAs and the glass therein. Therefore, the general validity of the present results cannot be ensured by a single experiment, as the IBA composition depends on seasonal and regional factors, such as the extent of separate collection [71,72]. Moreover, the composition of Austrian IBAs strongly depends on the incinerated waste stream, which can include sewage sludge, industrial waste, or other materials, but also on the incineration conditions [47]. Further uncertainties arise from the sampling and manual sorting procedures. Although special attention was paid to representative sampling by a high number of increments and incremental shoveling to reduce sample masses, only limited amounts of the fractions could be sorted manually, especially in the case of some extraneous material fractions. Due to the strict limit values (e.g., 2 mg/kg of ferrous metals), more material should have been sorted. According to Bunge and Bunge [73], even dozens of tons would have been necessary to obtain valid results and a general conclusion about whether the packaging glass requirements can be met. This is not feasible in scientific research concerning personnel, time and money resources. However, the present results report the composition of glass from FB-IBAs for the first time in scientific literature and show the potential of glass recovery from IBA. Further assessments with expanded sample sizes and the implementation of statistical models can help to improve the reliability of future findings.

A practical issue that occurred at the Brantner treatment plant and deteriorated the glass quality reported is the fact that some valves of the glass sorting device at the Brantner plant, which eject extraneous material, were not working during the sampling campaign. This was only identified weeks after the sampling campaigns. It cannot be assumed to what extent this impaired the investigated glass fractions. Repaired valves could lead to improved results.

4. Conclusions

The present work shows that high amounts of glass are contained in FB-IBAs from MSWI, which can be removed technically by sensor-based sorting. The glass fraction produced from FB-IBAs primarily contains clear glass, followed by green glass; but also, extraneous material, such as CSP or metals, was found in the range of up to 13%. For high-grade recycling in the packaging glass industry, the content of extraneous material has to be reduced by upgrading. In this study, it was found that glass fractions with >99% purity can be produced by upgrading steps. Despite this high value, the stringent regulations of the packaging glass industry could not be met in the experimental setting. To further improve the glass quality, adapted upgrading should be investigated. Moreover, other recycling paths for the glass should be assessed, e.g., foam glass or expanded glass. Therefore, the landfilling of this secondary resource could be reduced. Nevertheless, the recovery and purification of glass from FB-IBAs is not only limited economically, but the ecological feasibility also depends on the processing effort and the transport distance. Since Austria is seen as a forerunner regarding waste management [34,74], the amount of glass that can potentially be recovered from mixed MSW is comparably low. Regarding other European countries with lower collection rates, however, considerably more glass might be found in IBAs from MSWI, which could make the present approach more relevant [75]. Glass recovery from MSW IBA can also be advantageous compared to recovery from mixed MSW since organic contaminants are destroyed and the mass of the MSW is reduced by incineration. Therefore, potential economic and ecological benefits should be examined more closely. In general, fluidized bed combustion for MSW should be investigated in more detail. The potential of glass in FB-IBAs contributes to the advantages of FB-IBAs compared to G-IBAs, which were demonstrated in several Austrian studies hitherto [37,47,48,62]. Additionally, the pretreatment of MSW before fluidized bed combustion could have positive ecological effects, as more recyclable material can be recovered [33]. A holistic approach would be required to determine if fluidized bed combustion of MSW is generally advantageous, also considering the downsides of this incineration technology, like higher amounts of fly ash.

Supplementary Materials: The following supporting information can be downloaded at: https://www.mdpi.com/article/10.3390/recycling10020063/s1, Figure S1: Pictures of glass fractions of FB-IBAs before upgrading; Figure S2: Sensor-based glass sorter used for the upgrading steps; Figure S3: Crushed glass <2 mm after crushing and sieving; Figure S4: Pelleting of glass powder for XRF analysis; Figure S5: Fluorescence of lead glass through UV-C radiation; Table S1: FB-IBA B: Compositions of glass fractions produced in the upgrading setups; Table S2: Composition of extraneous material fractions produced in the upgrading setups; Table S3: FB-IBA B: Compositions of particle size fractions of upgrading setup US_I-IV determined by manual sorting of the sieved fractions; Table S4: FB-IBA C: Compositions of particle size fractions of upgrading setup US_I-IV determined by manual sorting of the sieved fractions; Table S5: Compositions of fractions of upgrading setup US_8-16 determined by manual sorting; Figure S6: Pictures of the glass fractions GL 0 of FB-IBA before upgrading; Figure S7: Pictures of the glass fractions GL IV from upgrading setup US_I-IV; Figure S8: Manually sorted compounds of the fraction GL 8-16 from FB-IBA C; Figure S9: Manually sorted compounds of the fraction EM 8-16 from FB-IBA B; Table S6: Results of XRF analysis for Pb, Cd, Hg and Cr(VI) in different fractions; Table S7: Calculation of the Pb contents in the input glass fractions; Table S8: Calculation of the Pb contents in the input glass fractions (GL 0) by means of material flow analysis of upgrading setup US_8-16; Table S9: Results of the XRF analysis for additional elements; Table S10: Results of manual lead glass sorting using UV-C light; Table S11: FB-IBA B: Compositions of glass fractions produced in the upgrading setups; Table S12: FB-IBA C: Compositions of glass fractions produced in the upgrading setups.

Author Contributions: Conceptualization, J.M. and J.L.; methodology, J.M., S.M., A.T.-A. and J.L.; validation, J.M.; formal analysis, J.M.; investigation, J.M., S.M. and A.T.-A.; resources, A.T.-A.; writing—original draft preparation, J.M.; writing—review and editing, J.M., S.M. and J.L.; visualization, J.M.; supervision, J.M. and J.L.; project administration, J.L.; funding acquisition, J.L. All authors have read and agreed to the published version of the manuscript.

Funding: This research was funded by the Austrian Federal Ministry of Labour and Economy, the National Foundation for Research, Technology and Development and the Christian Doppler Research Association. Open Access Funding by TU Wien Bibliothek.

Data Availability Statement: The original contributions presented in this study are included in the article/Supplementary Material. Further inquiries can be directed to the corresponding author.

Acknowledgments: The financial support by the Austrian Federal Ministry of Labour and Economy, the National Foundation for Research, Technology and Development and the Christian Doppler Research Association is gratefully acknowledged. Furthermore, we thankfully acknowledge the financial and non-financial support of our company partners, which are, in alphabetical order: Abfallbehandlung Ahrental GmbH, Altstoff Recycling Austria AG, Brantner Österreich GmbH, Holding Graz Kommunale Dienstleistungen GmbH, Lenzing Aktiengesellschaft, Linz Service GmbH, MM Board & Paper, Wien Energie GmbH, and Wopfinger Transportbeton Ges.m.b.H. In addition, we thank Magistratsabteilung MA 48, the public Waste Management provider of Vienna, for its non-financial support, Binder + Co., Ltd. AG for their experimental support and all student assistants involved for their hard work and persevering hand sorting. The TU Wien Bibliothek is thanked for financial support through its Open Access Funding Program.

Conflicts of Interest: The authors declare no conflicts of interest. The funders had no role in the design of the study; in the collection, analyses, or interpretation of data; in the writing of the manuscript; or in the decision to publish the results.

Abbreviations

The following abbreviations are used in this manuscript:

CSP	Ceramic, stones, porcelain and other non-glass mineral-based extraneous material
EU	European Union
XRF	X-ray fluorescence

FB-IBA	Fluidized bed incineration bottom ash
IBA	Incineration bottom ash
ICP-OES	inductively coupled plasma optical emission spectrometry
MSW	Municipal solid waste
MSWI	Municipal solid waste incineration
UV	Ultraviolet
VIS	Visible (spectrum)
XRF	X-ray fluorescence

References

1. Scalet, B.M.; Garcia Munoz, M.; Sissa, A.Q.; Roudier, S.; Delgado Sancho, L. Best Available Techniques (BAT) Reference Document for The Manufacture of Glass: Industrial Emissions Directive 2010/75/EU Integrated Pollution Prevention and Control. EUR 25786 EN, Luxemburg. 2013. Available online: https://eippcb.jrc.ec.europa.eu/sites/default/files/2019-11/GLS_Adopted_03_2012_0.pdf (accessed on 14 January 2022).
2. Larsen, A.W.; Merrild, H.; Christensen, T.H. Recycling of glass: Accounting of greenhouse gases and global warming contributions. *Waste Manag. Res.* **2009**, *27*, 754–762. [CrossRef] [PubMed]
3. Testa, M.; Malandrino, O.; Sessa, M.; Supino, S.; Sica, D. Long-Term Sustainability from the Perspective of Cullet Recycling in the Container Glass Industry: Evidence from Italy. *Sustainability* **2017**, *9*, 1752. [CrossRef]
4. Dhir, R.K.; de Brito, J.; Ghataora, G.S.; Lye, C.Q. *Sustainable Construction Materials: Glass Cullet*; Woodhead Publishing: Duxford, UK, 2018; ISBN 978-0-08-100984-0.
5. Dyer, T.D. Glass. In *Handbook of Recycling*; Elsevier: Amsterdam, The Netherlands, 2024; pp. 445–461, ISBN 9780323855143.
6. Abdel Alim, D.; El-Haggar, S.M. Innovation in the Glass Industry: Upcycle of Glass Waste: Foam Glass. In *Sustainability and Innovation*; El-Haggar, S.M., Anderson, L., Eds.; American University in Cairo Press: Cairo, Egypt, 2016; pp. 171–228, ISBN 9789774166471.
7. Arulrajah, A.; Disfani, M.M.; Maghoolpilehrood, F.; Horpibulsuk, S.; Udonchai, A.; Imteaz, M.; Du, Y.-J. Engineering and environmental properties of foamed recycled glass as a lightweight engineering material. *J. Clean. Prod.* **2015**, *94*, 369–375. [CrossRef]
8. da Costa, F.P.; da Silva Morais, C.R.; Rodrigues, A.M. Sustainable glass-ceramic foams manufactured from waste glass bottles and bentonite. *Ceram. Int.* **2020**, *46*, 17957–17961. [CrossRef]
9. Mohajerani, A.; Vajna, J.; Cheung, T.H.H.; Kurmus, H.; Arulrajah, A.; Horpibulsuk, S. Practical recycling applications of crushed waste glass in construction materials: A review. *Constr. Build. Mater.* **2017**, *156*, 443–467. [CrossRef]
10. Kazmi, D.; Williams, D.J.; Serati, M. Waste glass in civil engineering applications—A review. *Int. J. Appl. Ceram. Technol.* **2020**, *17*, 529–554. [CrossRef]
11. Dong, W.; Li, W.; Tao, Z. A comprehensive review on performance of cementitious and geopolymeric concretes with recycled waste glass as powder, sand or cullet. *Resour. Conserv. Recycl.* **2021**, *172*, 105664. [CrossRef]
12. Jani, Y.; Hogland, W. Waste glass in the production of cement and concrete—A review. *J. Environ. Chem. Eng.* **2014**, *2*, 1767–1775. [CrossRef]
13. Disfani, M.M.; Arulrajah, A.; Bo, M.W.; Sivakugan, N. Environmental risks of using recycled crushed glass in road applications. *J. Clean. Prod.* **2012**, *20*, 170–179. [CrossRef]
14. Delbari, S.A.; Hof, L.A. Glass waste circular economy—Advancing to high-value glass sheets recovery using industry 4.0 and 5.0 technologies. *J. Clean. Prod.* **2024**, *462*, 142629. [CrossRef]
15. Vinci, G.; D'Ascenzo, F.; Esposito, A.; Musarra, M.; Rapa, M.; Rocchi, A. A sustainable innovation in the Italian glass production: LCA and Eco-Care matrix evaluation. *J. Clean. Prod.* **2019**, *223*, 587–595. [CrossRef]
16. Gallucci, T.; Lagioia, G.; Piccinno, P.; Lacalamita, A.; Pontrandolfo, A.; Paiano, A. Environmental performance scenarios in the production of hollow glass containers for food packaging: An LCA approach. *Int. J. Life Cycle Assess.* **2021**, *26*, 785–798. [CrossRef]
17. Adekomaya, O.; Majozi, T. Mitigating environmental impact of waste glass materials: Review of the existing reclamation options and future outlook. *Environ. Sci. Pollut. Res. Int.* **2021**, *28*, 10488–10502. [CrossRef]

18. Bundesverband Glasindustrie e.V.; BDE Bundesverband der Deutschen Entsorgungs-, Wasser- und Rohstoffwirtschaft e.V.; bvse-Bundesverband Sekundärrohstoffe und Entsorgung e.V. *Leitlinie Qualitätsanforderungen an Glasscherben zum Einsatz in der Behälterglasindustrie*: *Standardblatt T 120* [Guideline Quality Requirements for Glass Cullet for the Use in the Packaging Glass Industry, 2014]. Available online: https://ec.europa.eu/eurostat/cache/metadata/en/cei_wm020_esmsip2.htm (accessed on 2 December 2024).
19. Bristogianni, T.; Oikonomopoulou, F. Glass up-casting: A review on the current challenges in glass recycling and a novel approach for recycling "as-is" glass waste into volumetric glass components. *Glass Struct. Eng.* **2023**, *8*, 255–302. [CrossRef]
20. Maier, G.; Gruna, R.; Längle, T.; Beyerer, J. A Survey of the State of the Art in Sensor-Based Sorting Technology and Research. *IEEE Access* **2024**, *12*, 6473–6493. [CrossRef]
21. Gundupalli, S.P.; Hait, S.; Thakur, A. A review on automated sorting of source-separated municipal solid waste for recycling. *Waste Manag.* **2017**, *60*, 56–74. [CrossRef]
22. Geueke, B.; Groh, K.; Muncke, J. Food packaging in the circular economy: Overview of chemical safety aspects for commonly used materials. *J. Clean. Prod.* **2018**, *193*, 491–505. [CrossRef]
23. Barbato, P.M.; Olsson, E.; Rigamonti, L. Quality degradation in glass recycling: Substitutability model proposal. *Waste Manag.* **2024**, *182*, 124–131. [CrossRef]
24. European Parliament and Council. Directive (EU) 2018/of the European Parliament and of the Council of 30 May 2018 Amending Directive 94/62/EC on Packaging and Packaging Waste, 14pp. Available online: https://eur-lex.europa.eu/legal-content/EN/TXT/PDF/?uri=CELEX:32018L0852 (accessed on 2 December 2024).
25. Eurostat. Recycling Rate of Packaging Waste by Type of Packaging. 2023. Available online: https://ec.europa.eu/eurostat/cache/metadata/en/cei_wm020_esmsip2.htm (accessed on 2 December 2024).
26. Close the Glass Loop. Container Glass Collection for Recycling in Europe. 2022. Available online: https://closetheglassloop.eu/wp-content/uploads/2023/06/CGL-Map-2022-Recycling-stats-scaled.jpg (accessed on 28 August 2024).
27. Westbroek, C.D.; Bitting, J.; Craglia, M.; Azevedo, J.M.C.; Cullen, J.M. Global material flow analysis of glass: From raw materials to end of life. *J. Ind. Ecol.* **2021**, *25*, 333–343. [CrossRef]
28. Butler, J.H.; Hooper, P.D. Glass Waste. In *Waste*; Elsevier: Amsterdam, The Netherlands, 2019; pp. 307–322, ISBN 9780128150603.
29. Majdinasab, A.; Yuan, Q. Post-consumer cullet and potential engineering applications in North America. *Resour. Conserv. Recycl.* **2019**, *147*, 1–9. [CrossRef]
30. Cimpan, C.; Maul, A.; Jansen, M.; Pretz, T.; Wenzel, H. Central sorting and recovery of MSW recyclable materials: A review of technological state-of-the-art, cases, practice and implications for materials recycling. *J. Environ. Manag.* **2015**, *156*, 181–199. [CrossRef] [PubMed]
31. Dias, N.; Máximo, A.; Belo, N.; Carvalho, M.T. Packaging glass contained in the heavy residual fraction refused by Portuguese Mechanical and Biological Treatment plants. *Resour. Conserv. Recycl.* **2014**, *85*, 98–105. [CrossRef]
32. Bourtsalas, A.C.T.; Themelis, N.J. Materials and energy recovery at six European MBT plants. *Waste Manag.* **2022**, *141*, 79–91. [CrossRef]
33. Lipp, A.-M.; Lederer, J. The circular economy of packaging waste in Austria: An evaluation based on statistical entropy and material flow analysis. *Resour. Conserv. Recycl.* **2025**, *217*, 108193. [CrossRef]
34. Pomberger, R.; Sarc, R.; Lorber, K.E. Dynamic visualisation of municipal waste management performance in the EU using Ternary Diagram method. *Waste Manag.* **2017**, *61*, 558–571. [CrossRef]
35. Bayuseno, A.P.; Schmahl, W.W. Understanding the chemical and mineralogical properties of the inorganic portion of MSWI bottom ash. *Waste Manag.* **2010**, *30*, 1509–1520. [CrossRef]
36. Eusden, J.; Eighmy, T.; Hockert, K.; Holland, E.; Marsella, K. Petrogenesis of municipal solid waste combustion bottom ash. *Appl. Geochem.* **1999**, *14*, 1073–1091.
37. Blasenbauer, D.; Huber, F.; Mühl, J.; Fellner, J.; Lederer, J. Comparing the quantity and quality of glass, metals, and minerals present in waste incineration bottom ashes from a fluidized bed and a grate incinerator. *Waste Manag.* **2023**, *161*, 142–155. [CrossRef]
38. Vateva, I.; Laner, D. Grain-Size Specific Characterisation and Resource Potentials of Municipal Solid Waste Incineration (MSWI) Bottom Ash: A German Case Study. *Resources* **2020**, *9*, 66. [CrossRef]
39. Huber, F.; Blasenbauer, D.; Aschenbrenner, P.; Fellner, J. Complete determination of the material composition of municipal solid waste incineration bottom ash. *Waste Manag.* **2020**, *102*, 677–685. [CrossRef]
40. Šyc, M.; Simon, F.G.; Hykš, J.; Braga, R.; Biganzoli, L.; Costa, G.; Funari, V.; Grosso, M. Metal recovery from incineration bottom ash: State-of-the-art and recent developments. *J. Hazard. Mater.* **2020**, *393*, 122433. [CrossRef]
41. Del Valle-Zermeño, R.; Gómez-Manrique, J.; Giro-Paloma, J.; Formosa, J.; Chimenos, J.M. Material characterization of the MSWI bottom ash as a function of particle size. Effects of glass recycling over time. *Sci. Total Environ.* **2017**, *581–582*, 897–905. [CrossRef] [PubMed]

42. Lederer, J.; Schuch, D. The contribution of waste and bottom ash treatment to the circular economy of metal packaging: A case study from Austria. *Resour. Conserv. Recycl.* **2024**, *203*, 107461. [CrossRef]
43. van Caneghem, J.; de Coster, E.; Vandenbergh, K.; de Broyer, S.; Lambrix, N.; Weemaels, L. Closing the household metal packaging cycle through recovery of scrap from waste-to-energy bottom ash: The case study of Flanders. *Resour. Conserv. Recycl.* **2019**, *144*, 115–122. [CrossRef]
44. Fletcher, C.A.; Dunk, R. Recovery and utilisation of municipal solid waste incineration bottom ash: Implications for European waste management strategy. *Detritus* **2023**, *23*, 43–57. [CrossRef]
45. Blasenbauer, D.; Huber, F.; Lederer, J.; Quina, M.J.; Blanc-Biscarat, D.; Bogush, A.; Bontempi, E.; Blondeau, J.; Chimenos, J.M.; Dahlbo, H.; et al. Legal situation and current practice of waste incineration bottom ash utilisation in Europe. *Waste Manag.* **2020**, *102*, 868–883. [CrossRef]
46. Makari, C. Optical Sorting for the Recovery of Glass from WIP Slags: Pilot Plant in Bratislava. In *Waste Management*; Thomé-Kozmiensky, K.J., Thiel, S., Eds.; TK-Verl. Thomé-Kozmiensky: Neuruppin, Germany, 2014; pp. 345–354, ISBN 978-3-944310-15-2.
47. Mühl, J.; Skutan, S.; Stockinger, G.; Blasenbauer, D.; Lederer, J. Glass recovery and production of manufactured aggregate from MSWI bottom ashes from fluidized bed and grate incineration by means of enhanced treatment. *Waste Manag.* **2023**, *168*, 321–333. [CrossRef]
48. Mühl, J.; Hofer, S.; Blasenbauer, D.; Lederer, J. Recovery of aluminum, magnetic ferrous metals and glass through enhanced industrial-scale treatment of different MSWI bottom ashes. *Waste Manag.* **2024**, *190*, 557–568. [CrossRef]
49. Pfandl, K.; Küppers, B.; Scheiber, S.; Stockinger, G.; Holzer, J.; Pomberger, R.; Antrekowitsch, H.; Vollprecht, D. X-ray fluorescence sorting of non-ferrous metal fractions from municipal solid waste incineration bottom ash processing depending on particle surface properties. *Waste Manag. Res.* **2020**, *38*, 111–121. [CrossRef]
50. Gerlach, R.W.; Nocerino, J.M. Guidance for Obtaining Representative Laboratory Analytical Subsamples from Particulate Laboratory Samples. 2003. Available online: https://clu-in.org/download/char/epa_subsampling_guidance.pdf (accessed on 14 December 2022).
51. Peukert, D.; Xu, C.; Dowd, P. A Review of Sensor-Based Sorting in Mineral Processing: The Potential Benefits of Sensor Fusion. *Minerals* **2022**, *12*, 1364. [CrossRef]
52. Wotruba, H.; Harbeck, H. *Sensor-Based Sorting. Ullmann's Encyclopedia of Industrial Chemistry*; Wiley: Hoboken, NJ, USA, 2003; ISBN 9783527303854.
53. Brunner, P.H.; Rechberger, H. *Handbook of Material Flow Analysis: For Environmental, Resource, and Waste Engineers*, 2nd ed.; CRC Press Taylor & Francis Group: Boca Raton, FL, USA; London, UK; New York, NY, USA, 2017; ISBN 978-1-4987-2134-9.
54. *EN 13656:2002*; Characterization of Waste—Microwave Assisted Digestion with Hydrofluoric (HF), Nitric (HNO3) and Hydrochloric (HCl) Acid Mixture for Subsequent Determination of Elements. European Committee for Standardization: Brussels, Belgium, 2022.
55. *DIN 38405-52:2020-11*; German Standard Methods for the Examination of Water, Waste Water and Sludge—Anions (Group D)—Part 52: Photometric Determination of Dissolved Chromium(VI) in Water (D 52). Deutsches Institut für Normung e.V.: Berlin, Germany, 2020.
56. Huber, R. Weiterentwicklung Optischer Sortiertechnik und Erweiterung der Einsatzmöglichkeiten in der Aufbereitung Primärer und Sekundärer Rohstoffe [Improvement of Optical Sorting Technology and Expansion of Possible Applications in the Processing of Primary and Secondary Raw Materials]. Ph.D. Thesis, Montanuniversität Leoben, Leoben, Austria, 2016.
57. Huber, R.; Leitner, K. Method and Device for Detecting Lead-Containing Glass. Pieces. Patent No. EP20100709457 20100226, 26 February 2010.
58. Viczek, S.A.; Aldrian, A.; Pomberger, R.; Sarc, R. Origins and carriers of Sb, As, Cd, Cl, Cr, Co, Pb, Hg, and Ni in mixed solid waste—A literature-based evaluation. *Waste Manag.* **2020**, *103*, 87–112. [CrossRef] [PubMed]
59. Morgan, T.J.; George, A.; Boulamanti, A.K.; Álvarez, P.; Adanouj, I.; Dean, C.; Vassilev, S.V.; Baxter, D.; Andersen, L.K. Quantitative X-ray Fluorescence Analysis of Biomass (Switchgrass, Corn Stover, Eucalyptus, Beech, and Pine Wood) with a Typical Commercial Multi-Element Method on a WD-XRF Spectrometer. *Energy Fuels* **2015**, *29*, 1669–1685. [CrossRef]
60. Götze, R.; Boldrin, A.; Scheutz, C.; Astrup, T.F. Physico-chemical characterisation of material fractions in household waste: Overview of data in literature. *Waste Manag.* **2016**, *49*, 3–14. [CrossRef] [PubMed]
61. Turner, A. Heavy Metals in the Glass and Enamels of Consumer Container Bottles. *Environ. Sci. Technol.* **2019**, *53*, 8398–8404. [CrossRef]
62. Mika, S.; Mühl, J.; Skutan, S.; Aschenbrenner, P.; Limbeck, A.; Lederer, J. Substance flows of heavy metals in industrial-scale municipal solid waste incineration bottom ash treatment: A case study from Austria. *Waste Manag.* **2025**, *195*, 240–252. [CrossRef]
63. Chen, X.; Kroell, N.; Feil, A.; Greiff, K. Sensor-based sorting. In *Handbook of Recycling*; Elsevier: Amsterdam, The Netherlands, 2024; pp. 145–159, ISBN 9780323855143.

64. Aldrian, A.; Pomberger, R.; Schipfer, C.; Gattermayer, K. Altglasrecycling—Anteil an Störstoffen im Altglas in Österreich. [Waste glass recycling—share of impurities in waste glass in Austria]. In *POSTER-Konferenzband zur 14. Recy & DepoTech-Konferenz*; Pomberger, R., Adam, J., Aldrian, A., Curtis, A., Friedrich, K., Kranzinger, L., Küppers, B.E., Eds.; Recy & DepoTech, Leoben, 07–09.11.2018; Abfallverwertungstechnik & Abfallwirtschaft Eigenverlag: Leoben, Austria, 2018; pp. 193–198. ISBN 978-3-200-05858-3.
65. Beigl, P. Auswertung der Restmüllzusammensetzung in Österreich 2018/2019: Ergebnisbericht [Evaluation of the Residual Waste Composition in Austria 2018/2019, Wien]. 2020. Available online: https://www.bmk.gv.at/dam/jcr:c034808f-c67d-4eab-b2a3-30a6bcd6d0eb/Restmuell-Zusammensetzung-2018-19.pdf (accessed on 7 June 2022).
66. Blengini, G.A.; Busto, M.; Fantoni, M.; Fino, D. Eco-efficient waste glass recycling: Integrated waste management and green product development through LCA. *Waste Manag.* **2012**, *32*, 1000–1008. [CrossRef] [PubMed]
67. Humbert, S.; Rossi, V.; Margni, M.; Jolliet, O.; Loerincik, Y. Life cycle assessment of two baby food packaging alternatives: Glass jars vs. plastic pots. *Int. J. Life Cycle Assess.* **2009**, *14*, 95–106. [CrossRef]
68. Deschamps, J.; Simon, B.; Tagnit-Hamou, A.; Amor, B. Is open-loop recycling the lowest preference in a circular economy? Answering through LCA of glass powder in concrete. *J. Clean. Prod.* **2018**, *185*, 14–22. [CrossRef]
69. Haupt, M.; Kägi, T.; Hellweg, S. Modular life cycle assessment of municipal solid waste management. *Waste Manag.* **2018**, *79*, 815–827. [CrossRef]
70. Meylan, G.; Ami, H.; Spoerri, A. Transitions of municipal solid waste management. Part II: Hybrid life cycle assessment of Swiss glass-packaging disposal. *Resour. Conserv. Recycl.* **2014**, *86*, 16–27. [CrossRef]
71. Costa, G.; Polettini, A.; Pomi, R.; Spagnuolo, R. Enhanced Separation of Incinerator Bottom Ash: Composition and Environmental Behaviour of Separated Mineral and Weakly Magnetic Fractions. *Waste Biomass Valorization* **2020**, *11*, 7079–7095. [CrossRef]
72. Beikmohammadi, M.; Yaghmaeian, K.; Nabizadeh, R.; Mahvi, A.H. Analysis of heavy metal, rare, precious, and metallic element content in bottom ash from municipal solid waste incineration in Tehran based on particle size. *Sci. Rep.* **2023**, *13*, 16044. [CrossRef] [PubMed]
73. Bunge, R.; Bunge, K. Probenahme auf Altlasten: Minimal notwendige Probenmasse. *Altlasten Spektrum* **1999**, *1999*, 174–179.
74. European Environment Agency. Many EU Member States Not on Track to Meet Recycling Targets for Municipal Waste and Packaging Waste: Briefing no. 28/2022. 2023. Available online: https://www.eea.europa.eu/publications/many-eu-member-states (accessed on 11 December 2024).
75. Chimenos, J.; Segarra, M.; Fernández, M.; Espiell, F. Characterization of the bottom ash in municipal solid waste incinerator. *J. Hazard. Mater.* **1999**, *64*, 211–222. [CrossRef]